US Army Corps
of Engineers
Construction Engineering
Research Laboratory

USA-CERL

TECHNICAL MANUSCRIPT M-86/15
September 1986

In Process Measurement of Hydrogen in Welding

by
Dawn R. White

The deleterious effects of atomic, or diffusible, hydrogen dissolved in welds on their mechanical properties have been known for over four decades. However, post weld inspection and repair of hydrogen induced cracks in welds remains the only means of correcting the defects produced by excess hydrogen in the arc atmosphere during welding. In this study, a spectroscopic technique for measuring the amount of hydrogen in the arc atmosphere during welding is presented. A relationship between the amount of hydrogen present in the weld arc atmosphere during welding and the diffusible hydrogen content of the resulting weld is developed. The results of mechanical tests are used to determine the hydrogen induced cracking susceptibility of an armor steel. The amount of hydrogen present in the arc atmosphere during welding is correlated with the mechanical properties of the weld. Methods for applying this work to real time detection of conditions likely to produce hydrogen induced cracking of production welds, and thereby reduce the amount of nondestructive inspection and weld repair required later, are suggested.

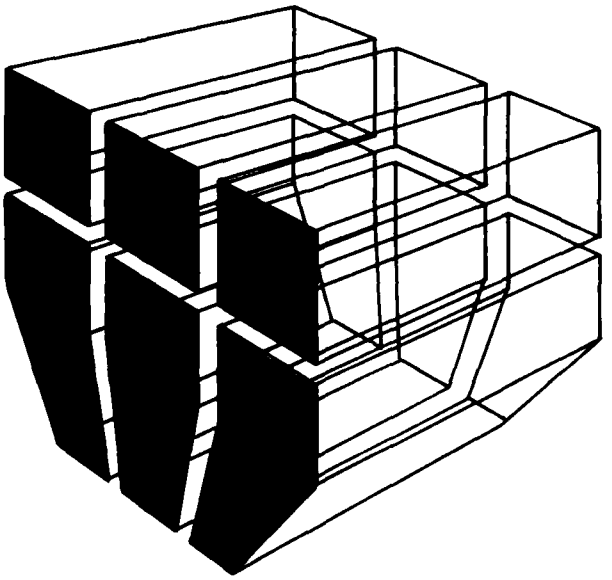

UNCLASSIFIED
SECURITY CLASSIFICATION OF THIS PAGE

AD-A173331

REPORT DOCUMENTATION PAGE

Form Approved
OMB No 0704-0188
Exp Date Jun 30 1986

1a REPORT SECURITY CLASSIFICATION UNCLASSIFIED	1b RESTRICTIVE MARKINGS
2a SECURITY CLASSIFICATION AUTHORITY	3 DISTRIBUTION/AVAILABILITY OF REPORT Approved for public release; distribution unlimited.
2b DECLASSIFICATION/DOWNGRADING SCHEDULE	
4 PERFORMING ORGANIZATION REPORT NUMBER(S) CERL-TM-M-86/15	5 MONITORING ORGANIZATION REPORT NUMBER(S)
6a NAME OF PERFORMING ORGANIZATION U.S. Army Construction Engr Research Laboratory 6b OFFICE SYMBOL (If applicable) USA-CERL	7a NAME OF MONITORING ORGANIZATION
6c ADDRESS (City, State, and ZIP Code) P.O. Box 4005 Champaign, IL 1820-1305	7b ADDRESS (City, State, and ZIP Code)
8a NAME OF FUNDING/SPONSORING ORGANIZATION HQ-USACE 8b OFFICE SYMBOL (If applicable)	9 PROCUREMENT INSTRUMENT IDENTIFICATION NUMBER
8c ADDRESS (City, State, and ZIP Code) 20 Massachusetts Ave., N.W. Washington, D.C. 20314-1000	10 SOURCE OF FUNDING NUMBERS PROGRAM ELEMENT NO: 61102 / PROJECT NO: T23 / TASK NO: A / WORK UNIT ACCESSION NO: 034

11 TITLE (Include Security Classification)

In Process Measurement of Hydrogen in Welding (Unclassified)

12 PERSONAL AUTHOR(S)
White, Dawn R.

13a TYPE OF REPORT	13b TIME COVERED	14 DATE OF REPORT (Year, Month, Day)	15 PAGE COUNT
Final	FROM _____ TO _____	86-09	101

16 SUPPLEMENTARY NOTATION
Copies are available from the National Technical Information Service
Springfield, VA 22161

17 COSATI CODES			18 SUBJECT TERMS (Continue on reverse if necessary and identify by block number)
FIELD	GROUP	SUB-GROUP	welds hydrogen cracks
13	08		

19 ABSTRACT (Continue on reverse if necessary and identify by block number)

The deleterious effects of atomic, or diffusible, hydrogen dissolved in welds on their mechanical properties have been known for over four decades. However, post weld inspection and repair of hydrogen induced cracks in welds remains the only means of correcting the defects produced by excess hydrogen in the arc atmosphere during welding. In this study, a spectroscopic technique for measuring the amount of hydrogen in the arc atmosphere during welding is presented. A relationship between the amount of hydrogen present in the weld arc atmosphere during welding and the diffusible hydrogen content of the resulting weld is developed. The results of mechanical tests are used to determine the hydrogen induced cracking susceptibility of an armor steel. The amount of hydrogen present in the arc atmosphere during welding is correlated with the mechanical properties of the weld. Methods for applying this

20 DISTRIBUTION/AVAILABILITY OF ABSTRACT	21 ABSTRACT SECURITY CLASSIFICATION
☐ UNCLASSIFIED/UNLIMITED ☒ SAME AS RPT ☐ DTIC USERS	UNCLASSIFIED
22a NAME OF RESPONSIBLE INDIVIDUAL D.P. Mann	22b TELEPHONE (Include Area Code) 217-373-7223 / 22c OFFICE SYMBOL CERL-IMT

DD FORM 1473, 84 MAR

83 APR edition may be used until exhausted
All other editions are obsolete

SECURITY CLASSIFICATION OF THIS PAGE
UNCLASSIFIED

BLOCK 19 (Cont'd)

work to real time detection of conditions likely to produce hydrogen induced cracking of production welds, and thereby reduce the amount of nondestructive inspection and weld repair required later, are suggested.

FOREWORD

This research was conducted for the Office of the Chief of Engineers under Project 4A161102AT23, "Basic Research in Military Construction"; Task A, "Base/Facility Development"; Work Unit 034, "Real Time Observation of Weld Pool Behavior."

This report was submitted in partial fulfillment of the requirements for the degree Doctor of Philosophy in Mechanical Engineering in the Graduate College of the University of Illinois at Urbana-Champaign. The advisor for this thesis was Professor Fred Leckie.

The author is a researcher in the Engineering and Materials Division (EM) of the U.S. Army Construction Engineering Research Laboratory (USA-CERL). Dr. Robert Quattrone is Chief of EM.

COL Norman C. Hintz is Commander and Director of USA-CERL. Dr. L.R. Shaffer is Technical Director.

TABLE OF CONTENTS

NOMENCLATURE

HAZ	heat affected zone
GMAW	gas metal arc welding
GTAW	gas tungsten arc welding
SMAW	shielded metal arc welding
SAW	submerged arc welding
FCAW	flux cored arc welding
t	time
T	temperature
C_H	hydrogen concentration in weld pool
S_H	solubility of Hydrogen in steel
P_{H_2}	partial pressure of hydrogen
I	emission line intensity
A	transition probability
g	statistical weight
k	Boltzmann's constant
λ	wavelength
N_n	number density of particles in state n
E_n	energy of atomic state n
h	Planck's constant
ν	frequency
B(T)	partition function for atoms
c	speed of light
R	Radiation
I^H_{REL}	relative intensity of the hydrogen emission line at 656.2 nm normalized to the intensity of the argon emission line at 696.5 nm

LIST OF FIGURES

LIST OF TABLES

l	diameter of weld plasma in the line of sight
A_s	area of spectrometer entrance slit
m	magnification of lens system
Ω_F	solid angle of weld plasma observed by spectrograph
V_p	photodiode output voltage
D	reciprocal dispersion of spectrograph grating
W	width of spectrometer entrance slit
$\Delta\lambda_s$	Stark width
C	diffusible hydrogen content of GMA weld made under nominally hydrogen free conditions
P_{cm}	hydrogen induced cracking susceptibility parameter

1. INTRODUCTION

1.1 Background

The one hundredth anniversary of the development of commercial welding processes occurred in 1985. Weld cracking problems have existed as long as welding has. It has been known for over 40 years that one of the primary causes of cracking in medium and high strength steel welds is the presence of diffusible, or atomic, hydrogen in the weld and heat affected zone (HAZ). Hydrogen induced cracking, also known as delayed or cold cracking because it occurs after the joint has cooled, occurs in steel when the following conditions are fulfilled: the existence of a susceptible weld metal or HAZ microstructure, the presence of tensile stresses, a sufficient quantity of diffusible hydrogen, and a temperature below 150°C. Common types of hydrogen induced cracks are depicted in Figure 1.1. Figures 1.2 and 1.3 show the appearance of cold cracks in weld metal and HAZ microstructures.

It is not difficult to show that conditions which cause hydrogen induced cracking often exist during welding. Hydrogen is introduced to the weld pool when moisture and organic contaminants in welding consumables, such as fluxes, filler wires and shielding gases, dissociate in the high temperature environment of the welding arc. The resulting atomic hydrogen is highly soluble in the molten weld pool and is absorbed rapidly. It is well known that shrinkage on solidification and transformation induced stresses produce tensile residual stresses around welds which approach the yield strength of the material.

Furthermore, the quenching effect of the cold plate around the molten weld pool produces high cooling rates in the HAZ. In many alloy steels, crack-susceptible, martensitic microstructures result. Since the operating temperature for most welded structures is in the susceptible regime, all the conditions for the occurrence of delayed cracking are fulfilled for many medium and high strength welded joints.

1.2 Objective

The objective of this study is to develop a method to predict the diffusible hydrogen content of a weld during processing and relate it to the susceptibility of the joint to hydrogen induced cracking. To accomplish this, three separate tasks were performed: (1) measurement of the amount of hydrogen present in the arc atmosphere during welding, (2) development of a model correlating the amount of hydrogen present during welding with the weld hydrogen content, and (3) determination of cracking susceptibility.

The first of these tasks was accomplished by the application of emission spectroscopy to the analysis of the composition of the welding arc. Light emitted by the welding arc was analyzed spectroscopically and the partial pressure of hydrogen in the welding arc determined. The second objective was completed by developing a model based on Sieverts' law to relate spectroscopic measurements of the hydrogen partial

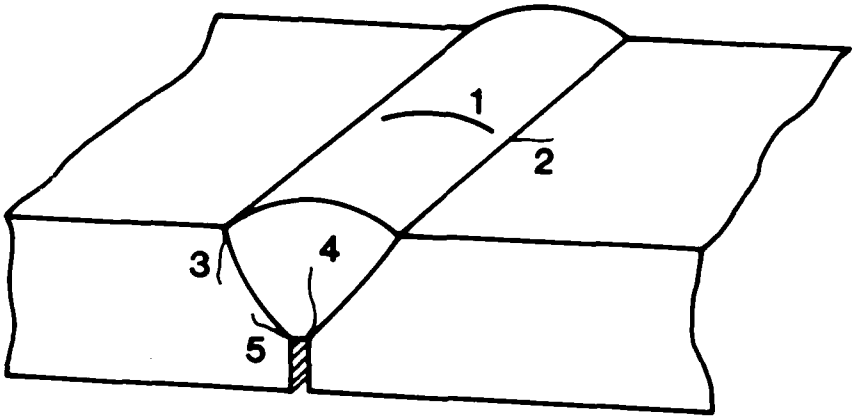

BUTT WELD

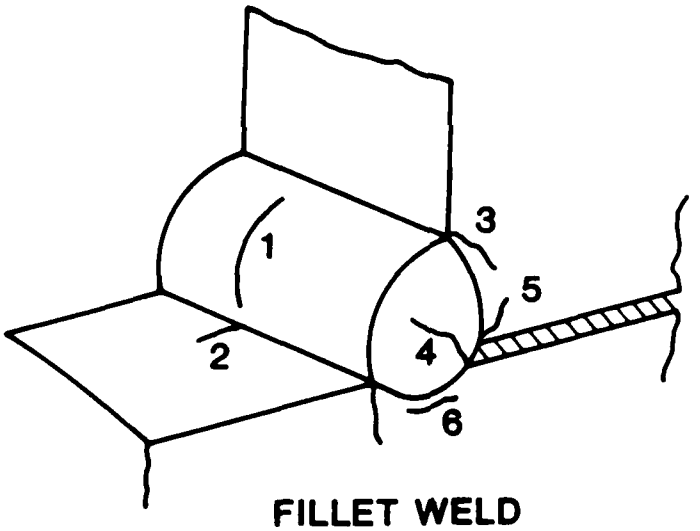

FILLET WELD

1 TRANSVERSE CRACK IN WELD METAL
2 TRANSVERSE CRACK IN HEAT AFFECTED ZONE
3 TOE CRACK
4 WELD METAL CRACK
5 ROOT CRACK
6 UNDERBEAD CRACK

Figure 1.1 Common types of hydrogen induced cracks in welds (after Graville).

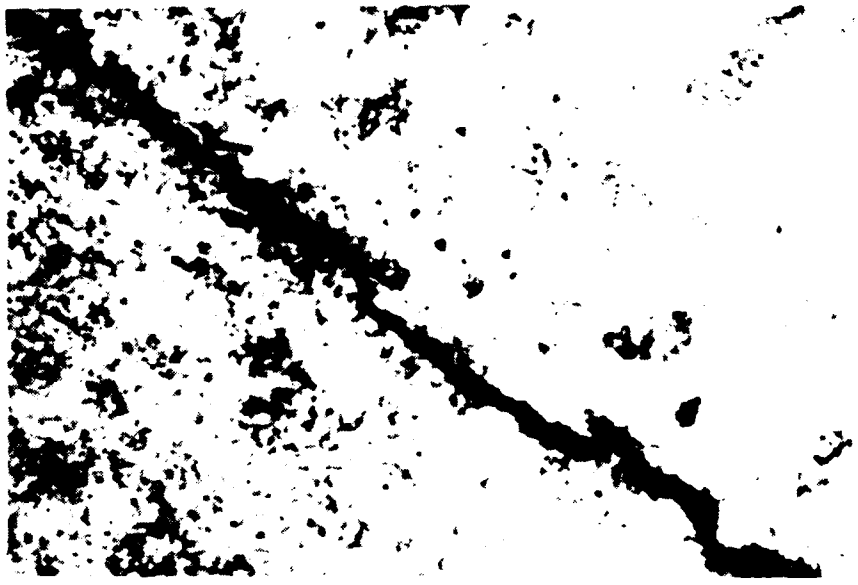

Figure 1.2 Appearance of hydrogen induced crack in weld heat affected zone (60X).

Figure 1.3 Appearance of hydrogen induced crack in weld metal (60x).

pressure in the weld arc atmosphere to the diffusible hydrogen content of the resulting weld. Implant tests were used to accomplish the third task. The implant rupture strength was used as an index of cracking susceptibility in the welding system involved in this study.

This report provides some background information on the problem of hydrogen cracking in medium and high strength steel welds and the use of emission spectroscopy in weld arc analysis. It describes the factors considered in selecting experimental techniques and predictive models. Experimental methods are given in detail and results reported. A predictive model for weld hydrogen content is developed and discussed and applied to the experimental data.

Susceptibility to hydrogen induced cracking is related to the amount of hydrogen present in a weld, and ways to use the experimental techniques employed to reduce cracking problems in production welds are suggested.

2. HYDROGEN IN WELDING

2.1 Background

Until the 1940's, cold cracking was thought to be due to multiaxial thermal and transformation stresses (which result from the welding process) acting on the brittle HAZ of the weld [1,2]. "Difficult" steels (those with higher carbon and alloying element contents and a higher susceptibility to cracking) were customarily welded using austenitic electrodes, although "oxidized ferritic" (low carbon, mild steel) electrodes were known to produce joints with a reduced tendency to crack [1]. In 1944, Hopkins [3] reported on a series of experiments performed to investigate the causes of cold cracking. He concluded that hydrogen embrittlement was the mechanism responsible for the delayed cracking. He further proposed that the source of hydrogen was the dissociation of hydrogen and hydrogen compounds present in electrode coatings to form atomic hydrogen, which is readily soluble in the weld pool. At approximately the same time, Herres [4] noted the influence of hydrogen in promoting underbead cracking. This hydrogen embrittlement mechanism for delayed cracking in welds was readily accepted, and a variety of papers were written describing sources of hydrogen in the welding arc, and absorption and diffusion of hydrogen in the welding arc [5-7]. However, as late as 1964, Makara and Mosendz concluded that the "hydrogen hypothesis" was "untenable" because no connection could be established between the weld metal composition and structure and the occurrence of cold cracking [8].

2.2 Hydrogen Sources in Welding

During the four decades since hydrogen was first recognized as the cause of delayed cracking in welds, a great deal of research has been devoted to welding. While some studies have indicated that the ambient atmosphere can be a significant source of hydrogen [9,10], due to air entrainment in the weld shielding gas, welding consumables are considered to be the primary source of hydrogen in the weld arc atmosphere [11]. The major influence on the hydrogen content of a weld is the welding process selected. Gas tungsten arc welding (GTAW) and gas metal arc welding (GMAW) have the lowest potentials for hydrogen pickup, while the flux-cored arc welding (FCAW) and submerged arc welding (SAW) processes will produce welds somewhat higher in hydrogen. Despite the development of low hydrogen electrodes, shielded metal arc welding (SMAW) is the process most likely to produce welds with a high hydrogen content (Figure 2.1).

2.2.1 Hydrogen Sources in Shielded Metal Arc Welding (SMAW)

In shielded metal arc welding (SMAW), the most important source of hydrogen is the electrode coating. In the case of cellulosic and rutile (TiO_2) based fluxes, this hydrogen is a part of the chemical formulation of the coating and cannot be eliminated. Low hydrogen electrodes (sometimes referred to as "basic electrodes") usually contain FeO, MnO, SiO_2 or CaF. Although hydrogen is not present in the combined form in these coatings nor generated by their decomposition in the welding arc, moisture may be absorbed by the flux binder (usually sodium

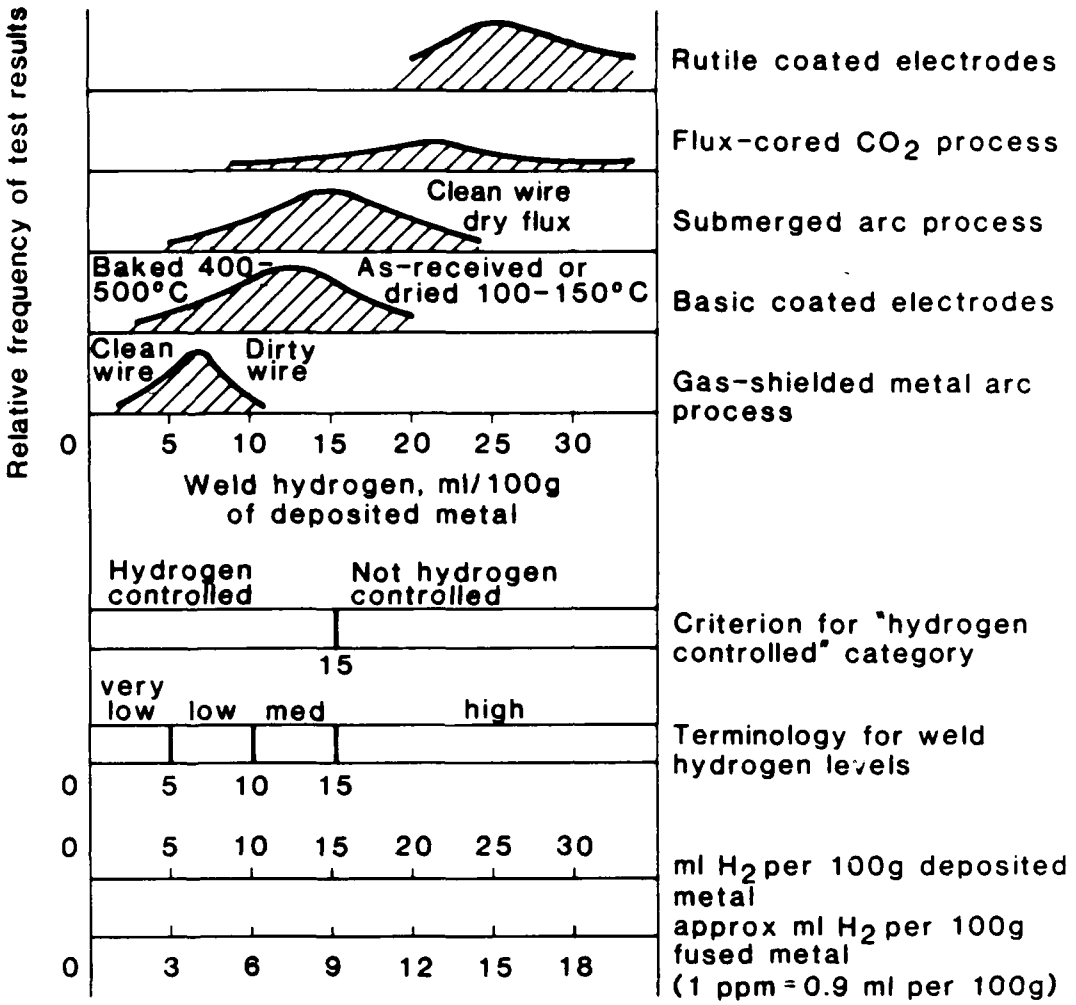

Figure 2.1 Characteristic hydrogen levels of various welding processes (after IIW).

silicate) when the electrodes are exposed to air. When low hydrogen electrodes are properly dried, stored, and used, very low weldment diffusible hydrogen contents [12] can be achieved. However, if such precautions are not taken, the hydrogen level in the weld may exceed that required to cause cracking in high strength steels.

Because of the cracking problems which result from moisture absorption by electrodes, their moisture absorption characteristics have been the subject of many studies [11,13-18]. It has been shown that moisture absorption is heavily influenced by the composition of the coating, density and particle size, as well as by the temperature and relative humidity to which it is exposed. Removal of absorbed moisture from electrode coatings has also been extensively studied and has been found to be controlled by the length of time and the temperature at which the electrodes are baked [13,15,16]. Test results indicate that electrodes should be baked at the highest temperature which will not damage their

shielding properties. There are two reasons for this. First, moisture loss is diffusion controlled, therefore moisture will be removed from the flux more rapidly at higher temperatures. Second, moisture in the coating may be either loosely bound in the form of water physically adsorbed or it can be tightly bound, as water combined with the silicate flux binder. Such water is far more difficult to remove than the more loosely bound moisture. Thus, some tightly bound water which would be removed from an electrode baked at 450°C, for example, might not be mobile if the same electrode was baked at 150°C [15]. At present, the most interesting research in the area of low hydrogen electrode coatings appears to be in the development of hydrophilic sol-gel coatings which would not absorb moisture if exposed to atmospheric humidity for long periods of time.

2.2.2 Hydrogen Sources in Other Arc Welding Processes

The flux coating on the electrode is the major source of hydrogen in manual welding, but in FCAW and SAW considerably less flux is consumed than in SMAW, while no flux at all is used in GTAW and GMAW. Thus the most important source of hydrogen in welding is either significantly reduced or completely eliminated in these processes.

GTAW and GMAW, particularly the former, are very clean welding processes; most data indicate that weld hydrogen contents of 8 ppm or less can be expected without special precautions [12]. The presence of hydrogen in these processes is due to organic compounds found on filler wire [19,20]. Lubricants used in wire drawing are often not completely removed when the wire is cleaned following drawing, and it is the dissociation of the lubricant remaining on the wire during welding which is the major source of hydrogen in GMAW and GTAW.

Although the FCAW process was originally considered an intrinsically low hydrogen welding process, research has shown that weld metal hydrogen contents in the neighborhood of 10 to 14 ml H_2/100 g deposited weld metal can be expected [12,21]. This is within the International Institute for Welding (IIW) specified limits for "controlled hydrogen" welding processes [12] but is more than enough hydrogen to induce cracking in most medium and high strength steels. In FCAW, the hydrogen source may be drawing lubricants as in the case of GTAW and GMAW, or it may originate in the flux core. It was initially believed that exposure to the atmosphere would not affect the moisture content of the flux core of the wires. However, recent work has shown that some moisture absorption may occur [21].

The other sources of hydrogen in welding are relatively minor and are easily recognized and removed. Rust, primer, paint, and grease on plates to be welded are all potential sources of hydrogen which can be avoided if proper cleaning procedures are used. Water vapor may contaminate shielding gas used in the gas shielded processes or may be present in gas lines. Interrante, et al. [14], noted that plates should be preheated to above the dew point of the ambient air when welding susceptible steels to prevent moisture condensation which might lead to

cracking. Most welding procedures for high strength steels require preheating of all joints prior to welding to increase cooling times and reduce HAZ hardness.

2.3 Diffusion of Hydrogen in Welds

2.3.1 Hydrogen Diffusion in Steel

The diffusion of interstitial hydrogen in steel is governed by classical Fick's law behavior, where

$$\frac{\partial C}{\partial t} = \frac{\partial}{\partial x} D\left(\frac{\partial C}{\partial x}\right) \qquad (2.1)$$

and

$$D = D_o \exp(-Q/kT) \qquad (2.2)$$

Here C is the concentration of hydrogen, t is time, x is distance, D is the diffusivity of hydrogen in steel, D_o is the diffusion coefficient for hydrogen, Q is the activation energy for diffusion, T is temperature, and k is Boltzmann's constant.

The exact solution to equation (2.1) is a function of the error function of $X/2(Dt)^{\frac{1}{2}}$. However, simple order of magnitude calculations can be made using the expression

$$X^2 = 4\ Dt \qquad (2.3)$$

to relate the diffusion coefficient, D, to the time, t, required for hydrogen diffusion across an average distance, X [22].

2.3.2 Hydrogen Diffusion in Welds

During welding, the atomic hydrogen present in the welding arc is absorbed by the molten weld pool in which hydrogen is extremely soluble. Upon solidification, and during the austenite to ferrite transformation, a considerable decrease in the solubility of hydrogen in steel occurs. As a result, a concentration gradient exists to drive the diffusion of hydrogen into the crack susceptible HAZ during the cooling of the weld.

Equation (2.3) can be used to show that hydrogen is capable of diffusing well into the HAZ of a weld as it cools to ambient temperature. Coe [23] gives D an average value of 10^{-4} cm $^{-2}$ sec^{-1} during cooling, and three minutes is a reasonable approximation of the time required for a typical gas metal arc weld to cool to room temperature. According to equation (2.3), hydrogen will diffuse an average distance of 0.135 cm in three minutes. Although the size of the HAZ is also dependent on the welding parameters and base plate conditions, the HAZ dimensions of GMA welds are typically 0.1 to 0.5 cm.

Equation (2.2) shows that D decreases as the temperature of the joint decreases, hence the rate of hydrogen diffusion from the weld into the HAZ also decreases. At about 150°C, Q, the activation energy for

hydrogen diffusion, begins to increase as temperature decreases, and the value of D decreases rapidly. As a result, the mobility of the hydrogen which diffused into the HAZ immediately after welding is greatly reduced, and it can no longer diffuse out the joint rapidly. Although hydrogen continues to diffuse out of the joing at a reduced rate, removal of the remaining hydrogen occurs over a period of hours or days; during this time the weld is susceptible to hydrogen induced cracking.

Classical diffusion theory has also been useful in developing procedures to prevent hydrogen induced cracking, as well as in describing the kinetics of hydrogen diffusion to the HAZ. Several workers [22-25] have used measurements of the diffusivity of hydrogen in steel to design post-weld heat treatments which prevent delayed cracking by allowing hydrogen sufficient time to diffuse out of the joint prior to cooling below 150°C.

2.4 Prediction of the Diffusible Hydrogen Content of Welds

One of the objectives of this study is to develop a technique for making real time determination of the diffusible hydrogen contents of gas metal arc welds. Despite the extensive literature concerning hydrogen in welds, relatively few workers have attempted to predict the hydrogen content of welds. The approaches taken to solving this problem can generally be broken down into two categories: (1) development of empirical relationships between the hydrogen content ot welds and the hydrogen content of the welding consumables used, and (2) correlation of the weld hydrogen content with the partial pressure of hydrogen present in the weld arc atmosphere during welding.

2.4.1 Empirical Techniques

In the first approach, various methods are used to determine the hydrogen content of the consumables. Most commonly, this approach is used to estimate the hydrogen content of SMA welds by relating the moisture content of the electrode coating to the hydrogen content of the weld. Electrodes are usually heated to a temperature between 400°C and 1200°C and the amount of moisture driven off is measured. Encapsulation [19] is another technique which can be used to determine the hydrogen content of electrode coatings or to determine the amount of hydrogen present on other consumables. A small sample of the material is placed in a sealed mild steel container and heated to 700°C or 1000°C. Since hydrogen diffuses through mild steel readily at these temperatures, the amount of hydrogen present can be determined by collecting and measuring the amount of gas given off.

Although it is simple to determine the amount of hydrogen present in consumables experimentally, it is not clear that any specific relationship exists between the "hydrogen potential" of the consumables determined in this way and the hydrogen content of the weld. It was noted by Christensen [26] that additional moisture in some electrode coatings may actually reduce the partial pressure of hydrogen in the weld arc atmosphere and the amount of moisture absorbed by the molten

pool during welding. It has also been observed that coating composition, density, and particle size, in addition to the temperature and relative humidity at which moisture is absorbed, affect the amount of hydrogen transferred to the welding arc [15]. Electrode gauge also affects weld hydrogen content with small gauge electrodes resulting in lower weld hydrogen levels [9].

Despite the hazy nature of the relationship between the hydrogen content of welding consumables and the hydrogen content of the weld produced with them, several investigators have attempted to establish correlations. Chew [27] found that weld hydrogen contents increased with increasing electrode coating moisture, but the rate at which diffusible hydrogen increased varied widely from electrode to electrode. He concluded that "reliable hydrogen control can best be achieved through direct specification of weld hydrogen." Coe [19] could not establish any direct relationship between the results of potential hydrogen measurements and weld hydrogen content either. Evans and Weyland [28] state flatly that there is no generally valid relationship between coating moisture content and the amount of diffusible hydrogen present in a weld. Hirai, et al. [29] attempted to establish a relationship between electrode, moisture content and weld hydrogen levels using Sieverts' law. Although predicted and actual values agree reasonably well, there are four experimentally determined constants in the expression developed in this work which vary from electrode to electrode requiring extensive testing for each type of consumable used.

2.4.2 Methods Based on Sieverts' Law

Sieverts' law is also used in the second common approach to prediction of weld hydrogen levels. Sieverts [30] observed that

$$C_H = S_H(P_{H_2})^{1/2} \qquad (2.4)$$

where C_H is the concentration of hydrogen in steel, S_H is the solubility of hydrogen in steel at the temperature of the molten material, and P_{H_2} is the partial pressure of hydrogen in the atmosphere above the molten steel. In the case of welding, it is the partial pressure of hydrogen in the weld arc atmosphere, the solubility of hydrogen at the temperature of the weld pool, and the diffusible hydrogen content of the weld which are of interest. Predictive models based on Sieverts' law generally produce better correlation between theoretical and measured values of weld hydrogen contents than empirical techniques based on "potential hydrogen" measurements.

In the first such study, conducted by Mallett in 1946 [7], the composition of the gas collected during welding in a closed, evacuated chamber was analyzed. Sieverts' law was used to predict the hydrogen content of the resulting welds from the partial pressure of hydrogen in the arc atmosphere determined in this way. In this study, excellent agreement between the predicted and actual values for weld hydrogen content was found. In further testing, Mallet and Rieppel [31] obtained similar results. In studies of underwater welds, Arata, et al. [32] found that a Sieverts' law expression modified to include a baseline

hydrogen content adequately predicted hydrogen contents of GTA welds. In another investigation, Sieverts' law was used to correlate the diffusible hydrogen content of pulsed GMA welds with the amount of hydrogen added to the shielding gas during their fabrication. Although the authors [33] note that the temperature of the weld pool (and hence the hydrogen solubility S_H) was selected to give a good fit to the data, the results demonstrated the dependence of weld diffusible hydrogen content on the partial pressure of hydrogen in the welding arc.

Aristov, et al. [10], also noted the dependence of the diffusible hydrogen content of welds on the partial pressure of hydrogen in the weld arc atmosphere, although he proposed an empirical relationship between log P_{H_2} and log C_H. Chew [27] proposed an expression using the partial pressure of hydrogen and the activity of dissolved hydrogen similar to that of Hirai et al. [29], which yielded good results when appropriate values for weld pool temperature were assumed. In an extensive study, Salter, Milner, and Howden found Sieverts' law applied to hydrogen absorption behavior in the weld pool [34,35] during arc melting of metal button samples and bead on plate welding.

2.5 Measurement of the Hydrogen Content of Welds

It is useful to be able to distinguish between the weld hydrogen levels produced by various welding processes in order to know the amount of hydrogen required to induce weld cracking in certain materials, or to be able to perform weld hydrogen content determinations for quality control purposes. In addition, such a technique is needed to determine the validity of predictions of weld hydrogen contents. Therefore, it is necessary to have a reproducible test to measure the amount of diffusible hydrogen in a weld.

Many procedures have been used for measuring weld hydrogen contents. These can generally be separated into one of two categories; carrier gas methods and immersion methods. In the former, specimens are permitted to outgas in some carrier gas, usually argon or nitrogen, and the resulting gas mixture is tested for hydrogen content. In the immersion methods, a specimen is allowed to outgas under some liquid and the gas which evolves (all of which is assumed to be hydrogen) is collected and measured in a eudiometer over the immersing fluid. In either procedure, data is normalized to standard temperature and pressure, and expressed in terms of mL H_2/100 g deposited weld metal. In some countries, the H_2 content is expressed in terms of mL H_2/100 g fused metal. The former method is the international standard, however.

2.5.1 Immersion Methods for Measuring Weld Hydrogen Content

Immersion methods are common because they are relatively cheap and simple. Using mercury as the immersing fluid provides the most accurate and reproducible results [36]. Glycerin, however, is more often used in the United States and Japan because of the health hazards associated with mercury. Water [34], alcohol [37], and silicone oil [33] have also been used in this application.

Whatever the collecting fluid, the sampling procedure used is essentially the same. A sample which varies in size from one standard procedure to another is placed between run-on and run-off tabs and the assembly is clamped in a copper chill block. A weld bead is laid over the test pieces and immersed in a dry ice and alcohol bath (or other low temperature bath). The run-on and run-off tabs are then removed and the specimen is stored in liquid nitrogen until the hydrogen analysis is to be performed. Prior to immersion, the specimen is cleaned to remove all traces of moisture (the solvent varies with the procedure followed) and dried in a blast of dry gas, usually argon or nitrogen. The specimen is then placed under the collecting fluid for a specified period of time at a specified temperature. Both immersion time and temperature vary depending on procedure. In the IIW mercury method, the specimen is immersed at room temperature for three days; the Japanese glycerin method calls for immersion of the specimen at 45°C for two days. Ball, et al. [33], proposed outgassing at 100°C under silicone oil for 90 minutes.

Clearly, with so much variation in experimental procedures, some variation can also be expected in experimental results. In fact, variations of 50 to 100 percent have been found in measurements made from one laboratory to another [38]. This is true of both the mercury and the glycerin method, although the IIW/ISO (International Standards Orangaization) mercury method is widely considered to be the most accurate and reproducible immersion test for diffusible hydrogen content. Boniszewski and Morris [38], in reporting the results of tests performed to determine the reliability of the mercury immersion method, concluded that the reliability of the procedure is inadequate and recommended that gas chromatography (one of the carrier gas methods) be used instead. Other investigators have also reported unacceptable levels of variation between laboratories in diffusible hydrogen measurements made using the mercury method [36,39].

If some uncertainties exist about the accuracy and reproducibility of the mercury test, even greater concern must be expressed about the glycerin test. It has been recognized for years that a certain amount of hydrogen is lost during the glycerin test because hydrogen is soluble in glycerin. A correction factor of the form

$$H_{glyc} = 0.79 \times H_{Hg} - 1.73 \qquad (2.5)$$

is used to calibrate glycerin test results to those of the IIW mercury method [40]. Recent studies, however, have indicated that the problems with the glycerin test are severe and include not only the solution of outgassed hydrogen by the collecting fluid, but also gas exchange in the fluid. Quintana [41] reported hydrogen contents as low as 49 percent when the composition of the gas collected over glycerin was analyzed. Other collecting fluids such as silicone oil fared even worse when similar analyses were performed.

2.5.2 Carrier Gas Methods for Measurement of Weld Hydrogen Contents

The immersion methods for measurement of weld hydrogen are time consuming, and it is not possible to guarantee accurate and reproducible results. As a result, carrier gas methods, particularly gas chromatography, are rapidly becoming more popular for measuring the diffusible hydrogen in welds, despite their considerably higher initial cost. Another reason for the popularity of gas chromatography is time; procedures exist to measure the diffusible hydrogen content, H_{diff}, of a weld in as little as ten minutes [40].

No specific standard yet exists for the use of gas chromatography in this application. A variety of procedures have been proposed, however, and the American Welding Society has generated a draft standard [41]. Initially, specimen preparation is similar to that used in the immersion methods; i.e. a specimen is welded, quenched, cleaned, and dried in a blast of dry gas. However, specimens are then outgassed in a carrier gas stream with continuous measurement of the hydrogen evolved by the specimen [40] or in a closed chamber containing an inert gas and some internal standard. In the latter case, the contents of the chamber are sampled following outgassing and the amount of hydrogen present determined [41,42]. The second procedure has the advantage of allowing multiple samples to be obtained for increased accuracy, while the former procedure can be performed more rapidly and may be more suitable for large scale testing under production conditions.

Outgassing of the specimens may be performed at any temperature below approximately 600°C; at 650°C the residual, molecular hydrogen in the weld becomes mobile, and while this is usually a very small quantity, the accuracy of the test is reduced. Pokhodnya and Palt'sevich [43] report outgassing in a carrier gas stream at 140 to 150°C, while other workers report outgassing temperatures ranging from 100°C to 400°C [40,41]. Yanaco markets a system in which outgassing takes place at 5°C for three days, thus sacrificing the timesaving feature of the method.

2.6 Mechanical Tests for Susceptibility to Hydrogen Induced Cracking

Although tensile stresses acting on a susceptible microstructure are known to be among the conditions required for hydrogen induced cracking of a weld to occur, the susceptibility of the weld and HAZ microstructures (as well as the magnitude of the residual stresses) are dependent on the weld process parameters, and base plate and filler wire composition. Therefore, knowledge of a weld's hydrogen content alone does not provide sufficient information to determine whether hydrogen induced cracking is likely. In addition, the experimental conditions used to ensure uniform specimen preparation in tests to determine the hydrogen content of a weld are not representative of the thermal history undergone by a production joint; they reflect a maximum possible weld hydrogen content rather than the actual hydrogen content of a weld as manufactured. Hence, mechanical tests must be performed on various welding procedures to determine the susceptibility of the welding system to hydrogen induced cracking in conjunction with tests for weld hydrogen content. Such tests provide a means of estimating safe levels of hydrogen for specific welding procedures.

A myriad of tests has been devised for this purpose [22]. These tests can be separated into two categories: those in which an external load is applied, and those in which the the tensile stresses are produced by the shrinkage stresses resulting from weld solidification and a highly restrained joint geometry. Both types have advantages; for example, the reproducibility of results is enhanced in externally loaded tests [22] while self-restrained tests may more closely simulate service conditions.

2.6.1 Self-Restrained Cracking Tests

The Lehigh and Tekken tests are two very similar self-restrained butt weld tests (Figures 2.2 and 2.3). The level of restraint may be varied by adjusting the test geometry slightly. These tests have been used extensively to evaluate HAZ cracking susceptibility and can be modified to allow testing of the weld metal.

Two well known self-restraining tests, the controlled thermal severity (CTS) and cruciform tests, are often used to evaluate underbead cracking susceptibility. The CTS test (Figure 2.4) is complicated and most suitable for evaluating cooling rate effects on susceptibility to cracking. The cruciform test (Figure 2.5) is particularly sensitive to the exact welding conditions used, which has caused difficulties in interpretation of test results [24].

2.6.2 Externally Loaded Cracking Susceptibility Tests

Reproducibility is the most difficult problem to overcome in testing for hydrogen induced cracking of welds. Since slight variations in processing parameters can cause changes in weld cooling rates, and thus in weld microstructure, hydrogen content, and residual stress level, welding conditions must be very closely controlled. Enhanced reproducibility is one of the advantages of externally loaded weldability tests because restraint levels are not entirely dependent on joint geometry and welding parameters.

The implant test is a versatile, externally loaded weldability test developed in the mid-1960's by Granjon [44]. A notched, cylindrical specimen is implanted in a support plate containing a circular hole, and a weld bead is laid over the specimen and plate assembly as shown in Figure 2.6.

The specimen may contain a circumferential or a helical notch. If the former specimen is used, welding parameters must be selected to ensure that the notched portion of the specimen is in the HAZ where hydrogen induced cracks usually occur. If a helically notched specimen is used, the notch will always be located in the HAZ. The test piece may be allowed to cool to ambient temperature naturally, or it may be quenched or subjected to some post-weld heat treatment. Following specimen fabrication, a tensile load is applied to the implant and the load required to produce rupture or crack initiation within a specified period of time is determined.

The implant test is useful in a variety of applications, including dissimilar metals weldability testing, measurement of thermal histories, and plate thickness effects [43]. Recently it has been widely used in evaluating the susceptibility of welds to hydrogen assisted cracking. The effect of weld microstructure, hydrogen content, and pre- and post-weld heat treatments on cold cracking susceptibility have been studied in this way [45] in a major study. A linear relationship was observed between the implant rupture strength and the logarithm of the weld diffusible hydrogen content as measured using the standard IIW procedure. Externally loaded tests such as the implant test are useful not only because of the improved reproducibility of their results, but also because knowledge of the applied load permits development of such relationships which may be of value in the design process.

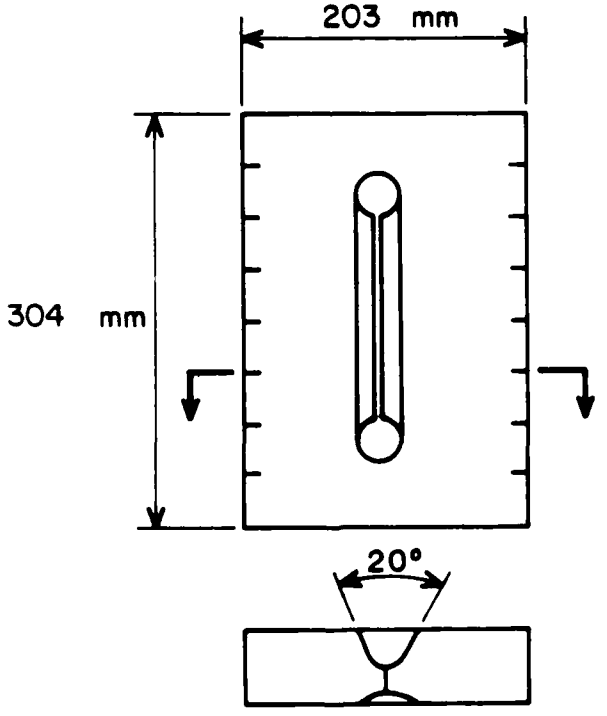

Figure 2.2 Lehigh test geometry.

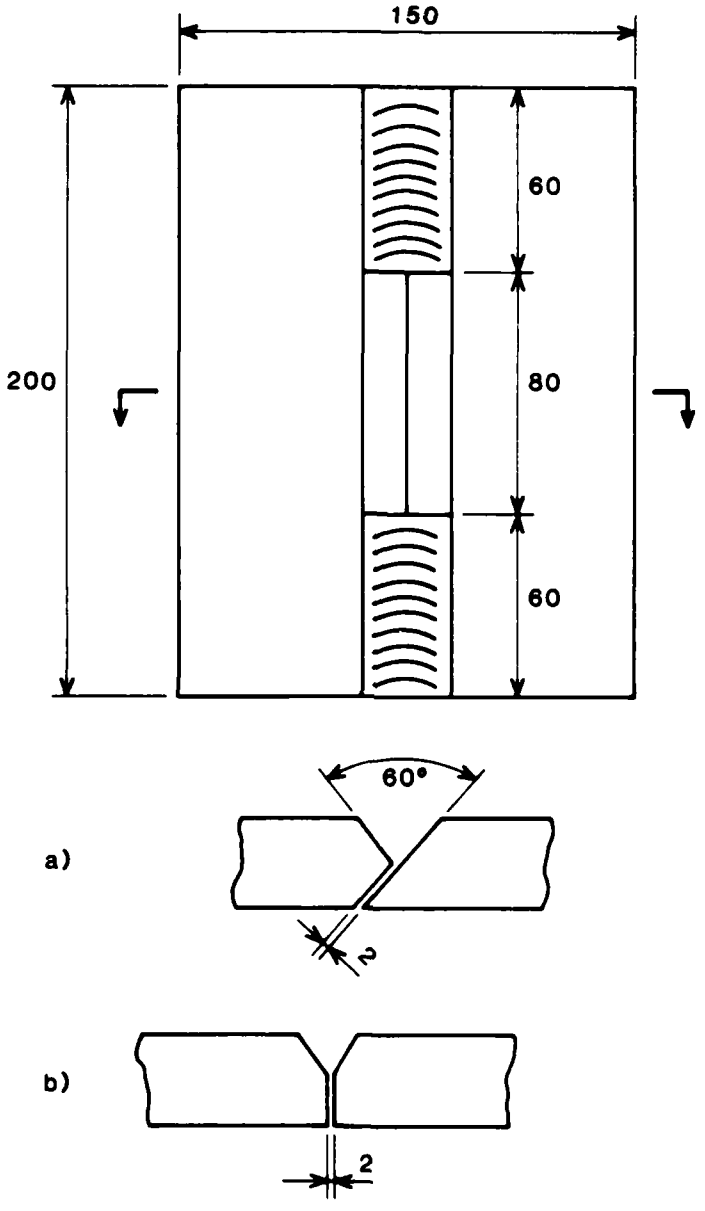

ALL DIMENSIONS IN mm

Figure 2.3 Tekken test geometry.
(a) Geometry of underbead cracking test.
(b) Geometry of weld metal cracking test.

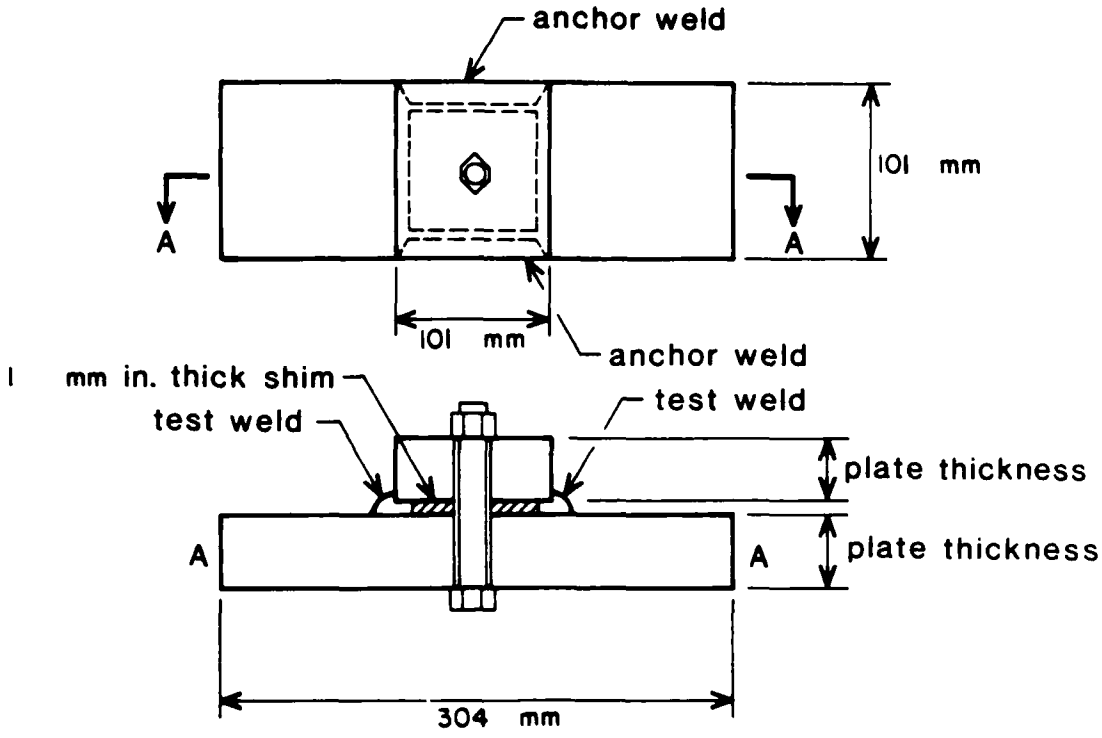

Figure 2.4 Controlled thermal severity test geometry.

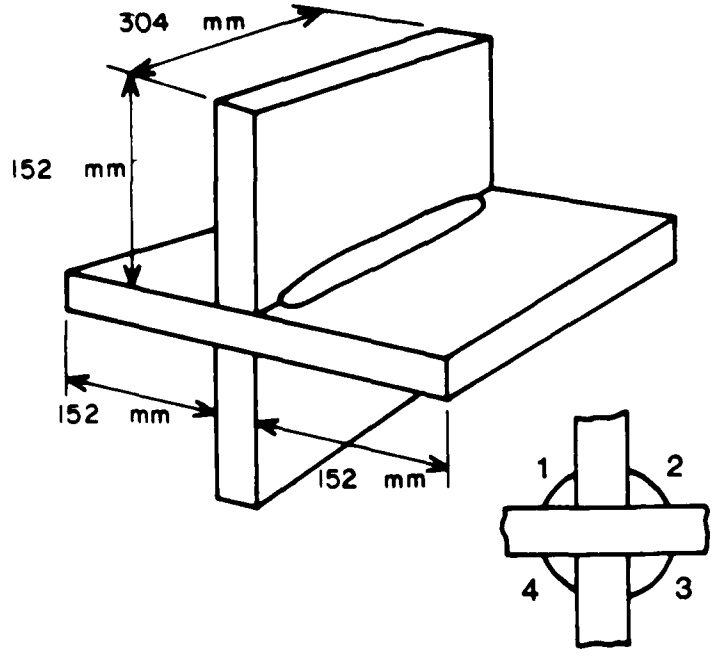

Figure 2.5 Cruciform test geometry.

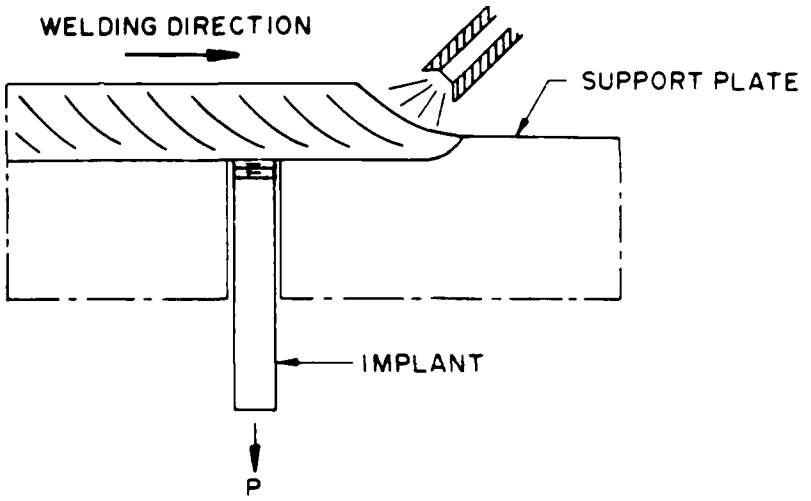

Figure 2.6 Implant test geometry.

2.7 Summary

The sources of diffusible hydrogen in welds have been considered, and the results of some previous investigations into hydrogen induced cracking have been reviewed. Various techniques for the experimental determination of weld hydrogen contents and susceptibility to hydrogen induced cracking have been discussed. Models which have been developed to predict the hydrogen content of welds have been evaluated.

Based on this review, gas chromatography and implant testing were the test methods selected for characterizing the hydrogen content of welded joints and their susceptibility to hydrogen induced cracking. Sieverts' law based methods were found to provide good agreement between predicted and measured values of weld hydrogen. However, all of the studies cited depended on cumbersome, post-weld methods for analyzing the hydrogen content of the weld arc atmosphere, or on indirect methods such as measurement of electrode moisture contents. A more desirable procedure would be to measure the partial pressure of hydrogen present in the arc during welding and use the information to predict the resulting weld hydrogen content during processing. The use of emission spectroscopy in this application will be discussed in the next chapter.

3. SPECTROSCOPIC ANALYSIS OF WELD ARC PLASMAS

3.1 Analytical Spectroscopy

The high temperature of a welding arc is an obvious impediment to in process determination of weld arc atmosphere composition and thus to prediction of weld hydrogen contents and cracking susceptibility. Analytical equipment must be remotely sited or capable of withstanding temperatures of 10,000°K or more. The intensity of the light produced during arc welding makes spectroscopy an attractive technique; an optical sensor may be distant from the arc and, using appropriate analytical techniques, plasma compositions may be determined.

Spectroscopy is the study of transitions of a system (in this case, atomic transitions) between energy states [46]. In atomic emission spectroscopy, the investigator is concerned with spectra generated by electron transitions between quantized energy levels in states of the outer electron shells of atoms. Although the quantum physics required to explain many phenomena which can be studied spectroscopically is extremely complex, optical spectroscopy originated over 200 years ago and is today a principal analytical technique used to determine the composition of a variety of substances. There are two major spectroscopic techniques in optical spectroscopy for observing orbital electron transitions: emission spectroscopy and absorption spectroscopy.

3.1.1 Emission and Absorption Spectroscopy

Electromagnetic radiation is emitted at discrete frequencies (wavelengths) in the visible and ultraviolet region by atoms, which have been excited to energy levels above the ground state, as they return to their normal energy state. This radiation generates specific arrays of lines in a spectral display on which analytical measurements are made in atomic emission spectroscopy. This is accomplished by collimating the light from the emitting source through a small slit and passing it through a prism or grating. The optical system breaks the light up into its wavelength spectrum which, unlike the blackbody radiation of high temperature solid surfaces, is concentrated at discrete wavelengths. Because the emission spectrum of each atomic species is unique, atomic emission spectroscopy provides an absolute means of identifying approximately 60 elements in the periodic table, including gases commonly used in welding.

Atomic species in the gaseous phase also possess unique absorption characteristics. If a cell containing a monatomic gas of interest is placed between a blackbody emitter and a prism or diffraction grating, continuous light will be observed at all wavelengths except at the discrete wavelengths at which the light has been absorbed by the atoms of the gas cell. These wavelengths will be characteristic of the gaseous species contained in the cell and can be used in analyzing its composition. Although every absorption line has a corresponding emission line, the reverse is not necessarily true. Because the atoms of interest in the gas cell will normally exist initially only in the ground state, n = 1, only transitions from the state where n = 1 to the state

where $n > 1$ can occur, unless the atoms of the absorbing gas are excited, as occurs, for example, in stellar atmospheres. Therefore, many lines found in emission spectroscopy, where excited atoms are observed, will not be present when absorption techniques are employed.

3.1.2 Plasma Diagnostics

Plasma diagnostics is the study of the properties of plasmas through experimental spectroscopy [47]. Plasmas are usually luminous, so that emission spectroscopy becomes important in their study. The shape and intensity of lines and the characteristics of the continuous spectra are the major considerations. Radiation is also commonly used for investigation of plasma properties, for example, absorption of laser radiation by plasmas has been used with success in plasma evaluation, including weld plasmas [48]. In this study, emission spectroscopy was the diagnostic tool used to study the weld arc plasma.

In the gas tungsten and gas metal arc welding processes, a high current electric discharge is passed through a region containing a gas or mixture of gases. Although there is no confining vessel, the result is similar to that obtained when a discharge tube is used in a plasma physics experiment. Collisions occur between the atoms of the gas and between atoms and electrons, a plasma is formed, and many of the atoms are excited to levels above their ground state. As the atoms return to their normal energy state, electromagnetic radiation is emitted. As a result, emission spectroscopy is an attractive tool for studying the composition of the weld arc plasma. It is also useful in determining other physical properties of the plasma, such as temperature, which can be measured using spectroscopic diagnostic techniques.

3.2 Application of Plasma Diagnostics to Welding

3.2.1 Temperature Measurements

A number of researchers have used spectroscopic diagnostic techniques to study the welding arc. The most common use of spectroscopy in this application is measurement of weld arc temperatures. Several investigators have conducted studies using a technique known as the two-line method to determine the temperature of the weld arc plasma. Unfortunately, errors can be extremely large in this procedure [47] if proper precautions are not taken, so that there is a great deal of variation in the reported values. For example, Kobayashi and Suga [49] measured temperatures of 15,000°K in the central part of the arc, while a maximum temperature of 11,000°K was reported by Glickstein [50]. Ludwig [51] observed temperatures of 16,000°K in the center of the arc, with temperatures of 10,000°K near the arc boundary, while Key, et al. [52], in measurements made on a higher current arc, measured temperatures of only 12,000°K at the center of the arc. The temperatures reported above were measured using the two-line method, with argon as the species used in making the determinations. Mills [53] did not report any measured temperature values, but suggested that manganese (Mn) lines could also be used in this capacity, and proposed the Mn I lines located at 534.1 and 537.7 nm for this application.

Obviously, considerable variation is found in the results of the differing investigations. To a certain extent, these variations are inherent in the approach used. The two-line method is a relative intensity technique in which the following equation is used to evaluate temperature.

$$\frac{I_1}{I_2} = \frac{A_1 g_1 \lambda_2 N_1 B_2 (T)}{A_2 g_2 \lambda_1 N_2 B_1 (T)} (\exp -(E_1 - E_2)/kT) \quad (3.2.1)$$

where I_1 and I_2 are the measured intensities of the lines used, A_1 and A_2 are transition probabilities, and g_1 and g_2 are the statistical weights.

It is clear that when the values of the constants and line intensity are substituted into this equation, it may be readily solved for temperature. However, line selection must be made very carefully as line intensity varies differently with these parameters. In each of the investigations cited, a different pair of lines was used to evaluate temperature, and reported results vary widely around an average value.

This highlights the fact that line selection for spectroscopic measurements on weld arc plasmas is critical and must be made carefully to ensure accurate results. Some of the factors which must be considered include using lines having the same degree of ionization and ensuring that there is a sufficiently wide energy gap between the pairs of lines used. The possibility of self-absorption by the plasma at the wavelength employed must also be considered.

3.2.2 Plasma Composition Analysis

One of the objectives of this study is to measure the partial pressure of hydrogen in a weld arc plasma. Emission line intensities are commonly used to determine plasma compositions, and while spectroscopy has not often been used in analyzing weld arc plasma, Vinogradov, et al. [54], reported that weld arc chromium (Cr) concentration, in the welding of copper to 18-8 stainless steel, could be correlated with Cr line intensities measured using a narrow pass band filter and a photoresistor. These workers also investigated the dependence of spectral line intensity, as measured in this way, on welding current and arc gap.

Despite the relatively small number of studies carried out using the technique, emission spectroscopy has proven to be a powerful tool for investigating the composition of the weld arc atmosphere and its effect on weld quality. The spectroscopic technique used in this investigation has been capable of detecting loss of shield gas [55], gaps in the flux shielding in flux cored arc welding wire, and the presence of hydrogen in the welding arc [56]. It has also been used successfully to analyze laser welding plasmas [57]. The objective of this study was to use emission spectroscopy to measure the partial pressure of hydrogen in the welding arc. These measurements were used to predict the diffusible hydrogen content of welds.

3.3 Application of Spectroscopic Techniques to Weld Plasma Hydrogen Determination

Spectroscopic measurements of several kinds can be made for different analytical purposes. In determining plasma composition, measurements of the intensity of emission lines characteristic of the element or elements of interest are most useful. Generally, there are two types of line intensity measurements used in analytical spectroscopy: relative intensity and absolute intensity. In relative intensity measurements, use is made of the relationships existing between the intensities of spectral lines when the state densities of the atomic species are in equilibrium. This requires an assumption of local thermodynamic equilibrium; this assumption is generally accurate for the weld arc plasma except very close to the anode [50]. In absolute intensity measurements, the optical system being used to make intensity determinations is calibrated to a National Bureau of Standards (NBS) calibrated, blackbody absolute intensity standard, to take into account the efficiency of the various components of the system. Once the initial calibration is performed, elemental emission line intensities are used to determine the number densities of particles in the various energy states.

Relative intensity measurements are the basis for quantitative spectral analysis; indeed much of the research in analytical spectroscopy has been focused on performing chemical analyses. In weld arc spectroscopy, relative intensity (internal standard) techniques have several advantages. For example, changes in the intensity of the line of interest caused by temporary variations in process parameters, rather than changes in the concentration of the analyte element, are normalized and do not incur false readings. The same is true when a loss of observed intensity occurs due to smoke particles in the optical path. While such systematic errors are eliminated, analysis of data must be performed by comparison to an empirical analytical curve generated by previous runs using weld plasmas of a series of known concentrations of the analyte element. However, it is difficult to produce a standard weld arc plasma, so errors in standard preparation are likely, and are reflected in the accuracy of results.

Absolute intensity measurements, calibrated to a blackbody with a known radiance, may theoretically minimize the need for an empirical standard, but in practice they have other shortcomings in diagnostic term due to the nonsteady state nature of welding plasmas. The population density of a species of particle can be determined from absolute intensity measurements. However, particle density may fluctuate widely over short periods of time when arc instabilities occur. It is, therefore, necessary to average values over a period of time or to integrate emission line intensity values over a long data acquisition period.

In this study, both absolute and relative intensity measurements were used to measure hydrogen concentrations in welding arcs as described in the following sections. However, different data reduction

procedures were used. In using relative intensity data, hydrogen emission line intensity at 656.2 nm, normalized to argon emission line intensity at 696.5 nm, was correlated with the relative hydrogen line intensity found in weld plasmas containing a known partial pressure of hydrogen. Absolute line intensities were used to calculate hydrogen ion density, and hydrogen partial pressure was evaluated by comparison with the total electron density (i.e., total atom density) of the plasma. In both cases, arc hydrogen partial pressure was used to predict the diffusible hydrogen content of resulting welds.

3.4 Relative Intensity Approach

3.4.1 Theory

It was noted in the previous section that the "two-line method" can be used to measure plasma temperature. This procedure makes use of the fact that population densities of particles in various excited states are proportional to the products of their statistical weights with the exponentials of the negative ratios of excitation energy and the thermal energy, kT, of the plasma. Because of the dependence on particle population as well as temperature, a two-line technique can also be used to estimate plasma composition [56]. Except very close to the anode, the weld arc plasma can be considered to be in a state of local thermodynamic equilibrium, with the excitation levels in the plasma having a Boltzmann distribution. Therefore,

$$N_n = g_n \exp\left(-\frac{E_n}{kT}\right) \qquad (3.4.1)$$

where E_n is the energy of an atomic state, g_n is the number of substrate having energy E_n, k is the Boltzmann constant, T is the plasma temperature, and N_n is the population density in state n. It is known that the optical energy emitted by an atom making a transition from state m to state n is

$$N_m A_{mn} \Delta v \qquad (3.4.2)$$

for a small volume of plasma, Δv, with a transition probability of A_{mn}. The intensity of a given spectral line is proportional to the atom population density. Therefore, the intensity of the line produced by the m to n transition can be expressed as

$$I_{nm} = A_{nm} h\nu_{nm} N_n \qquad (3.4.3)$$

Integrating over the entire volume of the plasma, the following expression is obtained

$$I_{nm} = \frac{1}{4\pi} A_{nm} \frac{hc}{\lambda_{nm}} N_n \qquad (3.4.4)$$

This allows the calculation of the total intensity of light emitted at a given wavelength. However, it is clear that any change in the temperature or volume of the plasma will result in corresponding alterations in the observed intensity of light produced.

Unfortunately, welding arcs are commonly subject to just such variations in plasma temperature and volume, due to changes in process parameters or random fluctuations such as those produced by magnetic arc blow. Various techniques exist for overcoming such obstacles to accurate analysis. The simplest is to select a normalizing procedure to factor out random variations in arc chemistry and optical receiver geometry.

As in the two-line method for temperature measurement, the ratio of the intensities of two lines is used for this purpose. However, while lines having widely differing excitation energies, E_{m_i}, are used in temperature measurement to maximize temperature dependency in the intensity ratio, lines having very similar excitation potentials are used in normalizing. Temperature dependence of the resulting ratio is thus minimized. Selecting lines having relatively close wavelengths will minimize wavelength dependent factors, such as the influence of blackbody radiation, and the ratio will remain nearly constant for a given concentration of the analyte elements, regardless of changes in process parameters.

From equation (3.4.4), the expression

$$\frac{I_{m_1 n_1}}{I_{m_2 n_2}} = \frac{\nu_1 N_1 g_{m_1} A_{m_1 n_1} \exp(-E_{m_1}/kT) B_1(T)}{\nu_2 N_2 g_{m_2} A_{m_2 n_2} \exp(-E_{m_2}/kT) B_2(T)} \qquad (3.4.5)$$

is obtained for the intensity ratio of emission lines produced by transitions of two different elements. In this expression, it is clear that the ratio of the number of atoms of each element present is equal to the ratio of their emission line intensities, multiplied by constants. The values of some of these constants, statistical weights, for example, are well known, while the values of others, such as transition probabilities, are not. So normalized, or relative, intensity measurements are made on plasmas of known composition, and these data are used to prepare empirical analytical curves. The empirical curve thus derived can be used to determine the concentration ratio of the element of interest in a plasma of unknown composition by comparing its relative line intensity to that found in a plasma of known composition.

It should be noted that, although this normalizing procedure will largely compensate for fluctuations produced by changing welding parameters or arc instabilities, the components of the weld arc atmosphere must remain unchanged. Adding carbon dioxide to an argon shielded welding arc, for example, would require recalibration and normalization specific to the altered system if the relative intensity approach was to be used in determining the hydrogen concentration in the arc plasma.

3.4.2 Application to Measurement of Weld Plasma Hydrogen Partial Pressure

Emission line intensity may be quantified by peak height or by integrating the area under the peak as seen in an analog chart or display. The latter is the preferred method and was the technique used in this study. However, the weld arc also emits significant background radiation resulting in measurable spectral continuum overlying the entire spectral range (Figure 3.1). This continuum must be compensated for when normalizing data.

The recorded level of the continuum is due in part to the electrical bias level produced by the photodiode array (Figure 3.2) and in part to the blackbody radiation emitted by incandescent metal droplets in the weld arc plasma and by the weld pool (Figure 3.3). The bias level of the photodiodes is a constant, while the continuum radiation produced by the blackbody effect increases slowly with wavelength. Despite this increase, it is possible to treat the blackbody background radiation level as a constant because only a 50.0 nm bandwidth of the spectrum is sampled at any one time. The change in the blackbody radiation level can be considered negligible in this bandwidth.

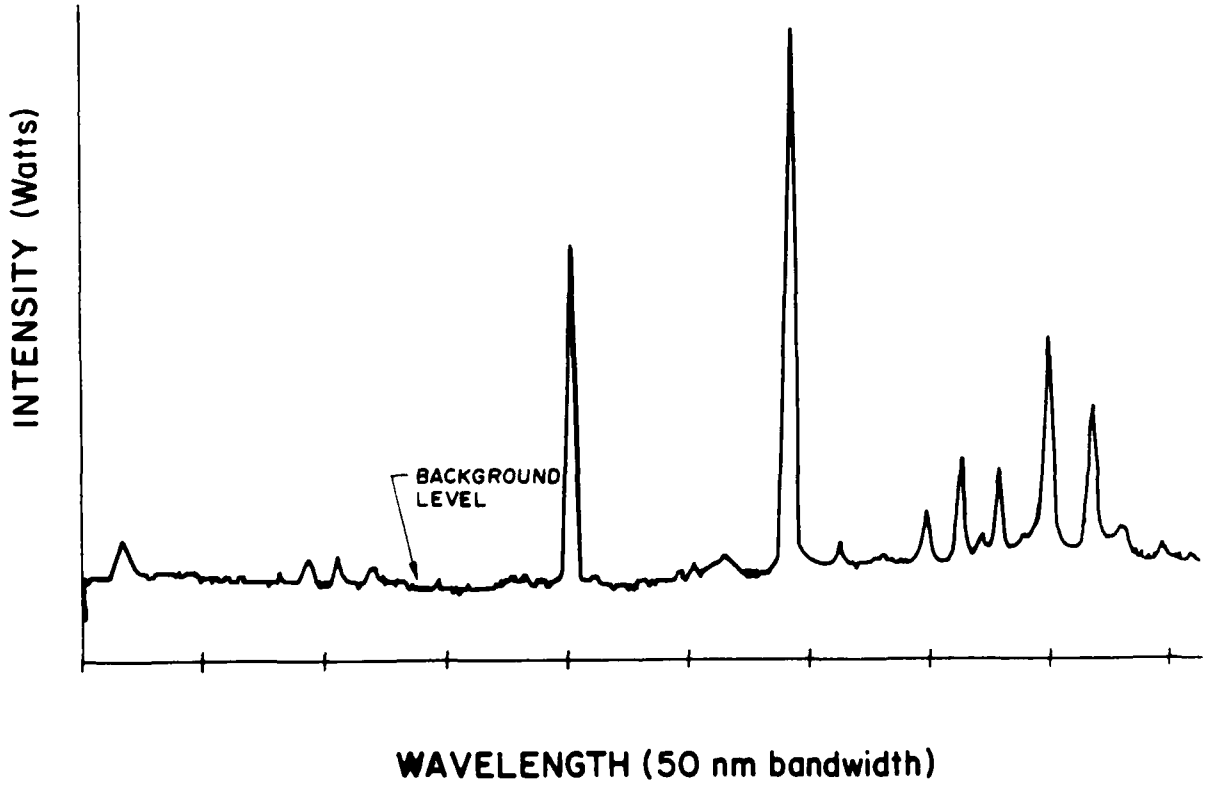

Figure 3.1 Typical 50 nm sample of weld arc spectrum showing background level and peaks.

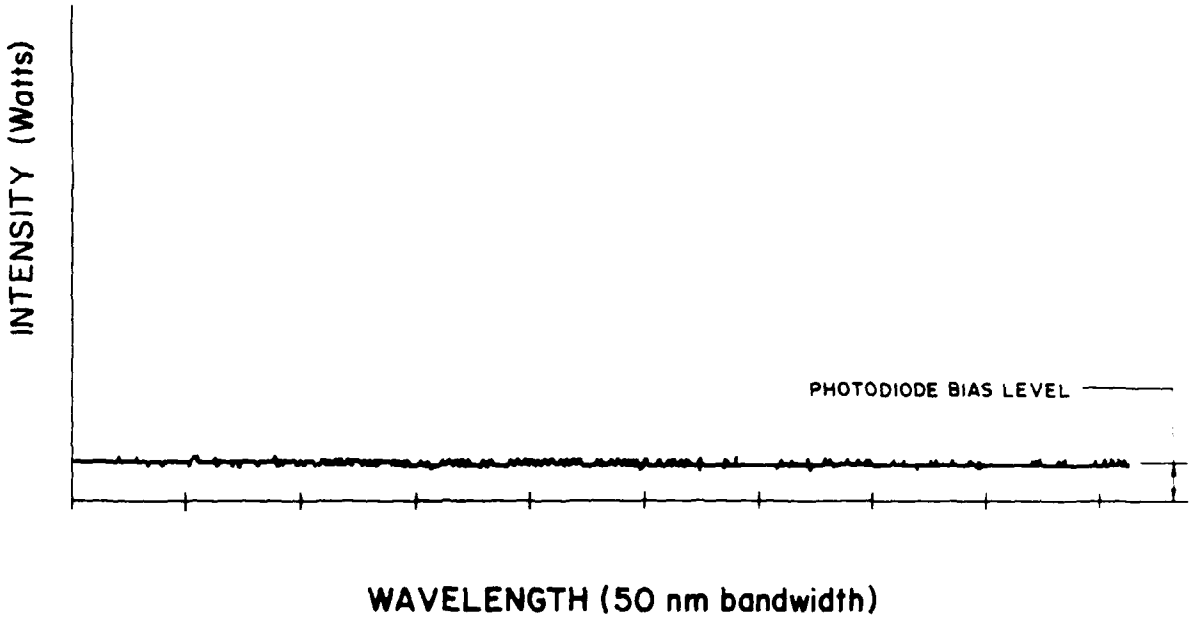

Figure 3.2 Characteristic photodiode bias level in any 50 nm bandwidth.

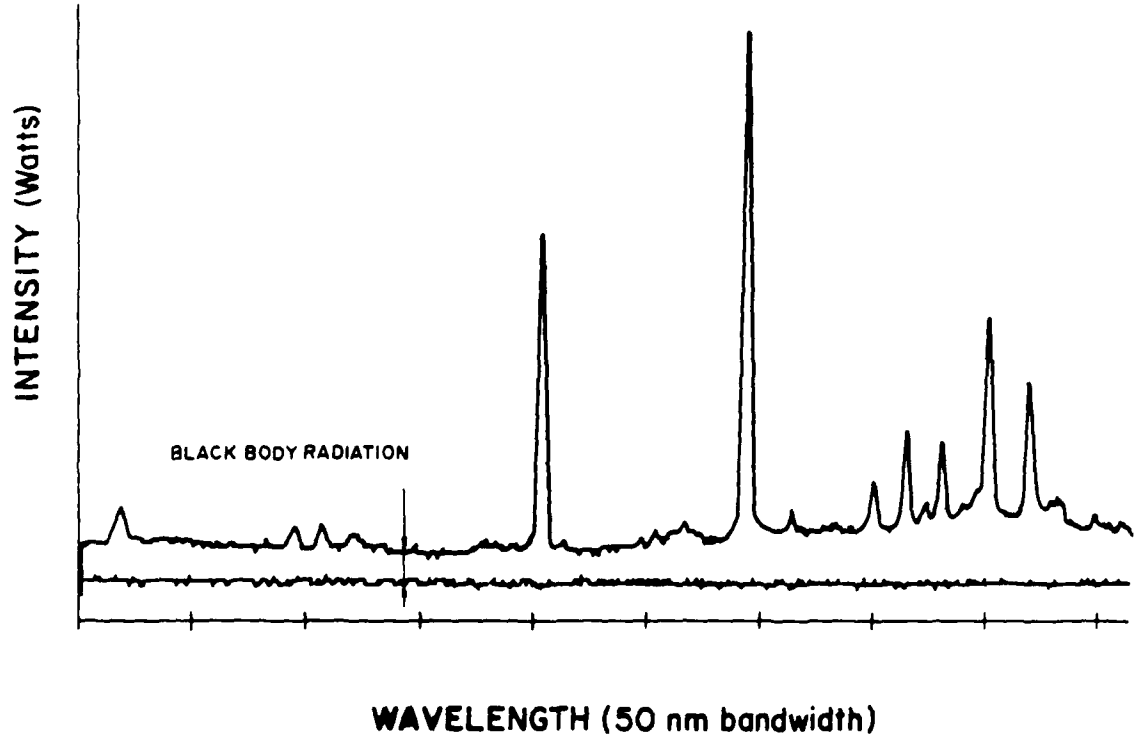

Figure 3.3 Contribution of blackbody radiation to background level.

Both blackbody radiation and photodiode bias can be compensated for in the normalizing procedure by selecting a region free of spectral lines and measuring the background level. This background value is then subtracted from the intensities of the lines being normalized (i.e. the area under the peaks) prior to taking the ratio of their intensities to obtain a relative intensity value. Once the background level has been subtracted from the observed intensity of the emission lines of interest (i.e., the hydrogen emission line at 656.28 nm and the nearby argon line at 696.5 nm), the ratio of the two lines is taken. This gives the relative intensity of the hydrogen emission line

$$I_{REL}^{H} = \frac{I_H - I_B}{I_A - I_B} \qquad (3.4.6)$$

where I_B is the background level, I_H is the intensity of the hydrogen emission line, and I_A is the intensity of the argon emission line (Figure 3.4). I_{REL}^{H} is calculated for weld arc plasmas containing known partial pressures of hydrogen and an analytical curve is developed. The partial pressure of hydrogen in a plasma of unknown composition is determined through comparison to the experimentally derived curve. The first ionization of metallic species can take place at temperatures far

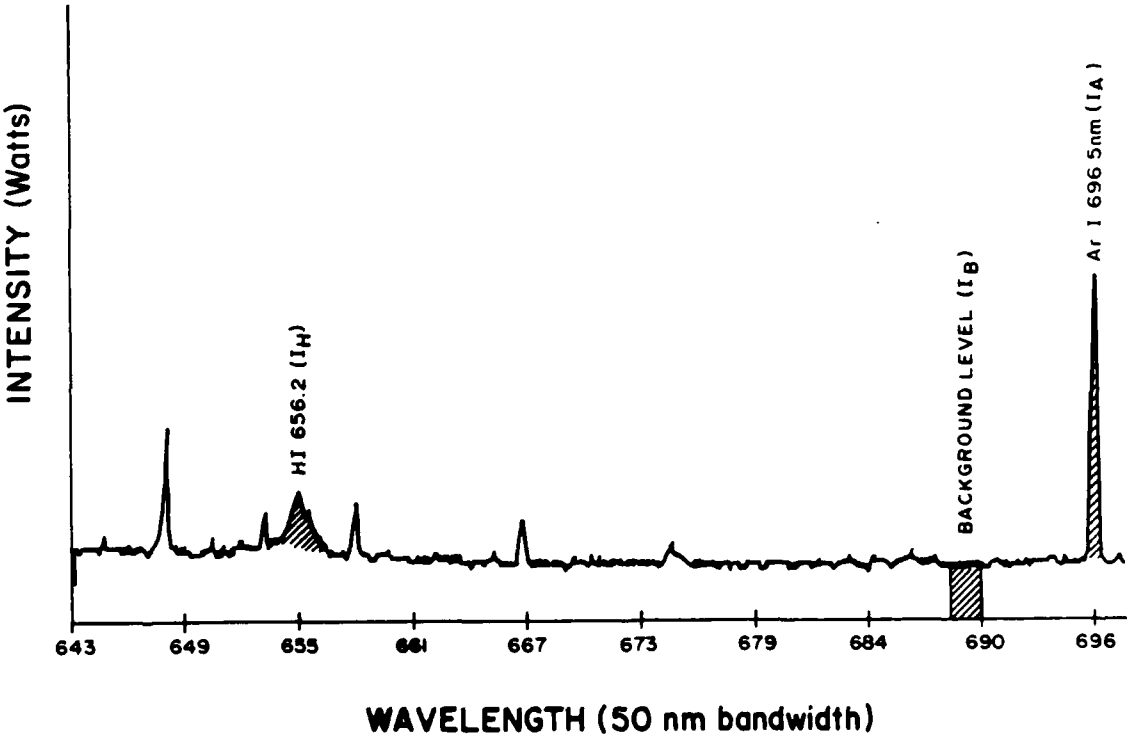

Figure 3.4 Graphical representation of quantities used in determining relative hydrogen emission line intensity.

lower than those required for ionization of gases such as hydrogen and argon. The presence in the plasma of the additional electrons can produce a "cascade" effect which lowers the temperature at which the species ionize. Many Mn, Fe, Cr, and other metal lines may be seen in the weld arc spectrum so this phenomenon undoubtedly affects apparent hydrogen line intensity. However, because a normalizing procedure is being used and an anlaytical curve is developed for plasmas of varying compositions, the problem is neglected.

3.5 Absolute Intensity Approach

3.5.1 Theory

To use the relative intensity approach described above to measure weld arc hydrogen content, empirical analytical curves must be developed. Determinations of weld arc plasma composition must be made by comparison with data acquired using arc plasmas of known composition. Any changes in shielding gas components require development of a new set of analytical curves. One way to overcome the necessity of preparing many sets of analytical curves would be to make direct measurements of the number of atoms of a certain element, N_n, in a given energy state.

Theoretically, such measurements are possible using absolute intensity measurements. Several difficulties associated with using absolute intensity measurements have already been mentioned. However, there are experimental techniques which can be used to compensate partially for these difficulties. The optical errors associated with pointing and focusing the fiber optic assembly can be minimized by calibrating the light collection and spectrographic system to a standard lamp. The other major difficulty with absolute intensity measurements (i.e., problems associated with absorption of the light emitted by the arc), can be limited if a smoke free process such as gas tungsten arc welding is used.

As shown earlier, the radiant intensity emitted from a unit volume of optically thin plasma in a spectral emission line of wavelength λ when atomic transitions from the higher energy state, n, to the lower energy state, m, occur is

$$I_{nm} = \frac{1}{4\pi} \frac{hc}{\lambda_{nm}} A_{nm} N_n \frac{\text{Watts}}{\text{cm}^3\text{-ster}} \qquad (3.5.1)$$

Here A_{nm} is the spontaneous emission transition probability, hc/λ_{nm} is the energy of the radiated quantum, and N_n is the number of ions per unit volume that have a bound electron in the excited atomic or ionic state, n. N_n is often referred to as the population density of the state n. In the case of the hydrogen induced cracking of welds, it is the hydrogen ion density in the welding arc which is of interest. Using the above equation, it is possible to determine the hydrogen ion density in the weld arc plasma from absolute intensity measurements.

Consider the hydrogen line with a wavelength of 656.28 nm which was used to determine plasma composition using relative intensity techniques. If this line is used in hydrogen ion density determinations, the following values may be substituted into the preceding equation:

$$\lambda_{nm} = 656.28 \text{ nm},$$

$$A_{nm} = 9.341 \times 10^{7} \text{ sec}^{-1},$$

$$h = 6.63 \times 10^{-34} \text{ joule-sec, and}$$

$$c = 3 \times 10^{8} \text{ m/sec} = 3 \times 10^{17} \text{ nm/sec.}$$

Solving for the hydrogen ion density N_n, we find that

$$N_n = \frac{4\pi \, I_{mn} \, \lambda_{mn}}{hc \, A_{mn}} \qquad (3.5.2)$$

Substituting numerical values, we obtain

$$N_n = 4.44 \times 10^{11} \, I_{nm} \text{ atoms/cm}^3 \qquad (3.5.3)$$

Here the population density, N_n, of the ionic state n is given as a function of the emission line intensity. An accurate value for this intensity is obtained by comparing the photodiode intensity values that are obtained during a welding experiment with those that are generated during calibration with a standard light source, using the same optical system.

3.5.2 Application to Weld Plasma Analysis of Hydrogen Partial Pressure

3.5.2.1 Hydrogen Ion Density Measurements

The characteristics of the optical system being used must be considered when attempting to measure population densities. The function of a spectrometer is to observe the radiation emitted by a given volume of plasma, which passes through a given solid angle, so the light can be broken up into discrete wavelengths. The volume of plasma observed and the solid angle are both functions of the optical system being used, and the relevant volume is essentially the plasma volume along the line of sight of the spectrometer and detector. Weld arc plasmas are known to have non-uniform properties in the axial direction, therefore, values of the population densities obtained must be considered to be average values along a given line of sight, approximately perpendicular to the arc.

A plasma which is uniform and optically thin will emit radiation with an intensity of Ω_E watts per unit volume, per solid angle. Thus the total emitted radiation, R, which is recorded by the spectrometer readout, will be primarily a function of the lens and the spectrometer entrance slit geometry.

$$R = Wl\ m\ A_s\ \Omega_F \qquad (3.5.4)$$

where m is the magnification of the lens system, Ω_F is the solid angle, A_s is the cross-sectional area of the spectrometer entrance slit, and l is the diameter of the plasma along the line of sight [58].

This equation is useful in reducing spectroscopic data. Since W is the generalized intensity of the radiation emitted by the plasma, in watts per unit volume per solid angle, it can be replaced with the voltage output of the photodiode array which occurs when the light which has been broken up by the spectrograph falls on it. Then the equation above can be rewritten as

$$R_p = I_{mn}\ lm\ A_s\ \Omega_F \text{ watts} \qquad (3.5.5)$$

Assuming that the spectrometer slit is adjusted to allow passage of all of the light emitted at the wavelength of interest, the resulting photodiode voltage, V_p, can be related to the intensity of the incident radiation by some calibration constant C. In this case, the form of the above equation becomes

$$I_{mn}\ lm\ A_s\ \Omega_F = CV_p \text{ volts} \qquad (3.5.6)$$

As noted above, the calibration constant is determined from tests using a standard tungsten ribbon filament lamp calibrated to NBS standards for spectral radiance. These optical calibration standards will be discussed further. However, let us consider the lamp to be calibrated in terms of the spectral radiance $N_\lambda(I_L)$ Watts/cm^2-ster-nm, as a function of the lamp current. When the standard lamp is placed so the filament is at the focal point of the optical system, the total radiation entering the optical system will be

$$R_L = N_{\lambda mn}\ (I_L)\ m\ A_s \Omega_F \text{ watts/nm} \qquad (3.5.7)$$

The lamp emits a spectral continuum of blackbody radiation calibrated against a primary standard, therefore, R_L has the units of intensity per unit wavelength. If W is the width of the spectrometer slit adjusted to pass all radiation at λ_{nm} and D is the reciprocal dispersion of the spectrometer grating, the following relationship is obtained

$$N_\lambda\ lm\ A_s\ \Omega_F\ WD = CV_L \qquad (3.5.8)$$

where V_L is the photodiode array output voltage generated during the calibration tests. When this is combined with the equation for the photodiode output voltage when the radiance of the weld arc plasma is being observed, the calibration constant, C, can be eliminated and we obtain

$$I_{nm} = \frac{V_p}{V_L}\ \frac{N_\lambda DW}{l} \qquad (3.5.9)$$

When a current of X amperes is passed through the spectral lamp, the spectral radiance, N_λ, is known as a function of wavelength and current. D and W are functions of the spectrometer conditions and are known. The photodiode array voltage at the wavelength of interest can be measured during calibration with a lamp and during a welding experiment, as can the plasma diameter. These values can then be substituted into the preceding equation to determine the absolute line intensity I_{nm} [58]. When this value is used in equation (3.5.3) for hydrogen ion density as a function of hydrogen line intensity, the population density of hydrogen ions is obtained.

The partial pressure of hydrogen ions present can then be calculated by measuring both the absolute hydrogen ion density and the electron density. The temperatures in the welding arc are not sufficient to produce a significant level of secondary ionization. Therefore, the electron density may be assumed to be approximately equal to the total ion (or atom) density. If the total number of particles present is known and the total number of hydrogen ions present is known, the partial pressure of hydrogen ions present is easily calculated.

3.5.2.2 Electron Density Measurements

Electron density in the weld arc plasma is calculated through measuring the Stark broadening of spectral lines [47]. Stark broadening is caused by the microfields surrounding the ions in a plasma. Use of Stark profiles permits determination of electron densities in plasmas of almost any composition, even if the plasma chemistry is not well known. Basically, electron density is determined by comparing measured full widths of lines (i.e., wavelength differences between the two points on either side of a peak where the intensity has fallen to one-half of the maximum) with their calculated values. Line widths and electron densities are almost exactly proportional to each other.

Conveniently, the theoretical values of line widths needed for this experiment are most accurate for hydrogen lines, and suitable hydrogen lines are indeed measurable in welding arcs. The Stark effect is linear and is proportional to the two-thirds power of the ion density [47]. It has already been noted that secondary ionization in the welding arc is insignificant and that, therefore, electron density is nearly equal to ion density. Electron density is given by

$$N_e = C(N_e, T)\ \Delta\lambda_s^{3/2} \qquad (3.5.10)$$

where N_e is the electron density, $\Delta\lambda_s$ is the full Stark width of the line, and $C(N_e, T)$ is a coefficient which is a weak function of the electron density. Griem [47] has calculated values for $C(N_e, T)$ (Table 3.1), and since these are rather slowly varying functions of the electron density and temperature for any given line, interpolation for intermediate values should always be sufficient.

3.6 Summary

Two spectroscopic methods for measuring the partial pressure of hydrogen in a welding arc have been presented. As discussed in section 1.3, this information can be used to predict the hydrogen content of a weld and its susceptibility to cracking. In the next chapter, the experimental methods used in this study to measure weld arc hydrogen levels, determine the diffusible hydrogen content of the resulting welds, and evaluate their susceptibility to cold cracking will be presented.

Table 3.1 Coefficients $C(N_e,T)$ in $Å^{-3/2}$ cm^{-3} for Electron Density Determinations From (Full) Half Widths of Stark-broadened Hydrogen (From Griem)

	T,°K	N_e, cm^{-3} 10^{14}	10^{15}	10^{16}	10^{17}	10^{18}
Hα	10,000			6.16×10^{15}	3.61×10^{15}	3.23×10^{15}
	20,000			7.13×10^{15}	3.88×10^{15}	2.79×10^{15}
	40,000			4.22×10^{16}	6.01×10^{15}	2.67×10^{15}
H_β	5,000	3.84×10^{14}	3.68×10^{14}	3.44×10^{14}		
	10,000	3.80×10^{14}	3.58×10^{14}	3.30×10^{14}	2.98×10^{14}	
	20,000	3.72×10^{14}	3.55×10^{14}	3.21×10^{14}	3.03×10^{14}	
	40,000	3.76×10^{14}	3.52×10^{14}	3.30×10^{14}	2.87×10^{14}	
H_γ	10,000		4.41×10^{14}	2.90×10^{14}	2.73×10^{14}	
	20,000		6.68×10^{14}	3.01×10^{14}	2.81×10^{14}	
	40,000		3.77×10^{15}	3.46×10^{14}	2.39×10^{14}	
H_δ	10,000	1.36×10^{14}	1.18×10^{14}	1.04×10^{14}		
	20,000	1.35×10^{14}	1.21×10^{14}	9.79×10^{13}		
	40,000	1.07×10^{14}	1.22×10^{14}	1.01×10^{14}		
H_{eII}	4,686 Å	5,000		1.58×10^{16}		

4. EXPERIMENTAL PROCEDURE

In this investigation, experiments were performed to determine the relationship between the intensity of hydrogen emission lines in the light emitted by a welding arc and the hydrogen content of the resulting welds. Mechanical tests were then performed to relate weld diffusible hydrogen content to susceptibility to hydrogen induced cracking in welds in armor steel.

To develop the relationships described, a series of shield gas hydrogen contents was selected and spectroscopic techniques were used to make measurements of the relative and absolute intensities of the hydrogen emission lines of interest at the various hydrogen levels. The diffusible hydrogen content of GTA and GMA welds made with varying shield gas hydrogen contents was determined, and implant tests were then performed on welds made with various shield gas compositions to determine the hydrogen induced cracking susceptibility of the welding system.

4.1 Welding

All gas metal arc welds were made using an automatic gas metal arc welder, a Linde SVI-600 power supply, and a Linde torch. Wire size was 1.5 mm in diameter. The welding voltage was 31 V. Some adjustment to filler wire feed speed was required to maintain arc stability as the arc hydrogen content increased from zero to 2 percent. As a result, welding current varied from 310 to 350 amps. Travel speed was 25 cm per minute. All welds were made on armor steel, the composition of which is given in Table 4.1. Linde 95 filler metal was used, the composition of which is given in Table 4.2. Electrode stickout was 19 mm.

All gas tungsten arc welds were made using a Hobart Cyber-TIG power supply. A 2 percent thoriated electrode with a diameter of 3.5 mm was used. Arc voltage and current were 14 V and 100 A, respectively.

Table 4.1 Composition of Armor Steel

C	Mn	P	S	Si	Mo	Cr	Ni
0.27	1.34	0.01	0.005	0.2	0.58	0.13	0.05

Table 4.2 Composition of Filler Metal

C	Mn	Si	P	S	Mo	Cr	Ni	V
0.08	1.3	0.4	0.005	0.005	0.04	0.01	2.0	0.02

4.2 Spectroscopic Measurements

Figure 4.1 is a block diagram of the system used to acquire weld arc spectra. A 50 mm focal length lens was used to collect the light emitted by the welding arc and focus it on the end of an armored Dolan-Jenner fiber optic bundle. A glass lens and bundle were used in relative intensity measurements; a quartz lens and bundle were used to make absolute intensity measurements because spectral data was needed for wavelengths at which the transmittance of glass fibers is very low. Figures 4.2 and 4.3 show the transmittance characteristics of the two fiber optic bundles.

The fiber optic bundle terminated at the entrance slit of an ISA HR-320 monochromator/spectrograph which uses a 0.32 m Czerny-Turner grating. A 1200 lines/mm holographic grating was used, which provided a bandwidth of 60 nm and a resolution of 0.06 nm. The monochromator was configured as a spectrograph, and a 1024 element Reticon photodiode array was used at the exit slit to observe the emitted light. An LSI 11/23 computer was used in conjunction with an ADAC 12 bit A/D converter and a direct memory access (DMA) unit to acquire and process spectral data. A parallel port and external synchronizing circuit provided the appropriate timing signals for A/D conversion of the Reticon video signal. Weld arc spectra were stored on floppy disks for later data reduction. The system described above acquires data in the following way. The Reticon video circuits continuously scan the photodiode array. One scan takes approximately 50 ms. Each scan consists of a 25 ms array video signal pulse followed by a 25 ms blanking pulse. The slow scan rate allows the charge coupled photodetectors to integrate over a long period of time, making it possible to observe weaker spectra.

The video circuits generate three signals: a start pulse which identifies the beginning of each scan, a 0-3 V video signal, and a clock which determines the scan rate. At the desired sampling time, one of the parallel interface outputs is set to synchronize the A/D converter and DMA with the Reticon start pulse and the Reticon clock. Conversions begin with the initiation of the start pulse. After an array scan is completed, the parallel interface output is reset.

Usually several consecutive array scans are made and summed together before being stored on a floppy disk. This helps to reduce noise and to factor out random variations in the arc behavior. The data acquisition sequence can be repeated up to 200 times during a weld pass with data being transferred to floppy disks at the rate of two scans per second.

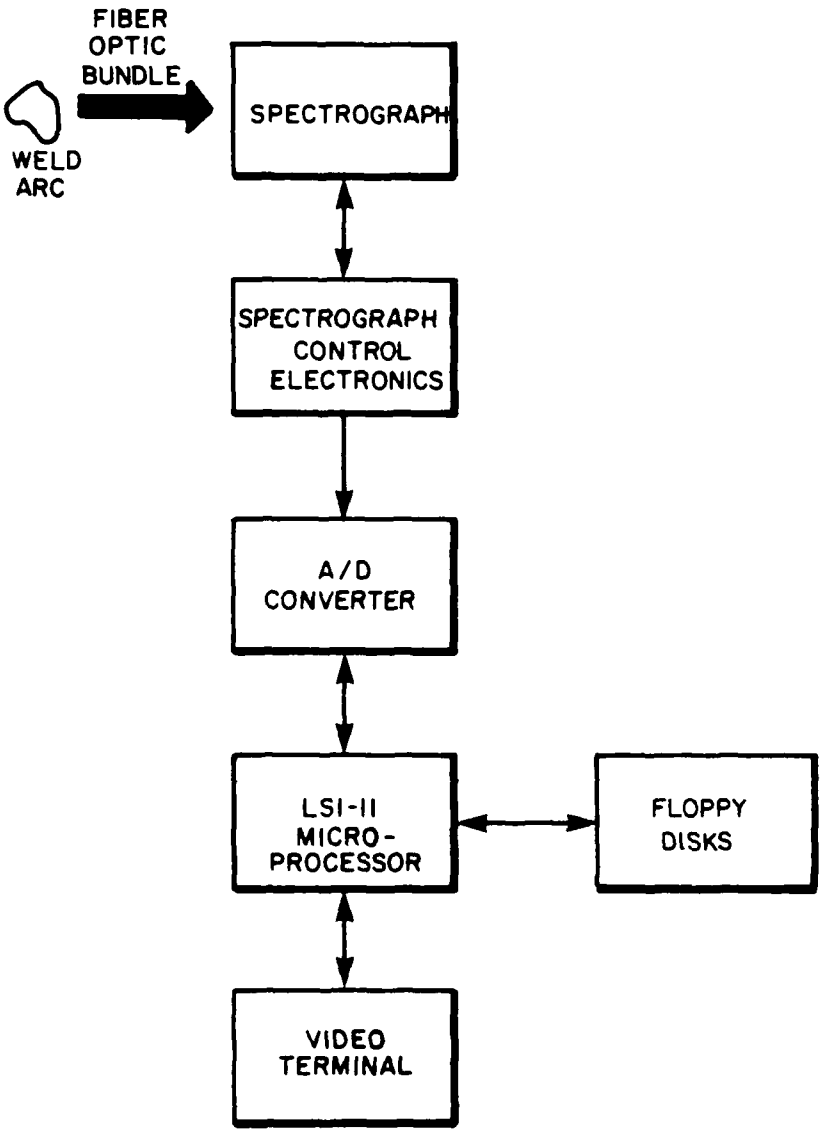

Figure 4.1 Block diagram of spectroscopic data acquisition system.

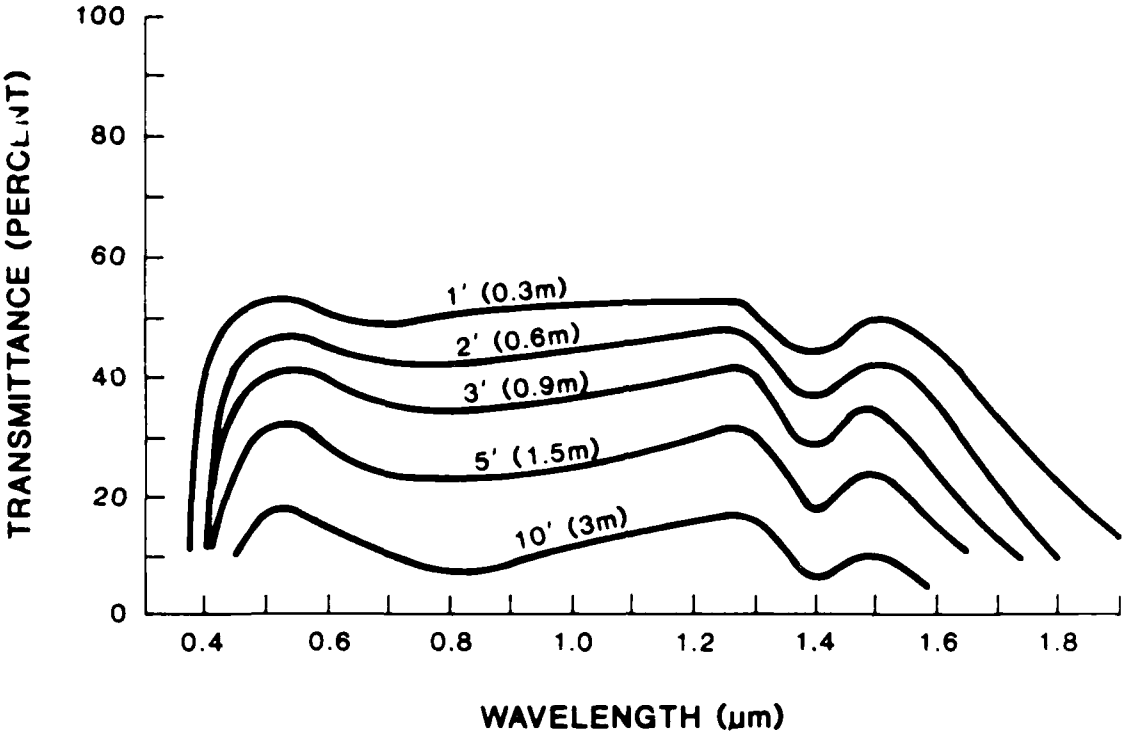

Figure 4.2 Transmittance characteristics of glass fiber optic bundle.

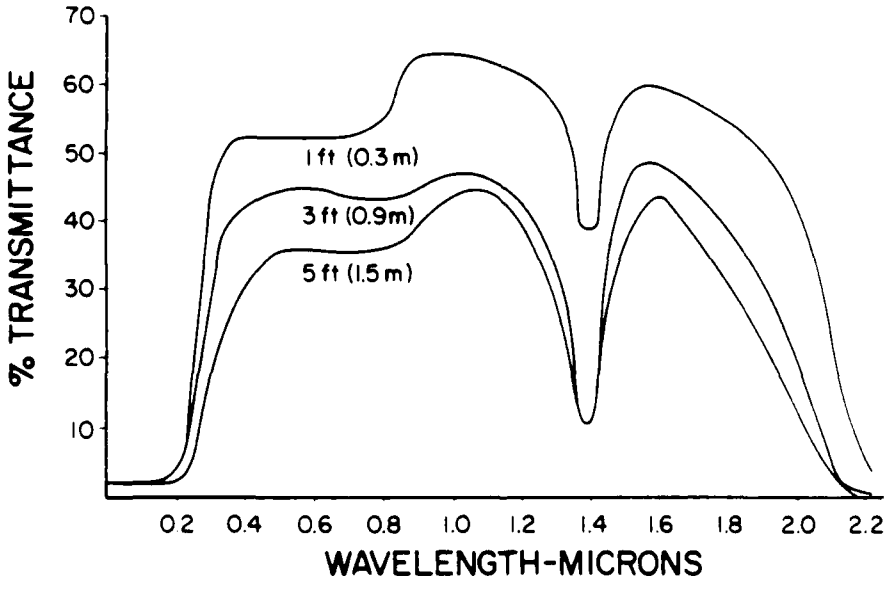

Figure 4.3 Transmittance characteristics of quartz fiber optic bundle.

4.2.1 Relative Intensity Procedure

All relative intensity data were collected using the data acquisition system described above, at a center wavelength of 672.5 nm during bead on plate GMA welding. The lens used to collect the light emitted by the welding arc was mounted on a bracket approximately 450 mm from the torch head. It was focused on the welding arc and traveled with the torch as shown in Figure 4.4.

Spectral data was collected at weld shield gas hydrogen contents of 0.00, 0.05, 0.10, 0.20, 0.25, 0.30, 0.50, 0.75, and 1.0 percent. The balance of the shielding gas was 98 percent argon and 2 percent oxygen; welding grade gas was used. The intensity of the hydrogen emission line at 656.25 nm was normalized to that of the argon line located at 696.5 nm, as described in section 3.4.2.

Spectroscopic data were taken during welding of specimens for the determination of weld diffusible hydrogen content.

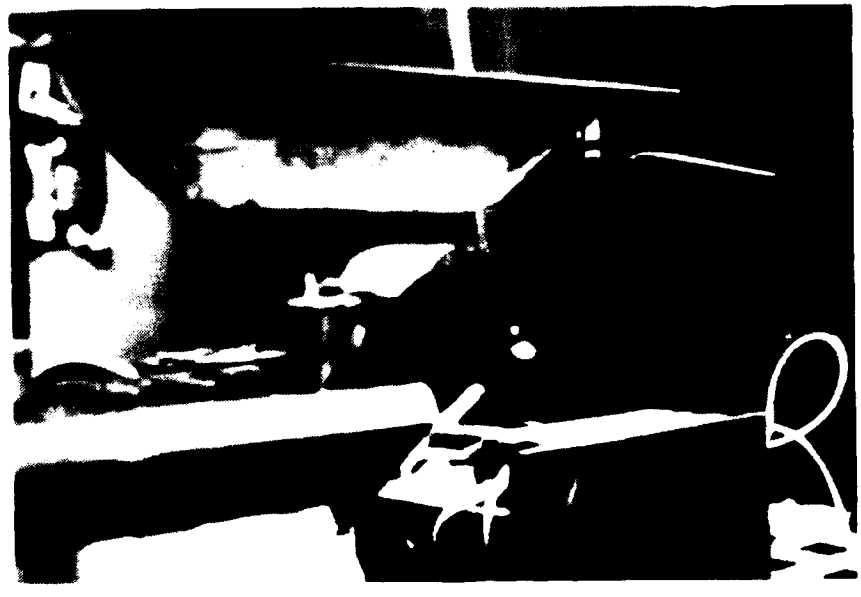

Figure 4.4 GMAW optical setup.

4.2.2 Absolute Intensity Procedure

All absolute intensity measurements were made using the system described above, during GTA welding without filler wire. Welding voltage and current were 14 V and 100 A, respectively. The light emitted by the welding arc was focused on the fiber optic bundle by a lens mounted approximately 150 mm from the GTA welding torch. The torch and optics remained stationary and the workpiece traveled beneath them. Spectral data was collected at weld shielding gas hydrogen contents of 0.0, 0.5, 1.0, 1.5, and 2.0 percent. The balance of the shielding gas was welding grade argon. Spectroscopic data was collected at center wavelengths of 656.2 nm and 460.0 nm.

An Optronics 550 tungsten filament lamp with a sapphire window (Figure 4.5) was used to calibrate the optical system as described in section 3.5.2.1. This lamp is a standard of spectral radiance and is used with a Optronics Model 95 lamp holder and Model 16 precision constant current dc power supply. This power supply is specially designed to operate tungsten filament lamp standards and is preset to operate at the current for which the standard lamp was calibrated.

Because an iron line located at 485.9 nm was known to interfere with accurate data acquisition at the hydrogen wavelength at 486.1 nm, absolute intensity data were collected as the GTAW arc traveled along a tungsten plate. The tungsten plate rested in a water cooled copper chill block during this procedure (Figure 4.6). The welding torch and optical detector remained stationary and the copper fixture moved beneath the torch at a speed of 7.5 cm per minute.

Figure 4.5 Calibrated lamp and lamp holder.

Figure 4.6 Copper chill block, tungsten test piece, steel specimen, and GTA torch.

4.3 Weld Diffusible Hydrogen Content Measurement

Because of the inaccuracies inherent in the immersion methods for the measuring the diffusible hydrogen content of welds described in section 2.5.1, gas chromatography was used to measure the hydrogen content of weld specimens. No standard exists for this procedure, however, the procedures used in this study followed those outlined by the American Welding Society (AWS) and IIW for specimen preparation.

4.3.1 Gas Chromatograph

All gas chromatography was performed using a Gow Mac Model 20-150 thermal equilibrium gas chromatograph equipped with a 15 ft packed column of molecular sieve type 5A 60/80. The output signal was sent to a Hewlett-Packard 3380A integrator. The absolute hydrogen content of specimens measured with this equipment was normalized to mL H_2/100 g of deposited weld metal at standard temperature and pressure.

4.3.2 Specimens and Procedures

Figures 4.7 and 4.8 show the dimensions of the diffusible hydrogen specimens used in the gas metal arc (relative intensity) and gas tungsten arc (absolute intensity) welding experiments, respectively. The specimen dimensions selected for the gas metal arc welding experiments conforms to the proposed AWS standard A 4.3-8X. Diffusible hydrogen specimen geometry for the gas tungsten arc welding experiments was selected to allow preparation of the samples immediately following spectral data acquisition.

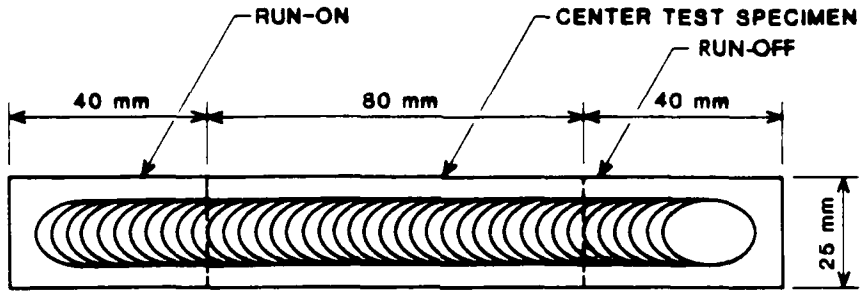

Figure 4.7 GMAW diffusible hydrogen specimen geometry.

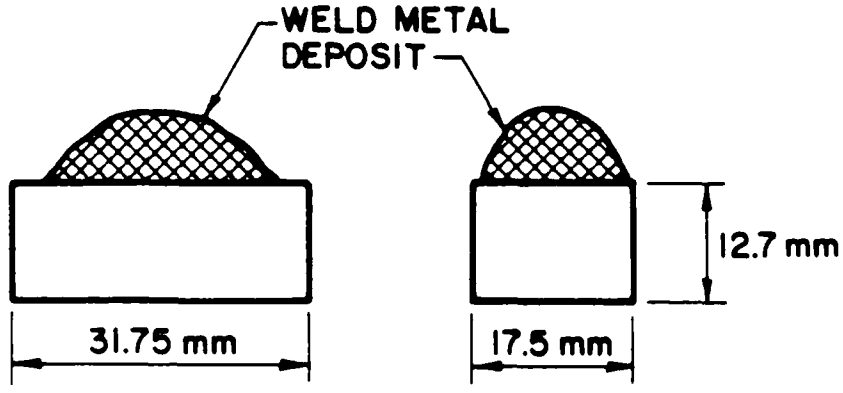

Figure 4.8 GTAW diffusible hydrogen specimen geometry.

4.3.2.1 Gas Metal Arc Weld Hydrogen Determination Procedure

The diffusible hydrogen content of welds made during the acquisition of relative intensity spectral data was measured using a procedure similar to that suggested in the proposed AWS specification. Gas metal arc welds with the shield gas hydrogen contents given in section 4.2.1 were made on 12 mm x 25 mm x 80 mm welding specimens, with run-on and run-off tabs at either end. Immediately after welding, the specimens were quenched in an ice water bath. Following quenching, the specimens were separated from the run-on and run-off tabs, and stored in liquid nitrogen while awaiting testing to prevent premature outgassing.

The following procedure was used to clean each specimen before degassing. Samples were placed in an ethanol bath followed by washing in anhydrous ethyl ether. Specimens were dried with a blast of ultra-high purity (UHP) argon gas. As required by the ISO procedure for preparing diffusible hydrogen samples for outgassing under mercury, the time taken for the cleaning procedure did not exceed 60 seconds. After cleaning, the specimens were placed in stainless steel degassing chambers of the type shown in Figures 4.9 and 4.10. The outgassing chambers were then purged with UHP argon. After purging with argon, the bombs were injected with a helium internal standard and heated at 150°C for eight hours. Following heating, samples of the gas in the fixtures were injected into the gas chromatograph system described in section 4.3.1 for analysis. When the analysis was completed, the specimens were removed from the bombs and reweighed. The hydrogen content of each specimen was normalized to mL H_2/100 g deposited weld metal at standard temperature and pressure.

4.3.2.2 Gas Tungsten Arc Weld Hydrogen Determination Procedure

The diffusible hydrogen content of gas tungsten arc welding specimens used in absolute intensity determinations of hydrogen ion densities was measured in the following way. After acquiring spectral data by allowing the GTA arc to travel along a tungsten plate at a constant speed, filler wire was fed into the arc as it remained stationary over an armor steel specimen of dimensions 12.7 mm x 17.5 mm x 31.75 mm. The specimen rested in a water cooled copper chill block as the metal was deposited. The filler metal was applied to the specimen in a small area so that as much of the deposited metal would remain molten as possible during deposition. The filler metal was deposited as rapidly as possible to reduce the length of time available for outgassing prior to specimen quenching. After the arc was extinguished, the specimens were quenched in an ice water bath and stored under liquid nitrogen while they awaited testing. The cleaning procedure described in section 4.3.2.1 was used to wash each specimen before placing it in an outgassing fixture and proceeding as described in the preceding section. Following outgassing, each specimen was weighed. The hydrogen content of the specimens was normalized to mL H_2/100 g of deposited metal.

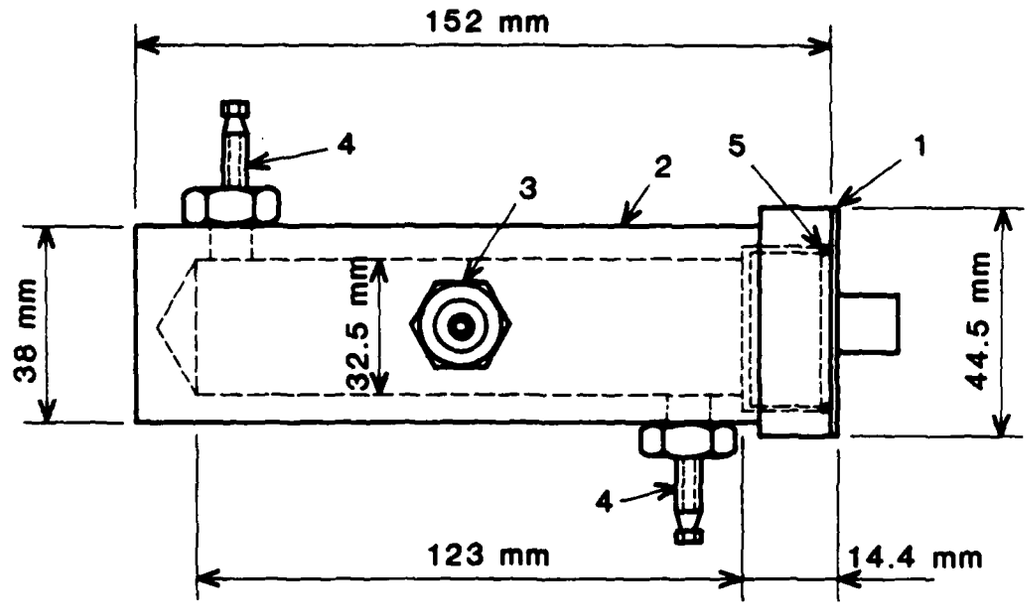

1 END CAP
2 BODY
3 SEPTUM PORT
4 ADAPTER FOR VALVE CONNECTION
5 O-RING

Figure 4.9 Schematic of specimen outgassing container for gas chromatography.

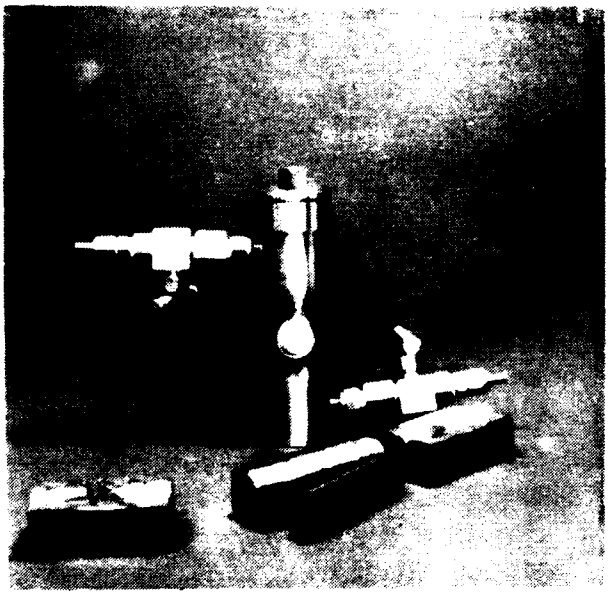

Figure 4.10 Diffusible hydrogen specimen with outgassing chamber, run-on, and run-off tabs.

4.4 Implant Testing

No standard procedure exists for the implant test. However, the International Institute for Welding has published a document containing guidelines for implant testing [61]. In general, the procedures in that document were followed in the implant tests performed in this study.

4.4.1 Specimens

All implant tests were performed using helically notched specimens of the type developed in the early 1970's (Figure 4.11). The support plate geometry is shown in Figure 4.12. Three holes were made in each each support plate to allow multiple tests. All implant specimens and support plates were fabricated from the same armor steel used in the spectroscopic tests and hydrogen analysis specimens.

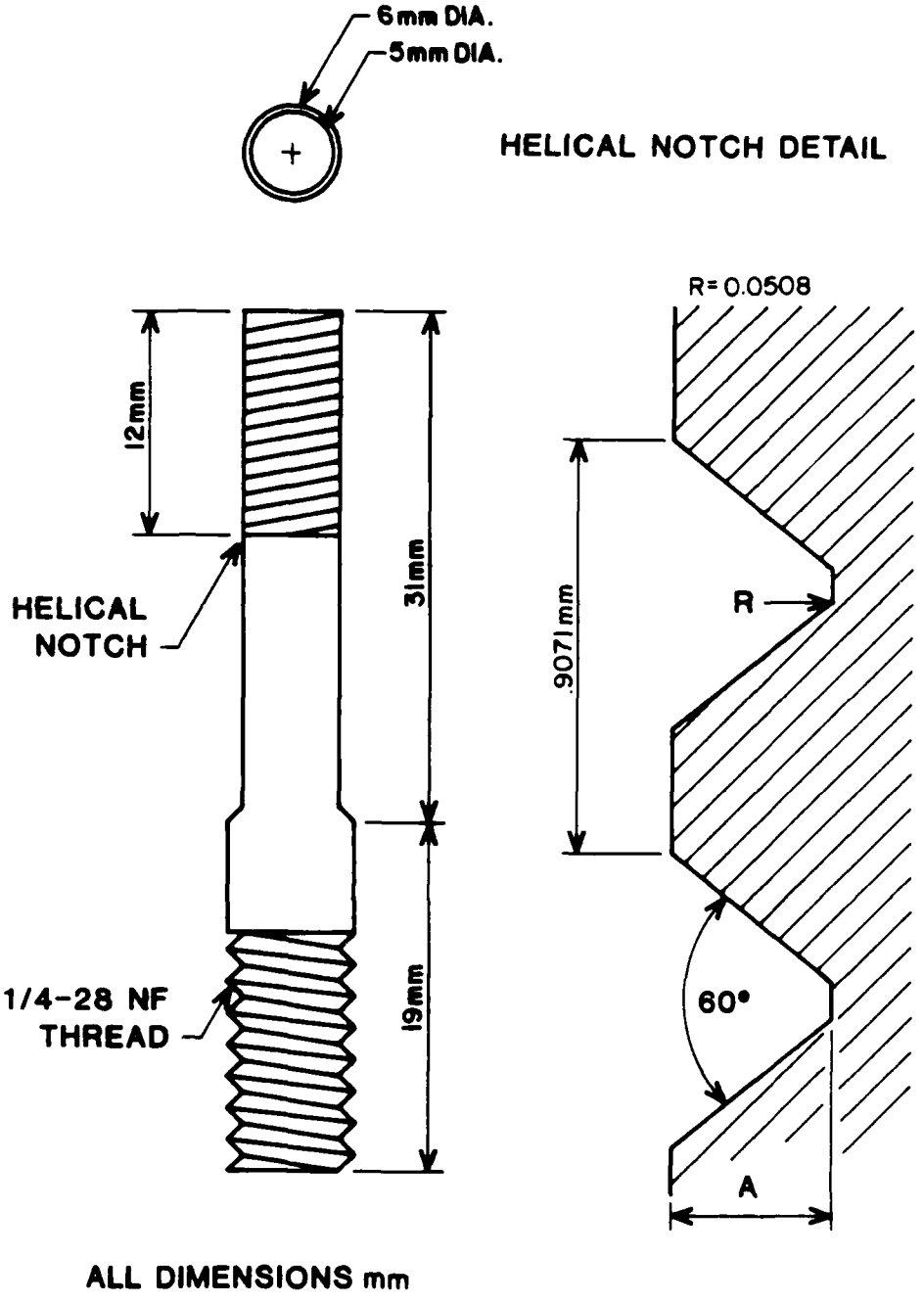

Figure 4.11 Helically notched implant specimen geometry.

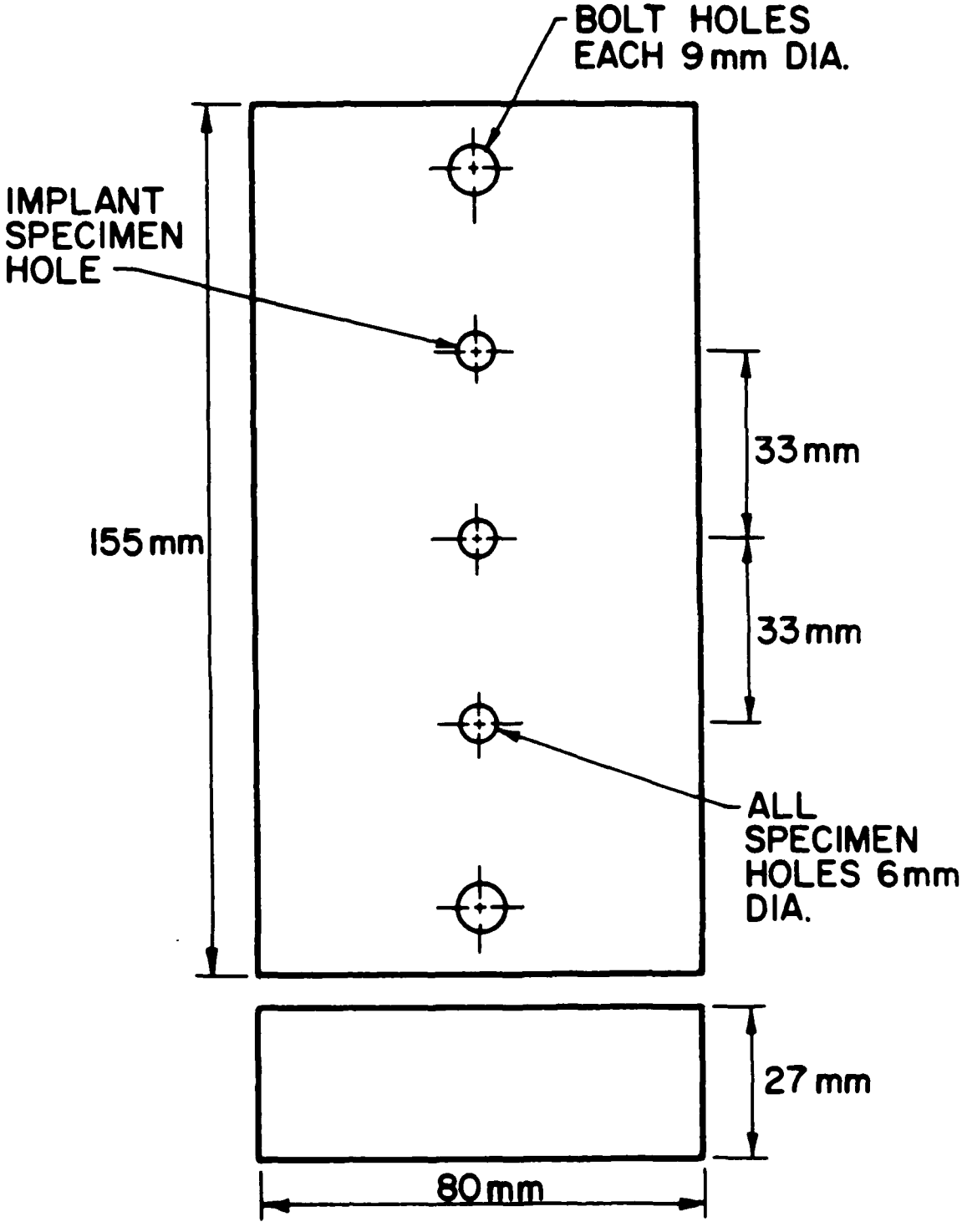

Figure 4.12 Implant test support plate geometry.

4.4.2 Equipment

A servo-controlled, electro-hydraulic implant testing machine was built for these tests (Figure 4.13). A 22 kip actuator with a 6-in. stroke was used. Tests were micro-processor controlled.

4.4.3 Procedure

Implant tests were performed on gas metal arc welds made with 98 percent argon, 2 percent oxygen, welding grade shield gas. Welding voltage and current were 31 V and 310 to 350 amps, respectively. Implant specimens were made with shield gas hydrogen contents of 0.0, 0.05, 0.1, 0.20, 0.25, and 0.5 percent. The filler metal was Linde 95, as in all other tests.

Prior to welding, the specimens and support plates were preheated to 150°F; this is the preheat temperature used when the material is fabricated commercially. Following welding, specimens were allowed to cool to 240°F. When the specimens had cooled to this temperature, the load was ramped up to the test load over a period of 20 to 60 seconds as recommended by the IIW in Document 802-84.

Either crack initiation or specimen rupture may be used as the criterion to determine the time to failure in the implant test. The latter is the more common approach and was used in this study. Specimens which did not fail within a test time of 24 hours at a particular load level were considered runouts. There is no standard for determining test length if no failure occurs. A minimum of 16 hours is recommended [60], and 24 hours has been used in many other studies.

The highest load which can be applied to a specimen under a given set of welding conditions without producing failure during the implant test within 24 hours is referred to as the lower critical stress. The lower critical stress is also sometimes referred to as the implant rupture strength. The lower critical stress was determined for each of the weld shielding gas hydrogen contents at which implant tests were performed.

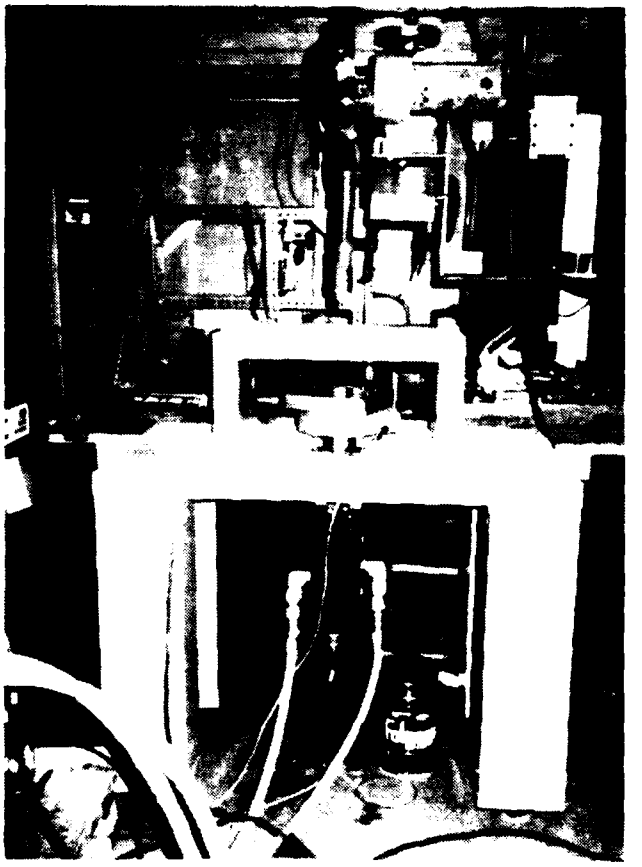

Figure 4.13 Implant testing frame and GMA torch.

5. RESULTS

5.1 Weld Arc Spectroscopy--Relative Intensity Measurements

The objective of these experiments was to correlate the intensity of the hydrogen emission line located at 656.2 nm, relative to that of an argon line located at 696.5 nm, with the partial pressure of hydrogen in the welding arc atmosphere.

Figures 5.1 and 5.2 show qualitatively the nature of the changes which occur in hydrogen emission line intensity as the hydrogen content of the weld shielding gas, and thus of the arc atmosphere, is increased from 0.0 to 1.0 percent. When the relative hydrogen emission line intensity is determined as described in section 3.4.2, and plotted against the hydrogen content of the shielding gas, a linear relationship is found to exist between the two parameters, as shown in Figure 5.3.

For the purposes of this portion of the investigation, the partial pressure of hydrogen in the weld shielding gas was assumed to be equivalent to the partial pressure of hydrogen in the weld arc atmosphere. Additional hydrogen is present in the weld arc atmosphere due to contamination by consumables and the inability of the shielding gas to completely exclude the ambient atmosphere from the vicinity of the welding arc. However, these effects were ignored and compensated for later. The following equation describes approximately the relationship between the partial pressure of hydrogen in the arc atmosphere and the relative intensity of the hydrogen emission line at 656.2 nm when sources of hydrogen outside the shielding gas are neglected.

$$I^{H}_{REL} = 287.5\ (P_{H_2}) + 0.7 \qquad (5.1)$$

As noted in Chapter 3, the presence of metal ions in the plasma affects hydrogen line intensity. However, it also affects argon line intensity and since different shield gas compositions ($25CO_2$-75Ar versus 98Ar $2O_2$, for example) require different calibration curves, the effect can be neglected. In Chapter 6 this relationship will be used to predict the diffusible hydrogen content of gas metal arc welds.

5.2 Weld Arc Spectroscopy--Absolute Intensity Measurements

In these experiments, standard spectroscopic calibration techniques were used to determine the absolute intensity of hydrogen emission lines located at 434 nm, 486 nm, and 656 nm. These data were used to calculate the average temperature of the welding arc, the average hydrogen ion density, and the average electron density as described in section 3.5. The partial pressure of hydrogen present in the welding arc was estimated by dividing the hydrogen ion density by the total electron density, which was assumed to equal the atom density. As noted in Chapter 3, this assumption can be made because little secondary ionization occurs in the welding arc.

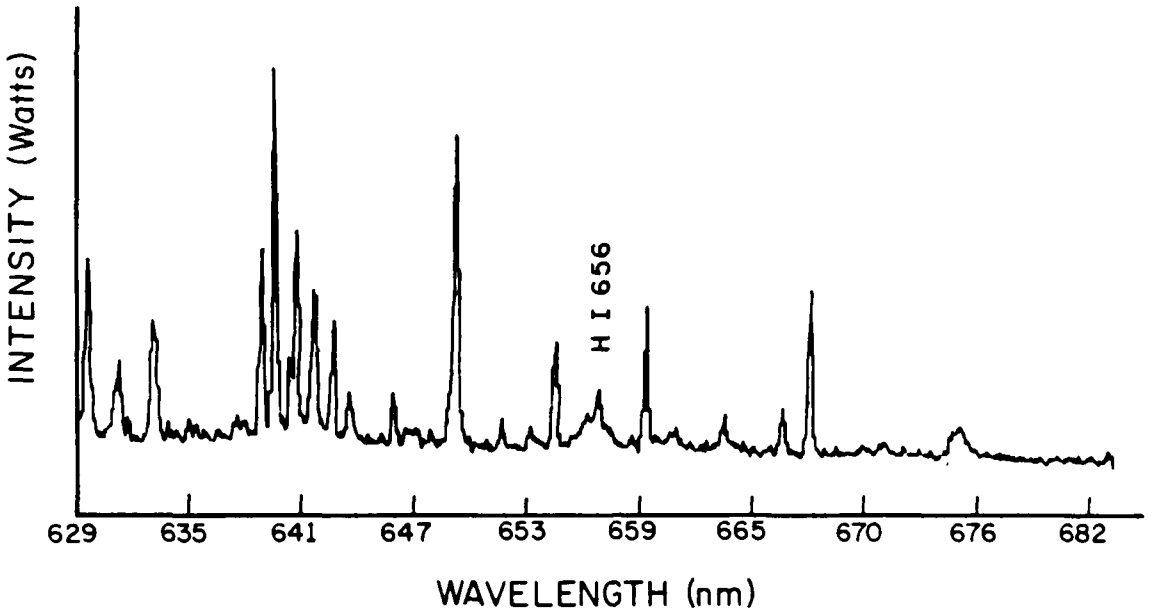

Figure 5.1 Appearance of weld arc spectrum at 656 nm when the shield gas hydrogen content is 0.0 percent.

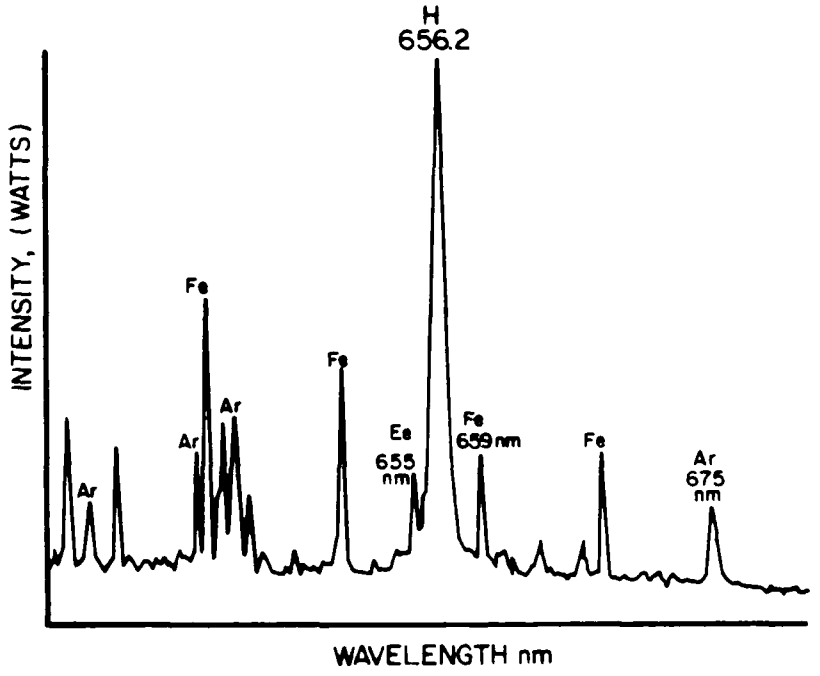

Figure 5.2 Appearance of weld arc spectrum at 656 nm when the shield gas hydrogen content is 1.0 percent.

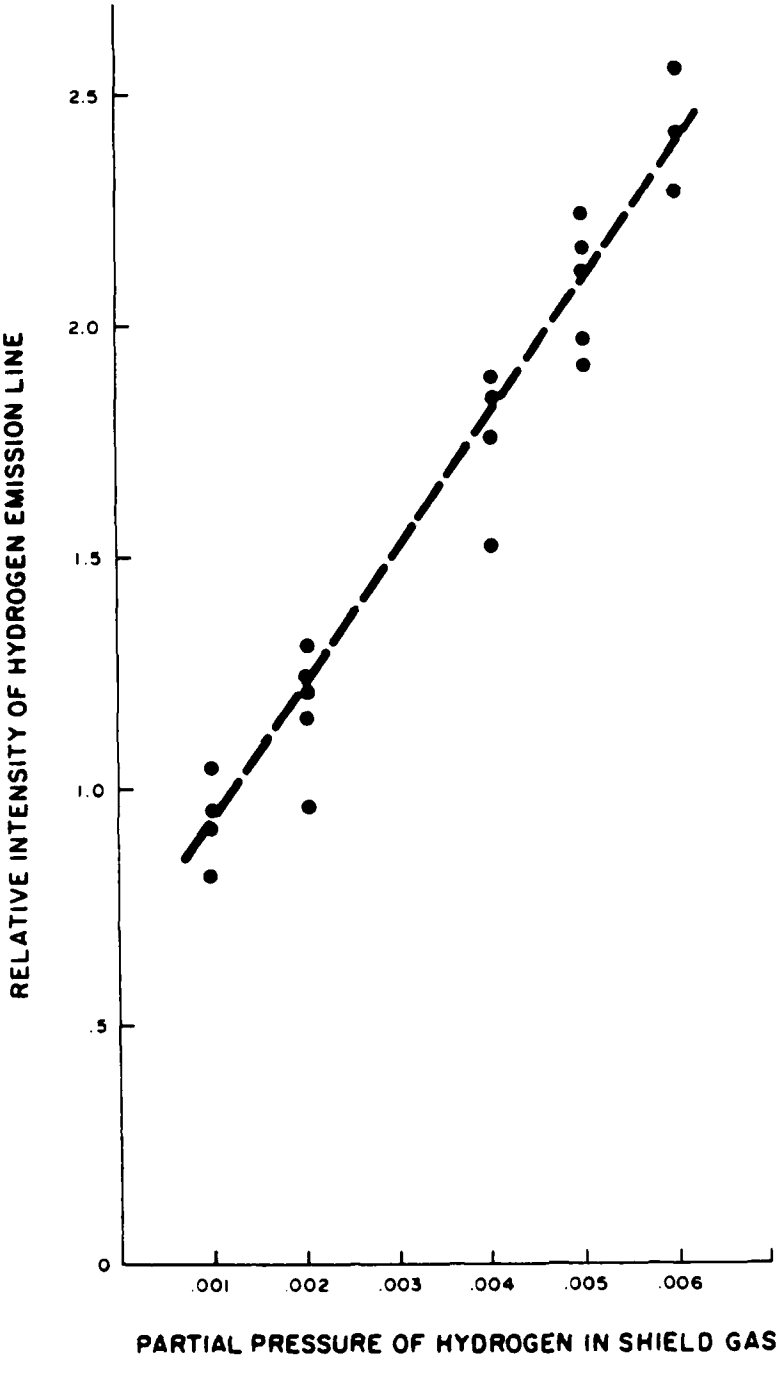

Figure 5.3 Relationship between relative hydrogen line intensity and partial pressure of hydrogen in weld arc atmosphere.

Figures 5.4 and 5.5 show the spectrum of light emitted by the welding arc in the 50 nm bandwidths surrounding the hydrogen lines which were used in making absolute intensity measurements of hydrogen ion density. The hydrogen lines of interest at 434.0 nm, 486.1 nm, 656.2 nm and other major peaks were identified using tables of spectral lines developed by the National Bureau of Standards [60].

Measurements of the weld arc temperature were made as described in section 3.5. When the number density of particles present in the state n, N_n, is plotted against E_n, the energy in the state n, the slope of the line will be 1/kT. This method was used to calculate the weld arc temperature from the absolute emission line intensities of three hydrogen lines. Figure 5.6 shows a typical plot of the data used in this calculation.

Table 5.1 displays the results of hydrogen ion density, electron density, and arc temperature measurements made on the welding arc as the hydrogen content of the shielding gas varies. The partial pressure of hydrogen in the weld arc atmosphere, as determined by dividing the hydrogen ion density by the electron density, is also listed. Weld arc temperature increased as the hydrogen content of the shielding gas increased. Figure 5.7 shows the change in weld arc temperature with increasing hydrogen content. Figures 5.8 and 5.9 display the averaged results of hydrogen ion density and electron density measurements, respectively. Figure 5.10 shows the average hydrogen partial pressure in the weld arc, as calculated spectroscopically, as a function of the partial pressure of hydrogen in the shielding gas.

In GTA welding, no hydrogen source in the form of filler wire lubricants is available to the welding arc. Therefore, the partial pressure of hydrogen in the weld arc atmosphere should closely approximate the partial pressure of hydrogen in the weld shielding gas. However, this result was not obtained in this experiment. Possible reasons for this will be discussed in Chapter 6.

The electron density and hydrogen ion density measurements are not inconsistent with results reported in the limited literature in this area [50]. Generally, the particle density measurements are close to the highest values reported in other studies.

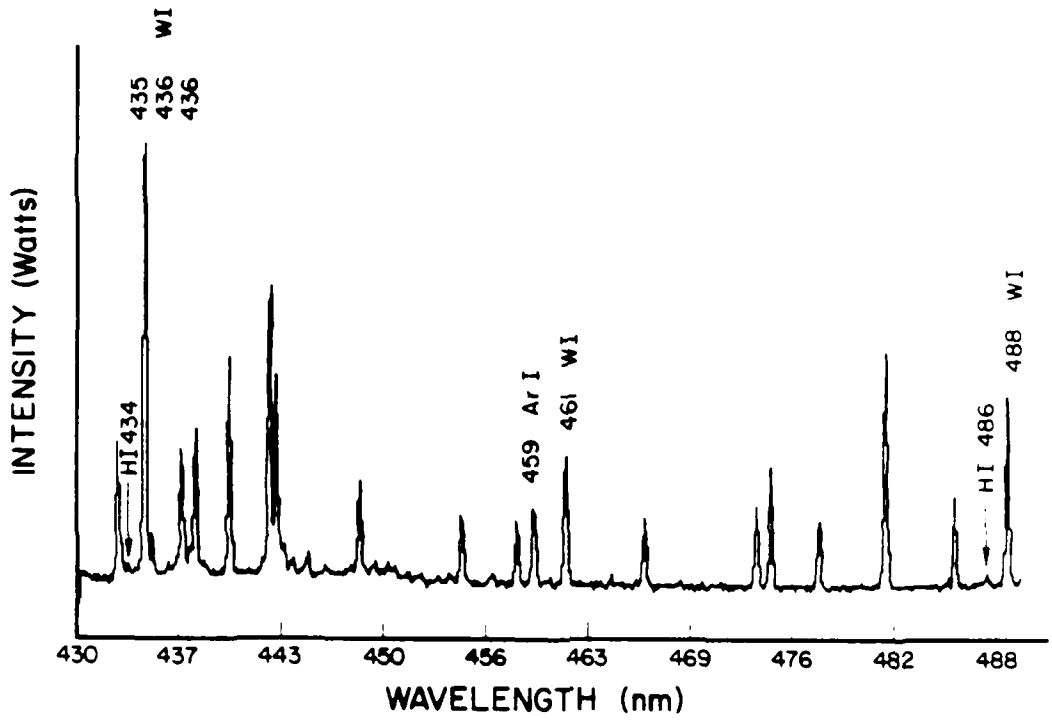

Figure 5.4 Weld arc spectrum in 60 nm bandwidth around the hydrogen lines at 434 nm and 486 nm.

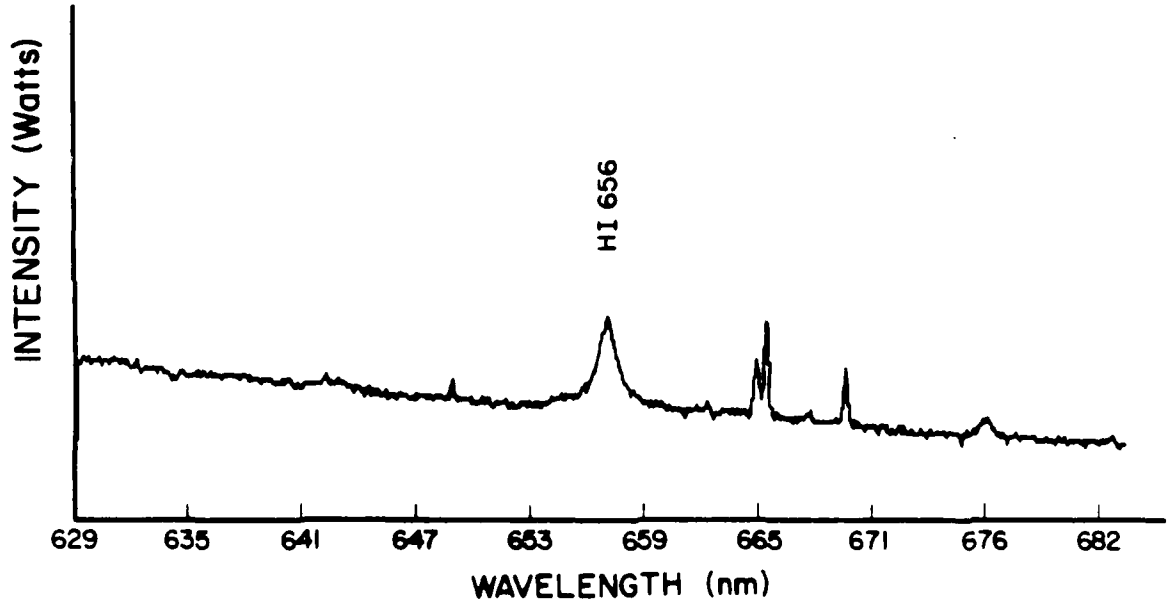

Figure 5.5 Weld arc spectrum in 60 nm bandwidth around hydrogen line at 656 nm.

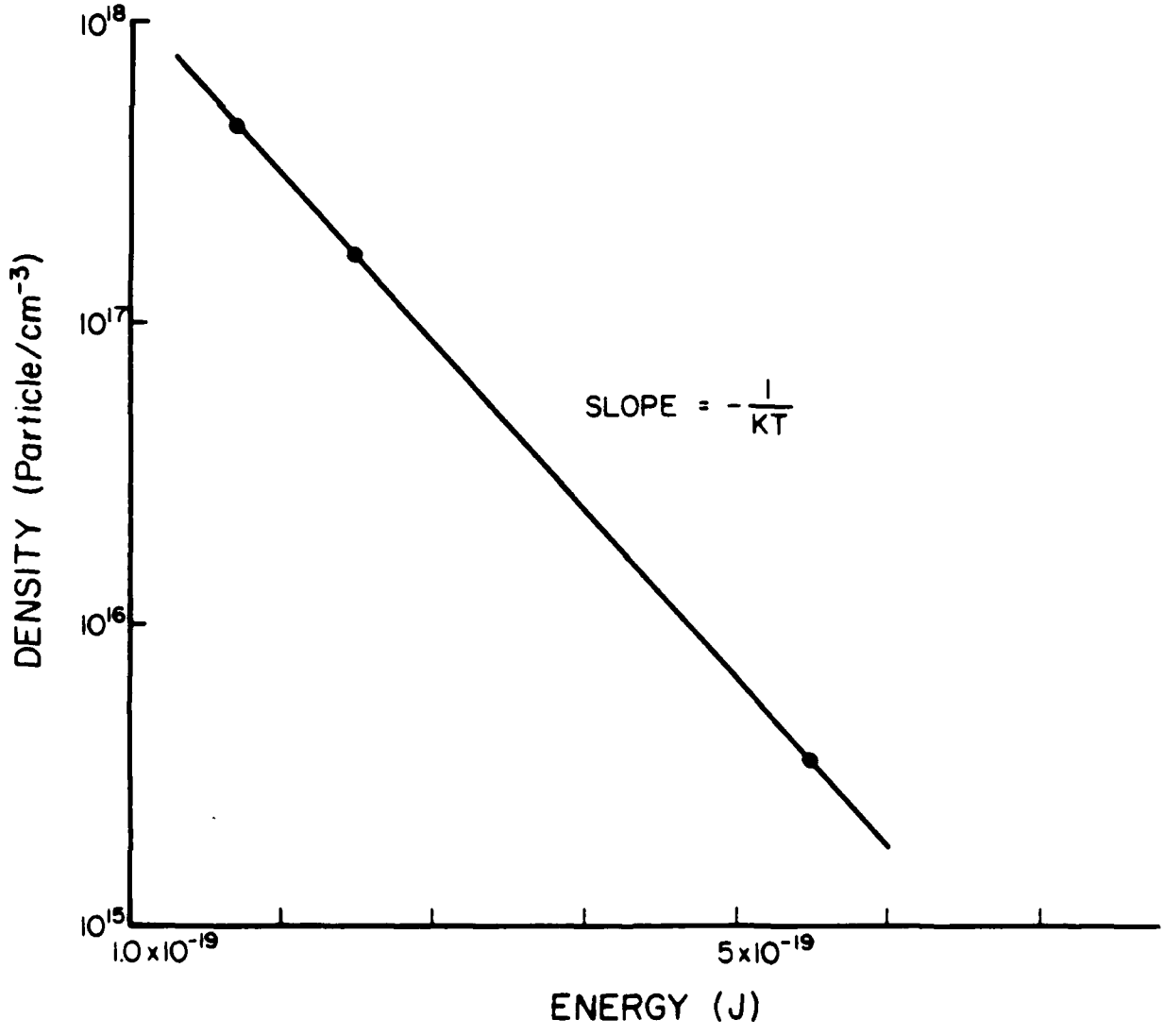

Figure 5.6 Method used to determine weld arc temperature.

Table 5.1 Results of Absolute Intensity Measurements on GTAW Arcs

% Hydrogen in Shielding Gas	Temperature (°K)	Calculated Hydrogen Partial Pressure	Hydrogen Ion Density (cm^{-3})	Electron (cm^{-3})
0	14400	0.83	1.28E+17	1.07E+17
0	14400	1.02	1.28E+17	1.3E+17
0	14400	5.4	5.4E+17	1.3E+17
0.5	19611	0.32	3.54E+17	1.12E+17
0.5	19611	0.56	2.07E+17	1.16E+17
0.5	19611	1.04	2.07E+17	1.16E+17
1	20200	0.46	3.51E+17	1.64E+17
1	20200	0.53	2.5E+17	1.34E+17
1	20200	0.656	2.5E+17	1.64E+17
1	20200	0.94	1.74E+17	1.64E+17
1.5	19131	0.445	3.55E+17	1.94E+17
1.5	19131	0.54	3.55E+17	1.94E+17
1.5	19250	1.26	1.53E+17	1.94E+17
2	22240	0.43	3.44E+17	1.48E+17
2	22300	0.52	3.44E+17	1.8E+17
2	22300	0.72	2.5E+17	1.8E+17

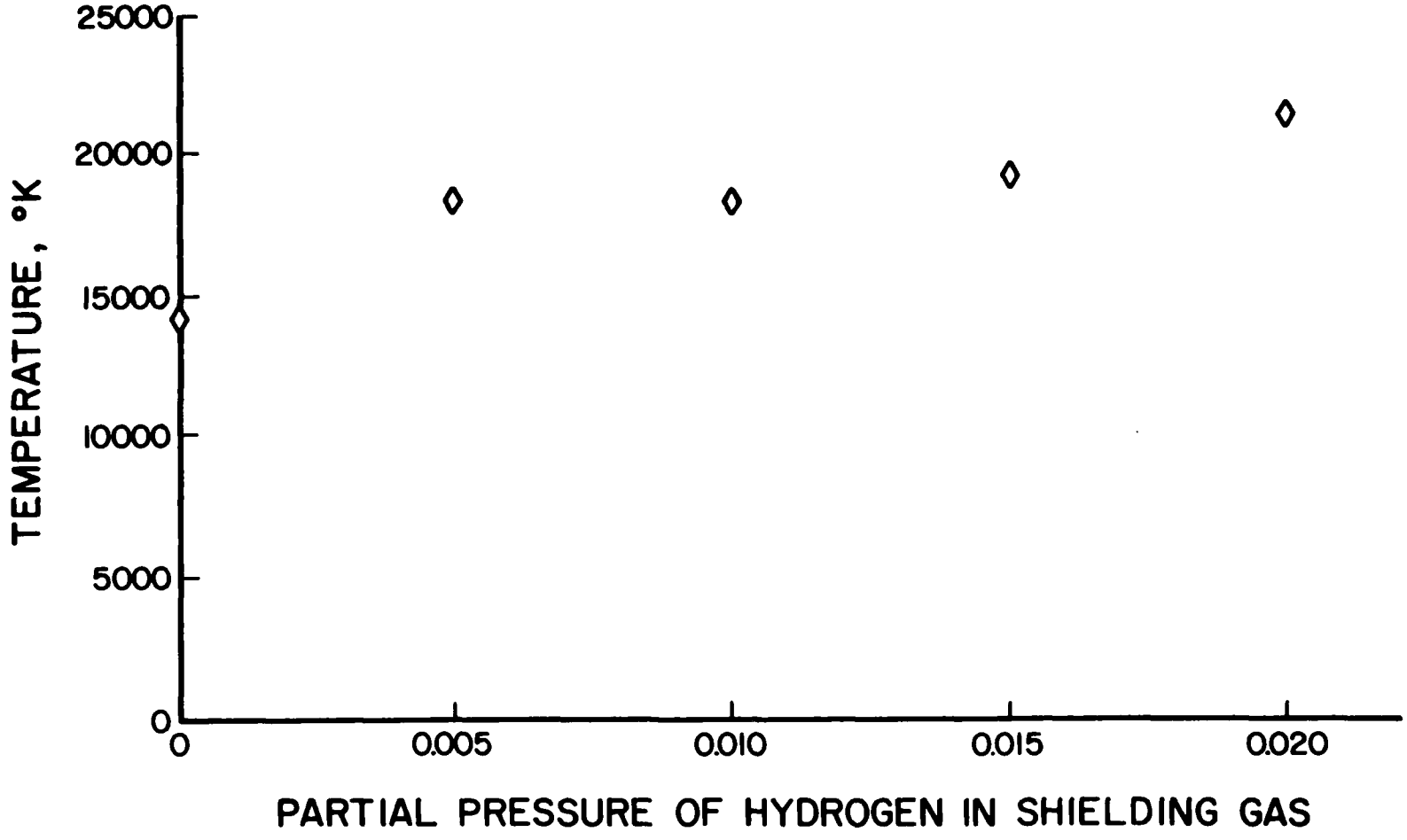

Figure 5.7 Effect of shield gas hydrogen content on spectroscopically measured weld arc temperature.

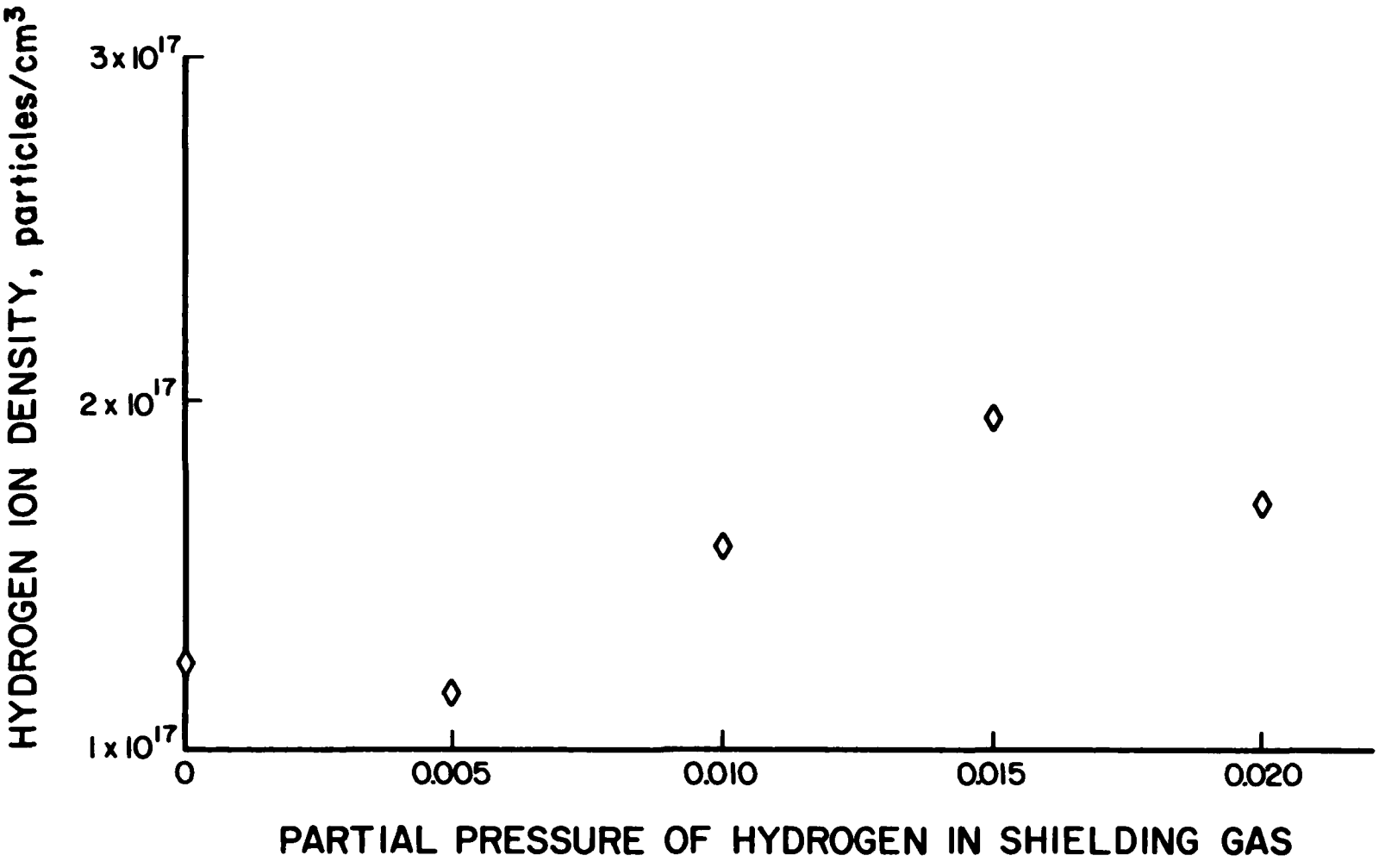

Figure 5.8 Effect of shield gas hydrogen content on spectroscopically measured hydrogen ion density.

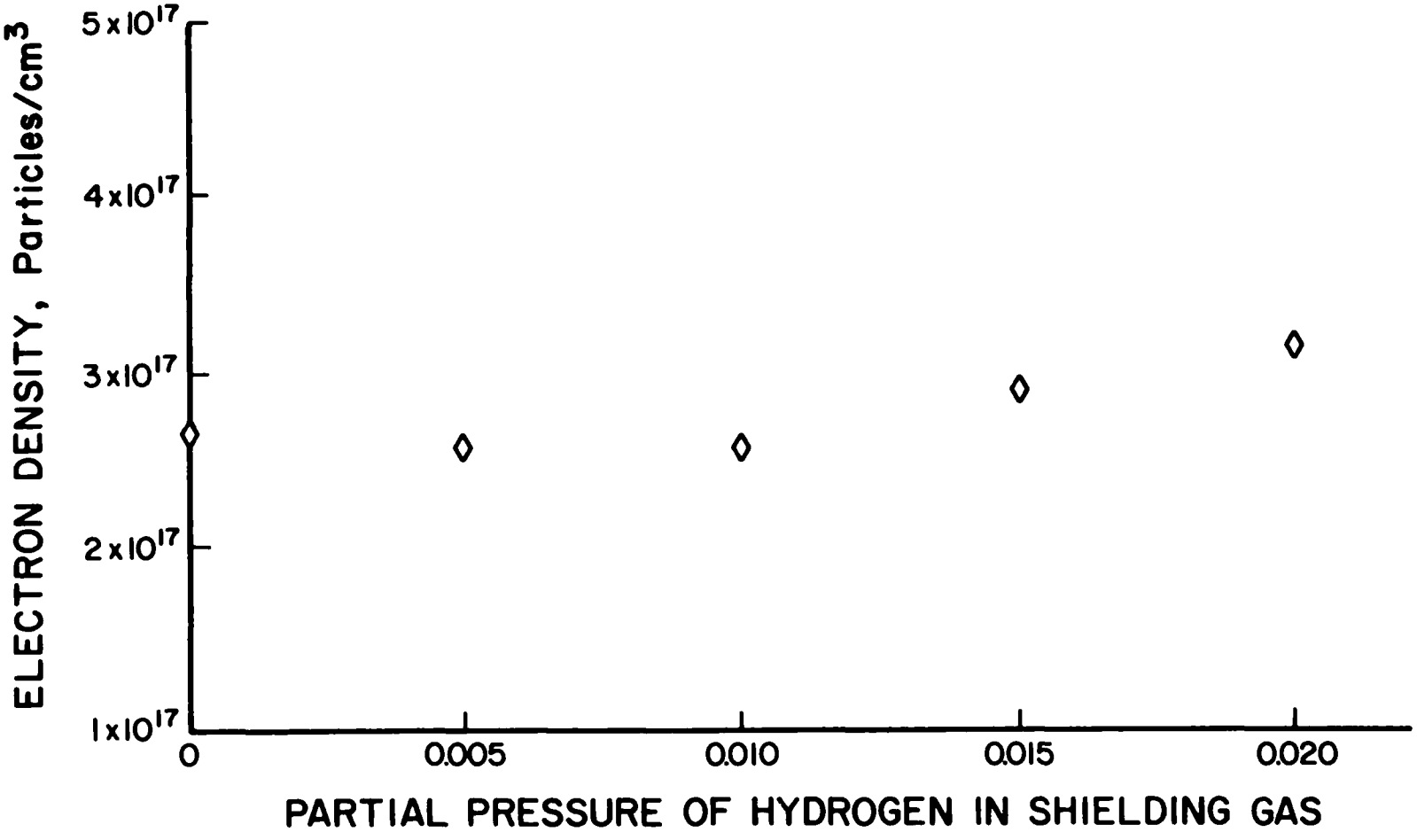

Figure 5.9 Effect of shield gas hydrogen content on spectroscopically measured electron density.

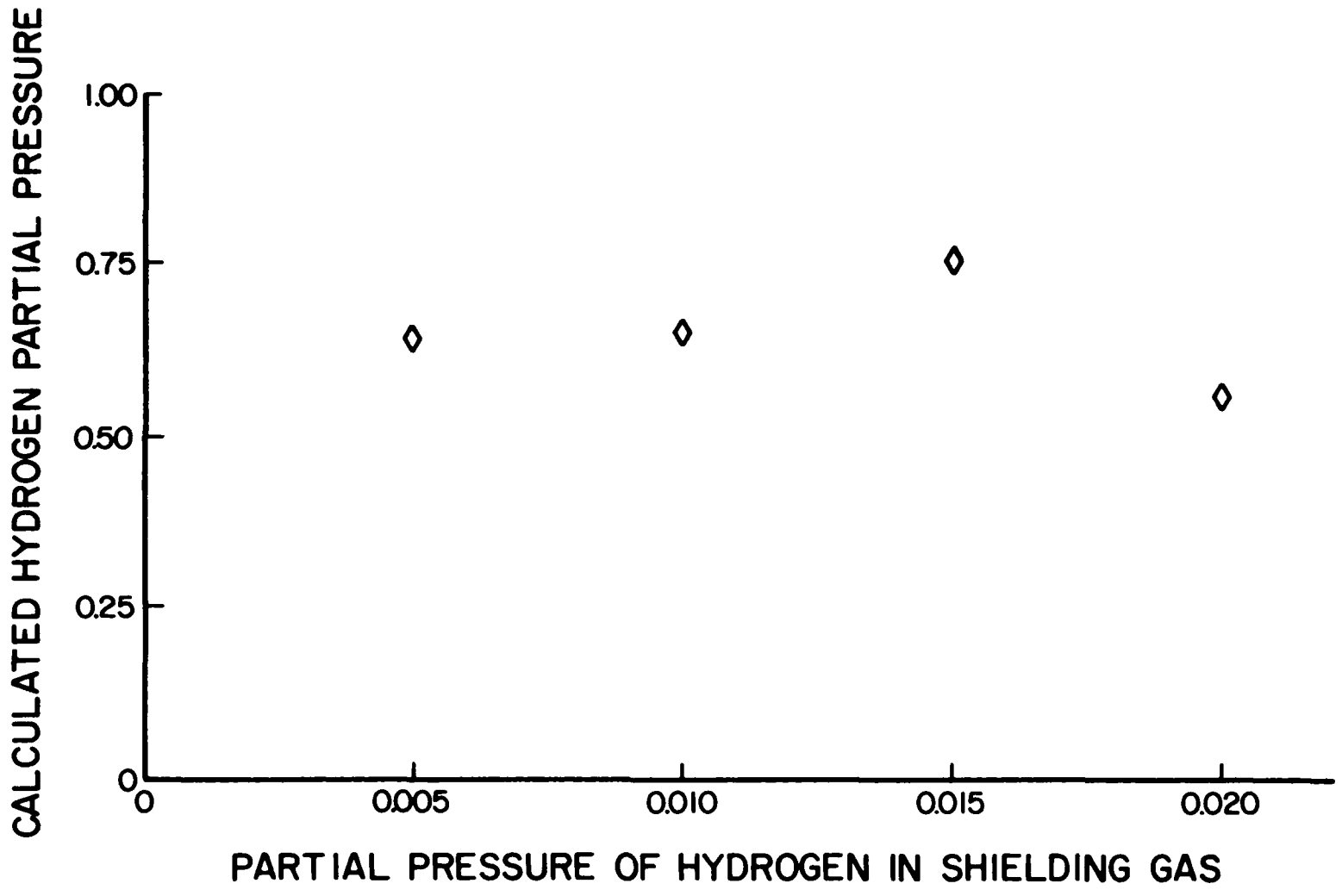

Figure 5.10 Results of absolute intensity determination of weld arc atmosphere hydrogen partial pressure.

5.3 Weld Diffusible Hydrogen Contents

The diffusible hydrogen content of GMA and GTA welding specimens was measured using various weld shielding gas contents to determine whether the results of spectroscopic measurements could be related to the hydrogen content of the resulting welds.

5.3.1 Gas Metal Arc Welds

GMAW diffusible hydrogen content specimens were prepared during acquisition of the spectroscopic data described in section 5.1 and analyzed as described in section 4.3.2. The rate at which hydrogen evolved from the specimens is shown in Figure 5.11, which demonstrates that no significant level of hydrogen remained in the specimens following outgassing. A recently published study showed that evolution of diffusible hydrogen from specimens of this type is complete within seven hours at 150°C [61].

Table 5.2 lists the results of the measurements of the diffusible hydrogen content of GMA welds. The hydrogen content of the welds increased as the hydrogen content of the weld shielding gas increased, as shown in Figure 5.12. In Chapter 6, the diffusible hydrogen content of the welded specimens will be correlated with the hydrogen content of the weld arc atmosphere and the relative intensity of the hydrogen emission line at 656.2 nm.

5.3.2 Gas Tungsten Arc Welds

The results of measurements of weld diffusible hydrogen content made on GTAW specimens are given in Table 5.3. The data are inconsistent. The average diffusible hydrogen content of the specimens increases up to shield gas hydrogen content of 1.0 percent and then decreases. This is apparently caused by the formation of porosity in the specimens as the shield gas hydrogen content increases.

Although it is possible to operate GTA welding equipment at voltages and currents as high as those commonly used in GMAW, these specimens were made using a far lower arc voltage and current than the GMAW specimens discussed above. The welding parameters were selected to prevent overheating during acquisition of spectroscopic data. The welding arc was in contact with the specimen for 45 seconds to 1 minute during these experiments. This lengthy contact was necessary to ensure that a sufficient quantity of hydrogen in solution would be present in the deposited metal to be measurable by the gas chromatography technique employed in this study.

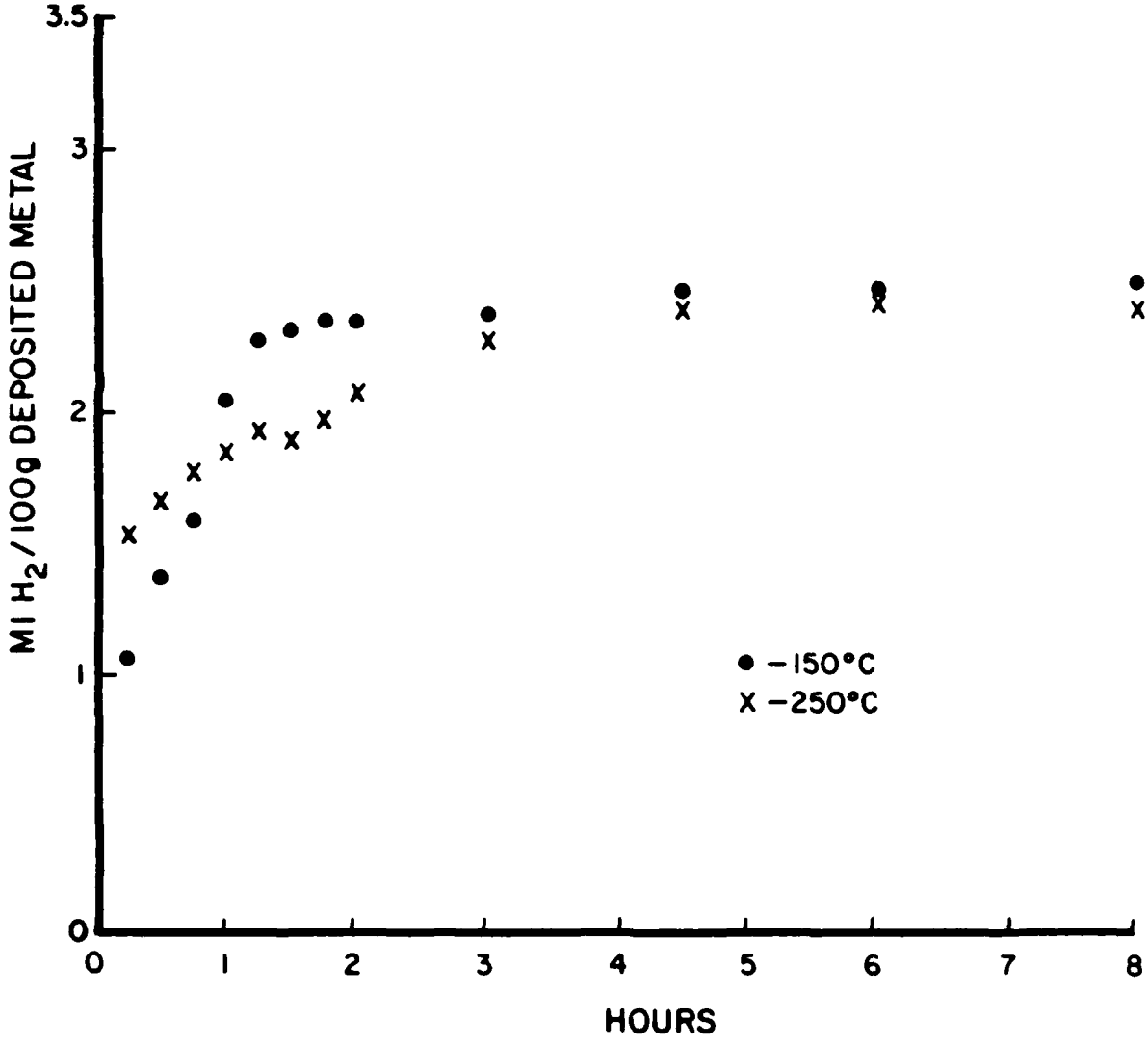

Figure 5.11 Outgassing behavior of diffusible hydrogen specimens at 150°C.

Table 5.2 Diffusible Hydrogen Content Data--GMA Welds

% Hydrogen in Shielding Gas	Diffusible Hydrogen Content of Test Welds (mL H_2/100 g deposited weld metal)				Average Diffusible Hydrogen Content of Test Welds (mL H_2/100 g deposited weld metal)
0.0	1.59	1.54	1.83		1.65
0.05	1.39	3.28	2.4		2.35
0.10	1.79	4.57	1.84		2.7
0.15	2.37	2.42	3.76		2.85
0.20	2.84	2.85	7.22		4.30
0.25	3.05	2.63	8.12		4.6
0.30	3.54	7.07	6.73		5.69
0.50	4.82	4.57	2.3	10.91	5.46
0.75	4.37	4.9	3.8	6.46	5.38
1.0	3.97	3.7	4.1		3.93

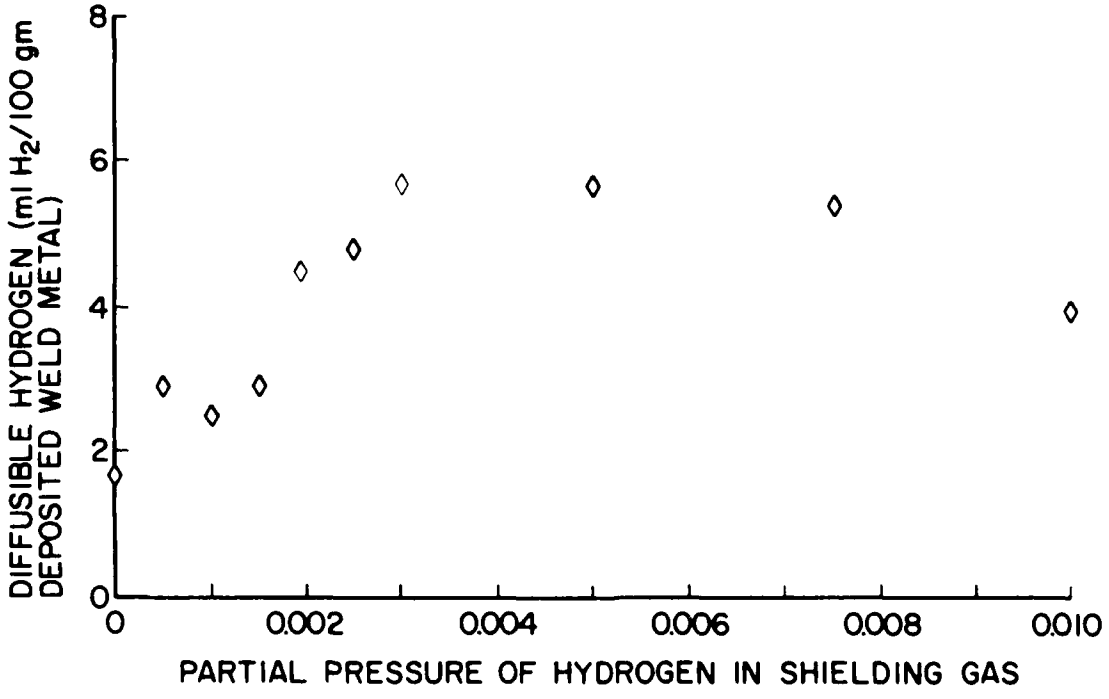

Figure 5.12 Change in weld diffusible hydrogen content with increasing shield gas hydrogen content.

Table 5.3 Diffusible Hydrogen Content Data--GTA Welds

% Hydrogen in Shielding Gas	Diffusible Hydrogen Content of Test Welds (mL H_2/100 g deposited weld metal)			Average Diffusible Hydrogen Content of Test Welds (mL H_2/100 g deposited weld metal)
0.0	2.04	0.94	0.5	1.16
0.5	3.59	5.6		4.59
1.0	2.95	10.18	19.38	10.84
1.5	1.30	2.0	0.642	1.3
2.0	2.20	3.71	5.11	3.67

An attempt was made to keep the deposited metal liquid during specimen fabrication. However, the use of the copper chill block to keep the base metal as cool as possible during welding (to prevent premature outgassing) makes this difficult. As a result, liquid circulation in the liquid pool is reduced. The liquid metal becomes supersaturated with hydrogen as the shield gas hydrogen content increases and porosity forms.

The hydrogen in these pores is present in the form of molecular H_2 gas which is not diffusible and is not measurable with this test. Hence, the measured diffusible hydrogen content of the welds decreases despite the increase in the partial pressure of hydrogen in the weld arc atmosphere.

5.4 Implant Tests

Implant tests were performed to determine the susceptibility of armor steel to hydrogen induced cracking. The objective was to determine how the mechanical properties of welds in armor steel are affected as the hydrogen partial pressure in the welding arc (and the diffusible hydrogen content of the welds) increase.

5.4.1 Metallography and Fractography of Implant Specimens

Figure 5.13 is a section through an implant specimen in which failure occurred, showing the geometry of the test and specimen failure in the heat affected zone. Figures 5.14 through 5.16 show the base metal, weld metal, and heat affected zone microstructures, respectively. No detailed analysis of microstructural effects was performed because fractography of the specimens showed that hydrogen trapping at inclusions was the most important factor in initiating hydrogen induced cracking. Although there was also evidence that some fracture occurred along the prior austenite grain boundaries, this was a minor effect compared to fracture initiation at inclusions.

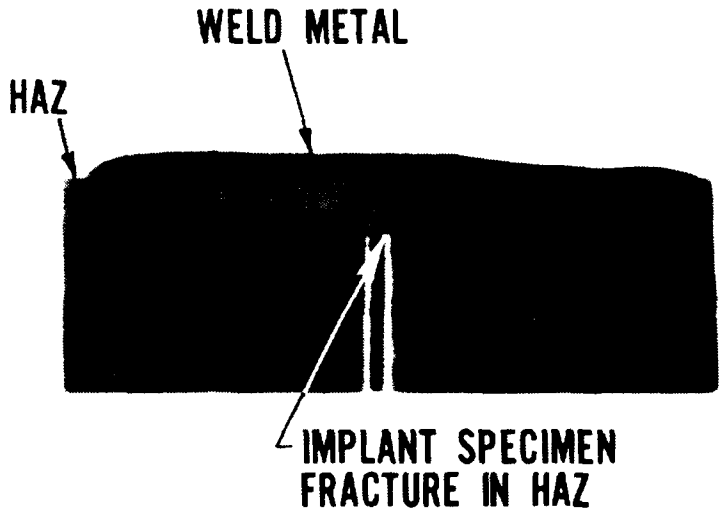

Figure 5.13 Section through implant specimen.

Figure 5.14 Armor steel base metal microstructure (160x).

Figure 5.15 Armor steel weld metal microstructure (160x).

Figure 5.16 Armor steel HAZ microstructure (160x).

Scanning electron microscopy was performed on the fracture surfaces of implant test specimens. The appearance of the fracture surfaces varied with the applied load and time to failure. Figure 5.17 shows an applied stress versus time to failure curve typical of the results of an implant test. It is divided into three regimes, each of which is characterized by a different type of fracture surface.

Regime A is composed of tests performed at high load levels (approaching the UTS) in which failure occurred in less than 10 minutes. The fracture surfaces of these specimens display mixed fracture characteristics. Areas of brittle fracture surround large inclusions as shown in Figure 5.18. Ductile, dimple rupture characterizes the fracture surface in areas not surrounding inclusions.

This type of failure occurs because atomic hydrogen dissolved in the weld diffuses preferentially to trapping sites such as inclusions. The hydrogen causes fracture of the inclusions as shown in Figure 5.19 and brittle crack growth in the metal surrounding it. The applied stress in these tests approaches the ultimate tensile strength of the material. Therefore, little hydrogen induced crack growth occurs before the final failure which takes place in a ductile fashion when the remaining section is too small to support the applied load.

The fracture surfaces in regime B are characterized by brittle, usually transgranular fracture, as shown in Figure 5.20. In this regime there is sufficient stress and sufficient time for hydrogen diffusion to the advancing crack tip, to permit extensive hydrogen induced cracking. Most of the brittle fracture occurs in a transgranular fashion. Some intergranular cracking is also found, however, as shown in Figure 5.21.

As in regime A, the fracture surfaces of specimens which did not fail during the 24-hour test period (region C) are dominated by ductile fracture. Brittle areas can be observed around inclusions as shown in Figure 5.22. While hydrogen diffused to trapping sites such as inclusions in these specimens just as in the short life specimens, insufficient hydrogen was present, or the applied load was too low for crack propagation to failure to occur. Instead, inclusion cracking is seen, accompanied by some brittle cracking in the metal matrix around the inclusions. Areas of ductile fracture are observed because tensile overloads were applied to specimens which did not fail within 24 hours to terminate the test and allow removal of the specimen. Hence, fracture of the uncracked material occurred in a ductile manner, as seen in Figure 5.22.

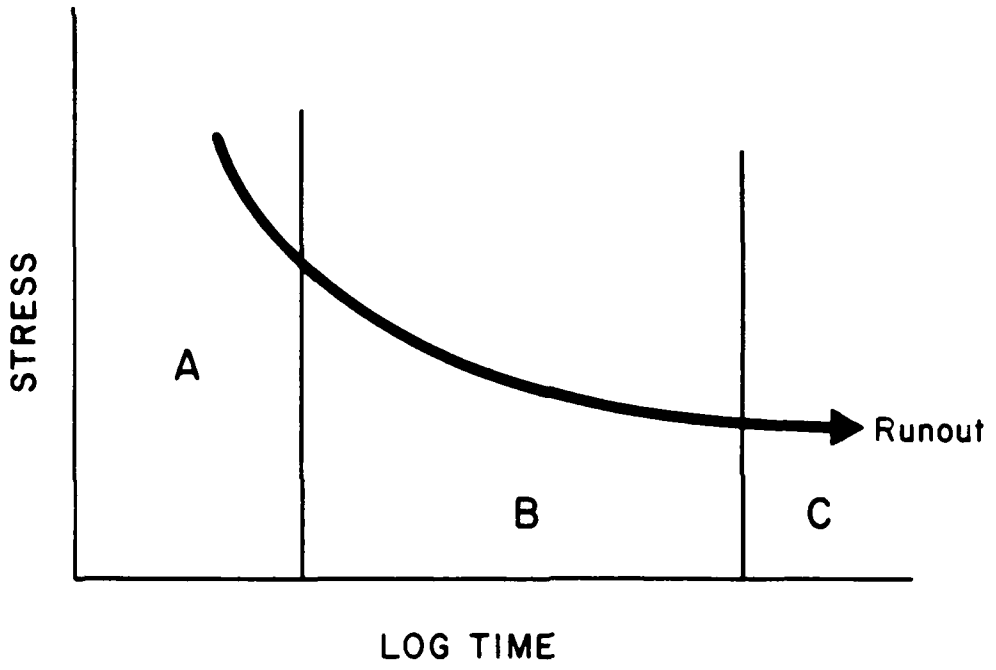

Figure 5.17 Load vs time to failure plot typical of implant test results showing three fracture type regimes.

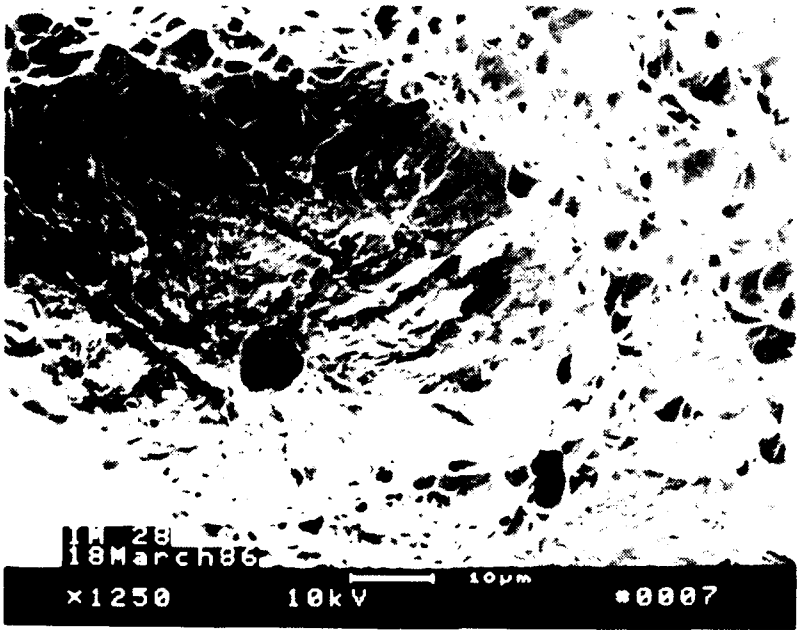

Figure 5.18 Brittle fracture surrounding inclusion site dimple ruture of surrounding area.

Figure 5.19 Brittle fracture of large inclusion.

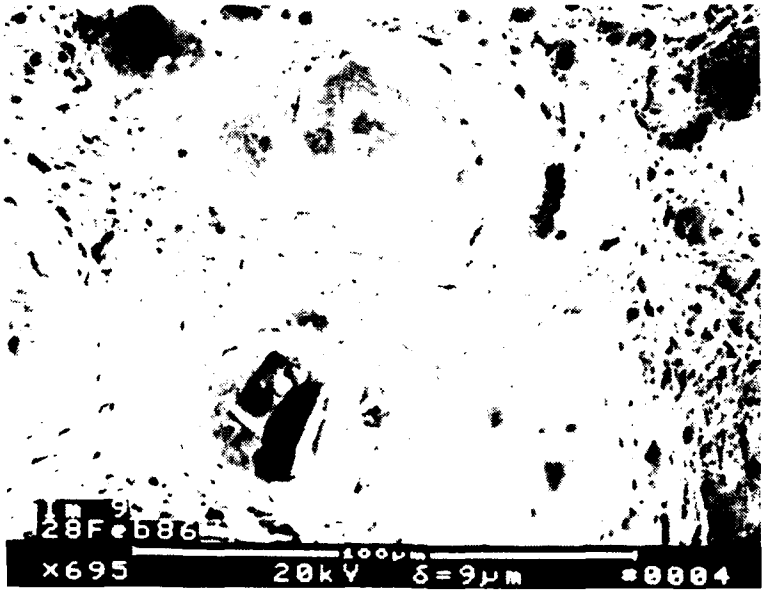

Figure 5.20 Brittle fracture surrounding inclusion in runout specimen.

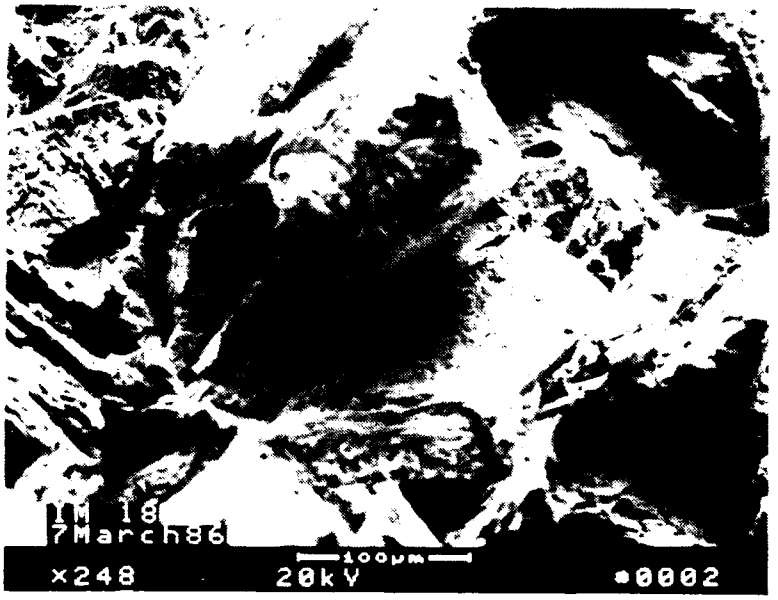

Figure 5.21 Brittle transgranular fracture characterized by large facets.

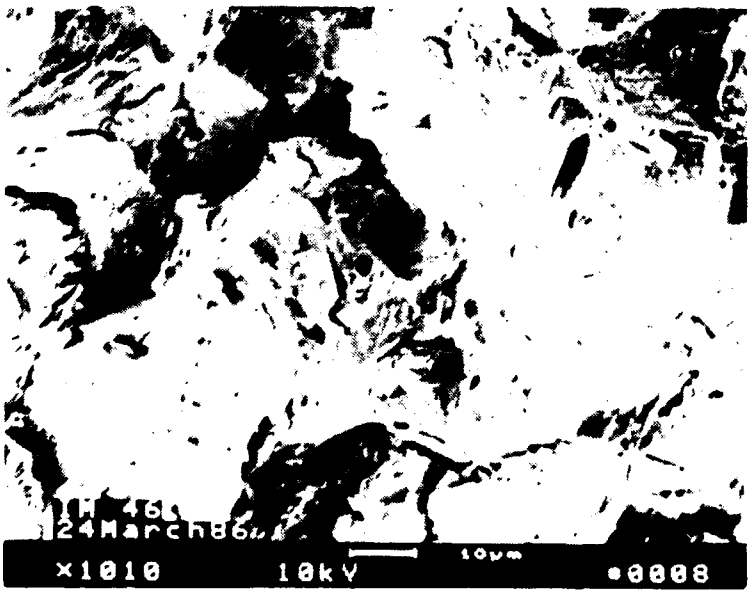

Figure 5.22 Intergranular and transgranular brittle fracture.

It is interesting to note that the results of the scanning electron microscopy support the theory that both a sufficient quantity of hydrogen and a sufficient level of tensile stress must be present for hydrogen induced cracking to occur. In implant tests in which the applied load was sufficiently low, brittle cracks initiated around hydrogen trapping sites but crack propagation did not occur.

5.4.2 Implant Testing Data

Figures 5.23 through 5.28 show the results of the implant tests performed as described in section 4.4.3. The tests were performed to determine how changes in the hydrogen content of the weld arc atmosphere affect the lower critical stress in this material. The lower critical stresses measured at each weld arc hydrogen content are listed in Table 5.4.

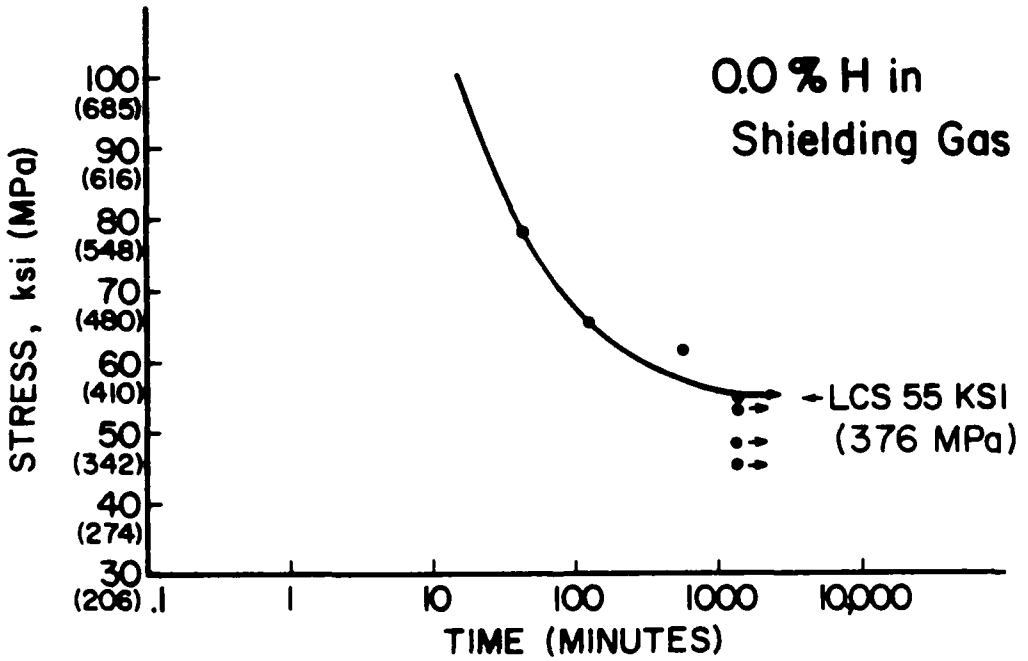

Figure 5.23 Implant test results--shield gas hydrogen content of 0.0 percent.

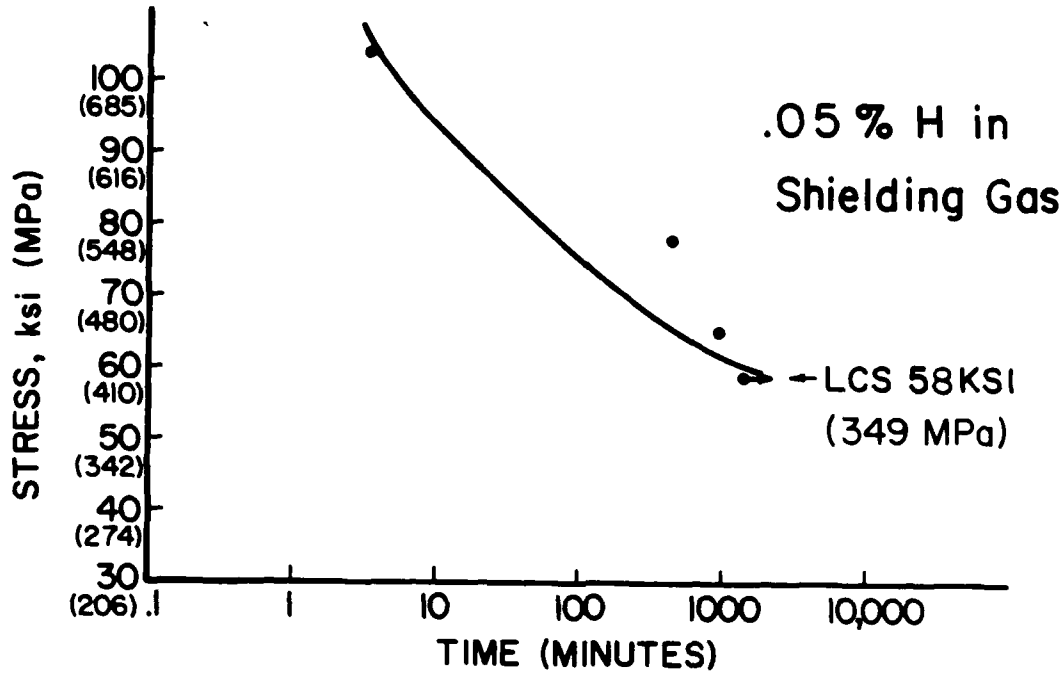

Figure 5.24 Implant test results--shield gas hydrogen content of 0.05 percent.

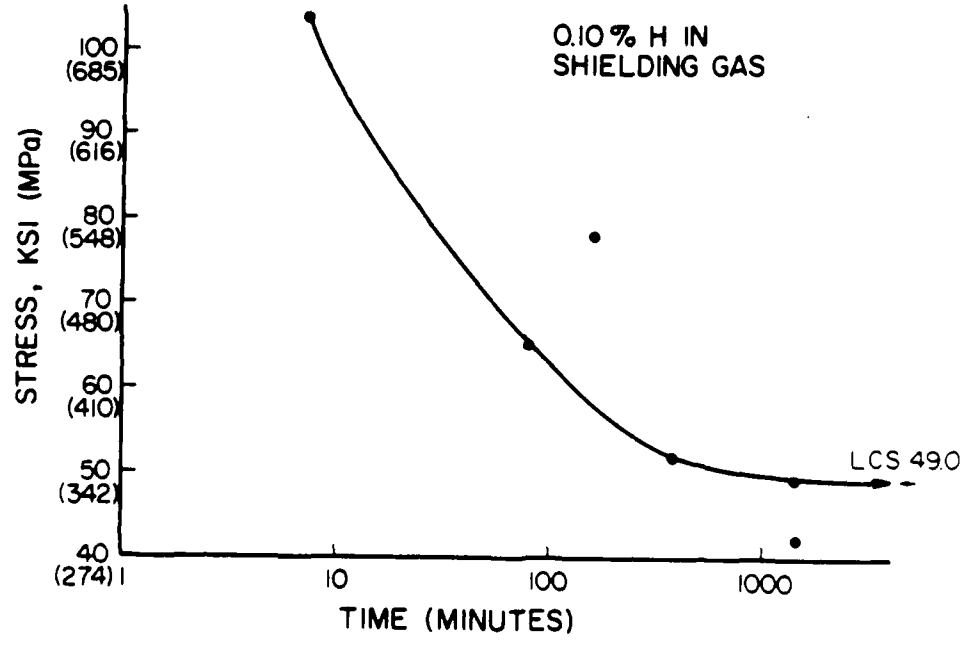

Figure 5.25 Implant test results--shield gas hydrogen content of 0.10 percent.

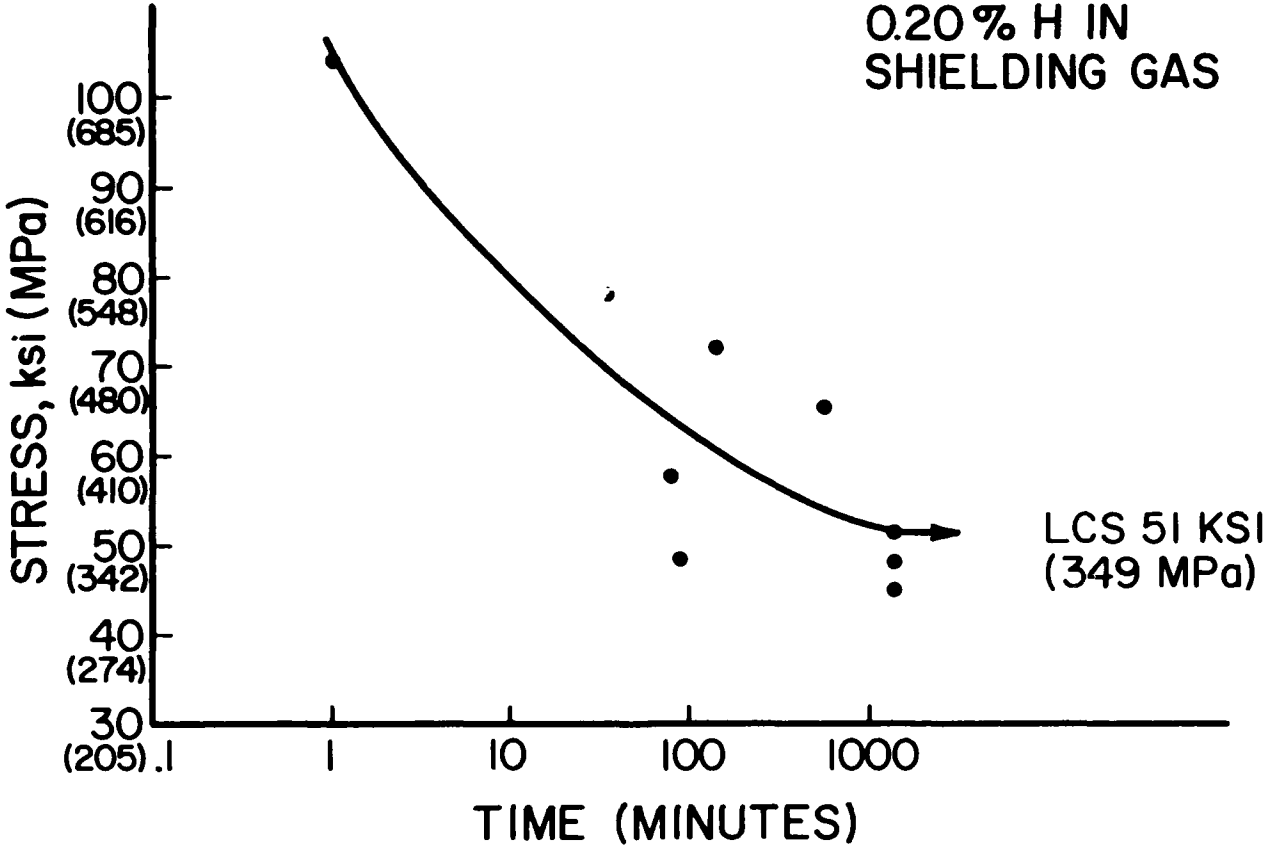

Figure 5.26 Implant test results--shield gas hydrogen content of 0.20 percent.

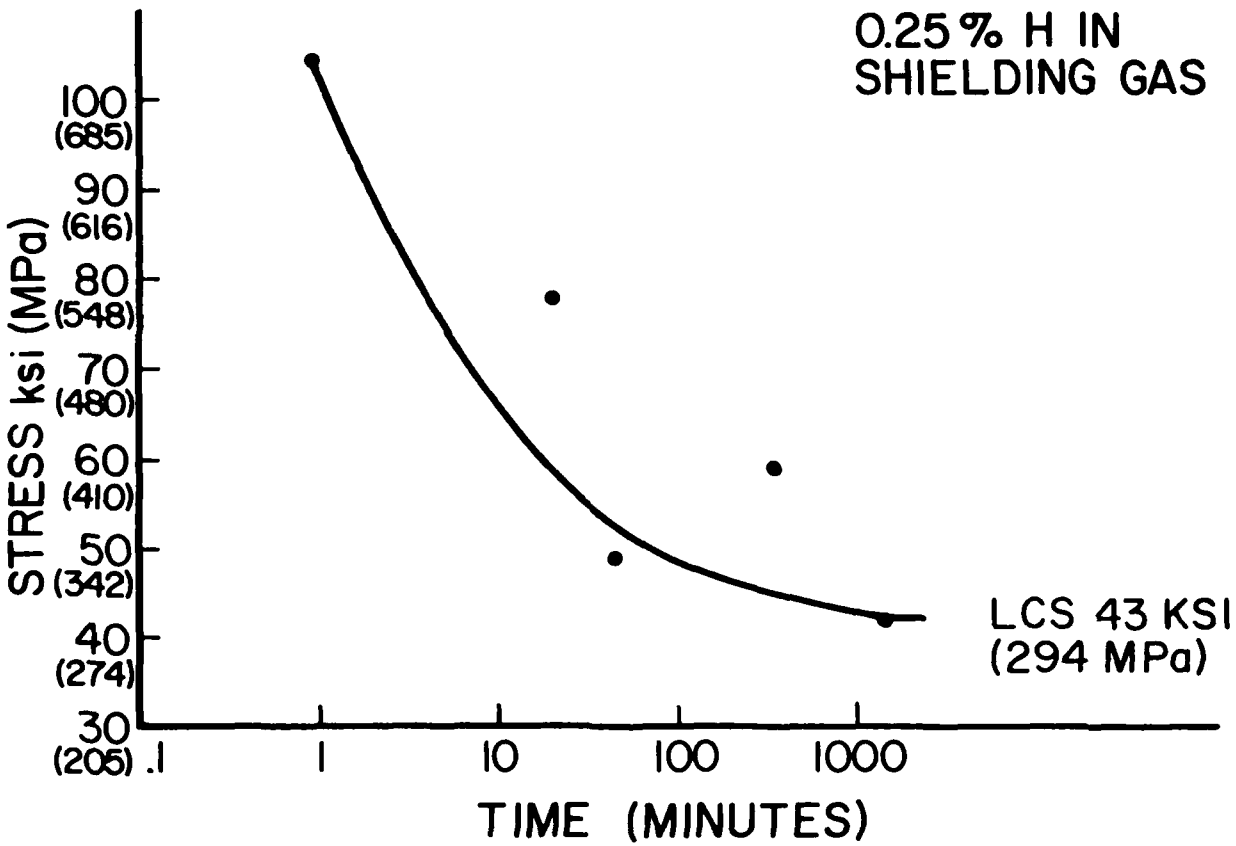

Figure 5.27 Implant test results--shield gas hydrogen content of 0.25 percent.

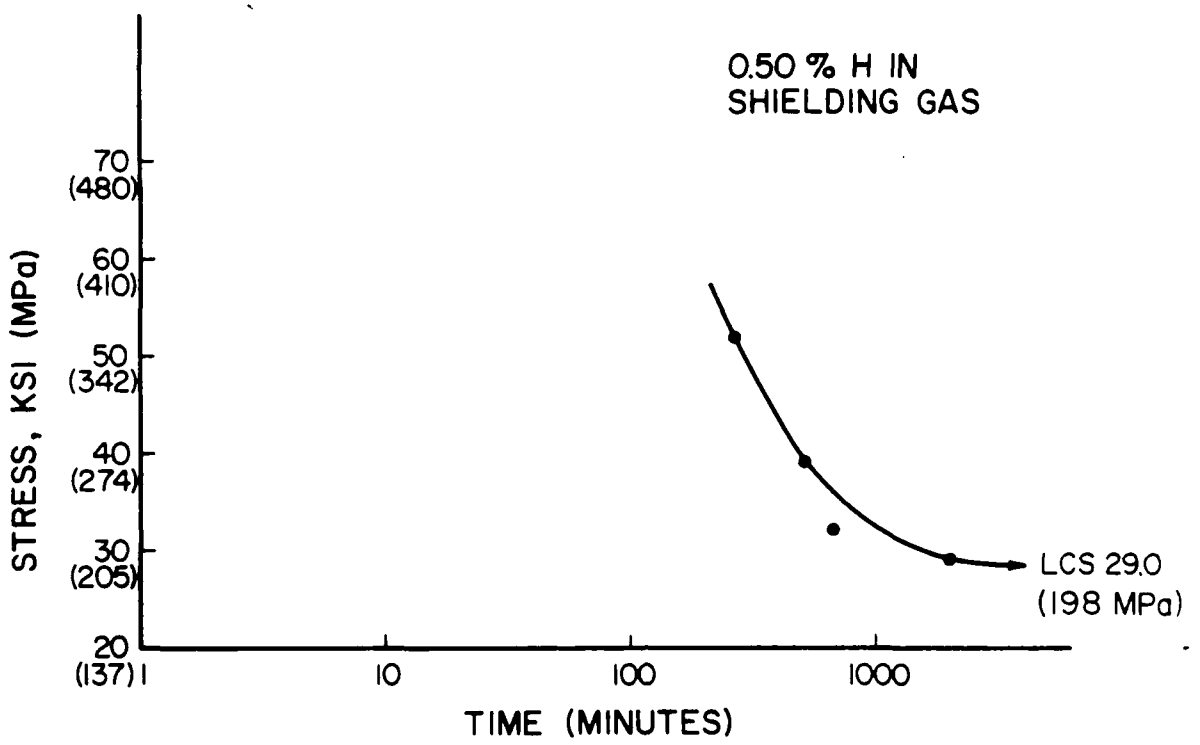

Figure 5.28 Implant test results--shield gas hydrogen content of 0.5 percent.

Table 5.4 Implant Test Data

% Hydrogen in Shielding Gas	Diffusible Hydrogen Content of Test Welds (mL H_2/100 g deposited weld metal)	Lower Critical Stress Ksi	MPa
0	1.65	55	377
0.05	2.35	58	397
0.1	2.7	53	365
0.2	4.30	51	350
0.25	5.46	43	295
0.5	6.05	29	199

The implant tests show that the lower critical stress decreases as the hydrogen content of the shielding gas (and weld arc atmosphere) increases. Figure 5.29 shows the change in lower critical stress as the shielding gas hydrogen content increases. Figure 5.30 shows the change in lower critical stress with the increase in weld diffusible hydrogen content (the result of increasing weld arc hydrogen content). As the hydrogen content of the weld shielding gas increased, the lower critical stress in the implant test generally decreased. When the shielding gas contained 0.50 percent hydrogen (the highest shield gas hydrogen content at which implant tests were performed) the implant rupture strength was only 55 percent of that measured when implant tests were run on specimens welded with hydrogen free shielding gas.

However, when 0.05 percent of hydrogen was added to the weld shielding gas, an increase in the lower critical stress over that measured under hydrogen free welding conditions occurred. This anomalous behavior could be the result of an increase in weld penetration due to the hydrogen addition to the welding arc [62]. Such an increase in penetration would increase the size of the molten pool. It is possible that the size of the fused metal and HAZ regions could increase enough to reduce the total hydrogen concentration in the joint, even though the hydrogen content of the weld arc atmosphere increased slightly.

The diffusible hydrogen content of welds made with a shield gas hydrogen content of 0.05 percent were slightly higher than those made with hydrogen free shielding gas. However, diffusible hydrogen measurements are made in terms of hydrogen/100 g deposited weld metal, not in terms of the total fused metal hydrogen content. Therefore, this very small hydrogen addition to the shielding gas could produce an increase in the amount of hydrogen/100 g of deposited weld metal, even though the hydrogen concentration in the entire joint decreased. A second reason for the observed increase in the implant strength could be slightly lower dislocation mobility caused by a small increase in hydrogen content of the joint. If the amount of additional hydrogen in the joint were sufficiently small, a slight strengthening might occur without causing significant embrittlement compared to the nominally hydrogen free condition.

Only 0.3 mL of additional H_2/100 g of deposited weld metal is added to the weld hydrogen content as the weld shielding gas hydrogen content goes from 0.0 to 0.05 percent. The reason for the observed increase in implant strength at a shielding gas hydrogen content of 0.05 percent is not important for the purposes of this investigation. Whatever the mechanism, the addition of small amounts of hydrogen to weld shielding gas is not recommended as a strengthening mechanism in armor steel welds on the basis of these results.

In the next chapter, changes in lower critical stress will be related to the diffusible hydrogen content of the weld, and the hydrogen content of the weld arc atmosphere.

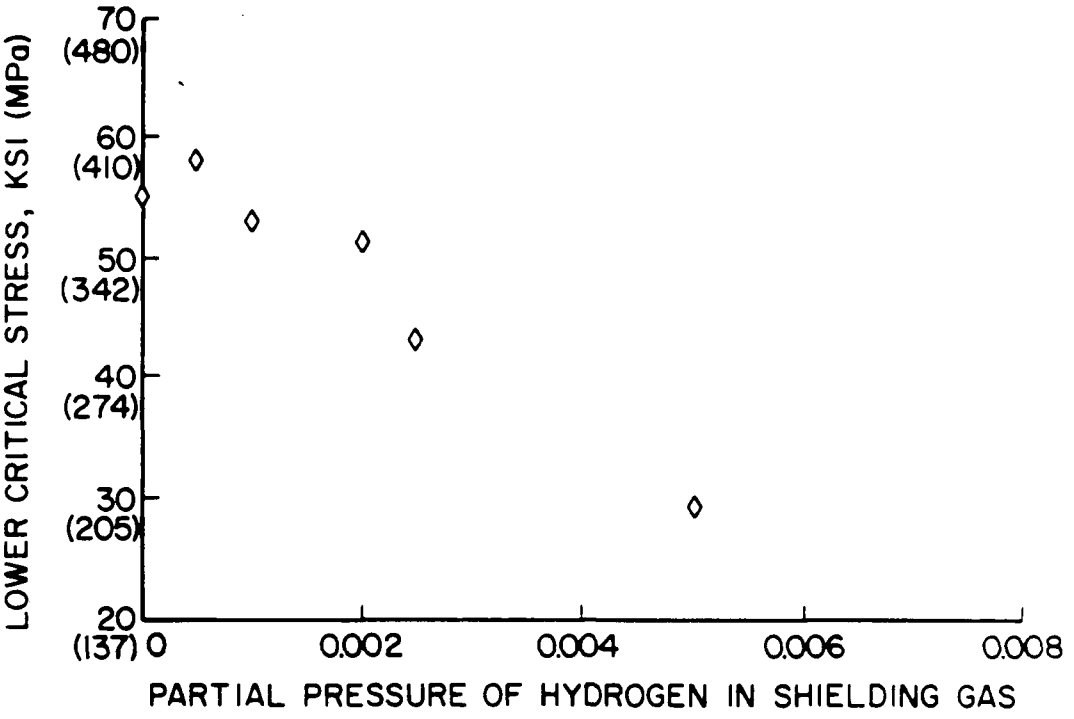

Figure 5.29 Change in lower critical stress with increasing shield gas hydrogen content.

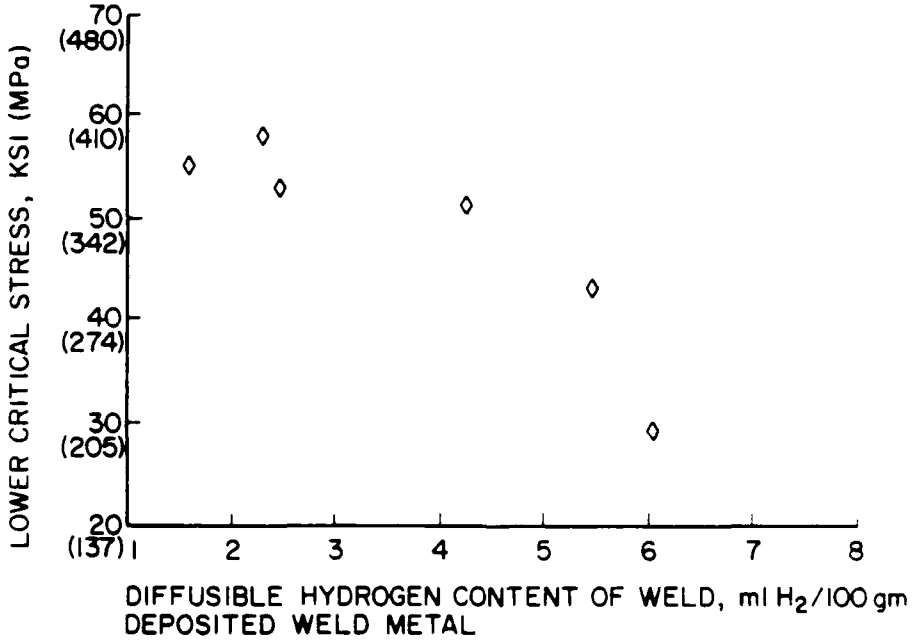

Figure 5.30 Change in lower critical stress with increasing weld diffusible hydrogen content.

6. DISCUSSION OF RESULTS

In the preceding chapter, the results of spectroscopic, diffusible hydrogen, and implant testing experiments were presented. In this chapter these results will be used together with Sieverts' law to develop a relationship between hydrogen emission line intensity and weld diffusible hydrogen content. Weld hydrogen content will be correlated with hydrogen induced cracking susceptibility in armor steel.

6.1 Sieverts' Law

In Chapter 2, previous uses of Sieverts' law in modeling hydrogen pickup during welding were discussed. Sieverts' law, which applies to the absorption of diatomic gases by metals, states that

$$C_H = S_H \, (P_{H_2})^{\frac{1}{2}} \qquad (6.1.1)$$

In the specific case of hydrogen absorption by steel during the welding process, C_H is the hydrogen content of the weld, P_{H_2} is the partial pressure of hydrogen in the atmosphere above the molten weld pool, and S_H is the solubility of hydrogen in steel at the temperature of the weld pool. Although Sieverts developed this expression empirically in the early part of the twentieth century [30], thermodynamic concepts can be used to arrive at the expression. For the reaction

$$H_2 \rightleftarrows [H] + [H] \qquad (6.1.2)$$

the reaction constant is

$$K = \frac{a_H^2}{P_{H_2}} \qquad (6.1.3)$$

In this expression, a_H is the activity of the dissolved hydrogen. The activity, a_i, of a substance is the ratio of the partial pressure of the substance, i, above a solution to the partial pressure of the pure substance, i. For small concentrations of hydrogen above steel, the activity of hydrogen is proportional to its concentration; hence

$$K = \frac{[\%H]^2}{P_{H_2}} \qquad (6.1.4)$$

or

$$[\%H] = K \, (P_{H_2})^{\frac{1}{2}} \qquad (6.1.5)$$

This expression is identical in form to equation (6.1.1).

To apply this expression to the prediction of the diffusible hydrogen content of arc welds, the solubility of hydrogen in the weld pool, S_H, and the partial pressure of hydrogen in the weld arc atmosphere must be determined.

6.1.1 Solubility of Hydrogen in the Weld Pool

The solubility of hydrogen in molten iron is a function of the temperature of the molten metal and its composition. Composition effects are relatively minor and were neglected in this study. It is difficult to determine the exact value of S_H as the temperature of the weld pool is neither uniform through the molten region nor well defined. Weinstein and Elliott [63] found that the expression

$$\log S_H = -\frac{1905}{T} + 2.455 \text{ ml } H_2/100 \text{ gm Fe} \qquad (6.1.6)$$

describes the solubility of hydrogen in iron. At a temperature of 2300°C, this equation gives a value of 51.8 mL H_2/100 g Fe. Howden and Milner [34] show a maximum solubility of approximately 48 mL H_2/100 g Fe, but do not provide an expression for estimating the value of S_H. The data of Weinstein and Elliott was used to assign a value to the solubility of hydrogen in the following sections.

6.1.2 Measurement of Hydrogen Partial Pressure in Weld Arc Atmospheres

The use of emission spectroscopy to measure the partial pressure of hydrogen in weld arc atmospheres was discussed extensively in Chapter 3. The two techniques presented (relative emission line intensity and absolute emission line intensity measurements) were used to determine the hydrogen partial pressures in GMA and GTA welding arc atmospheres respectively, and the values thus measured were used with equation (6.1.1) to predict weld hydrogen contents.

6.2 Prediction of the Hydrogen Content of GMA Welds: Relative Intensity Method

In section 5.1 it was shown that a linear relationship exists between the partial pressure of hydrogen present in the welding arc and the relative intensity of the hydrogen line at 656.2 nm. Thus, equation (6.1.1) can be written

$$C_H = S_H \left[f(I^H_{REL}) \right]^{\frac{1}{2}} \qquad (6.2.1)$$

Solving equation (5.1.1) for the partial pressure of hydrogen in the weld arc atmosphere, equation (6.2.1) can be rewritten as

$$C_H = S_H \left[(I^H_{REL} - 0.7)/(287.5) \right]^{\frac{1}{2}} \qquad (6.2.2)$$

This equation predicts the weld hydrogen content from a spectroscopically measurable quantity, i.e., the relative intensity of the hydrogen line at the wavelength 656.2 nm.

In this study, the calibration curve used to relate relative hydrogen line intensity to the partial pressure of hydrogen in the weld arc atmosphere was generated (as described in section 3.4.2) by equating the shield gas hydrogen partial pressure with the hydrogen partial pressure in the weld arc atmosphere. This introduces a slight error because the

effects of the dissociation of lubricants on filler wire, and any hydrogen present in the base plate on hydrogen line intensity, are neglected in generating the calibration curve. Thus, the spectroscopically measured hydrogen partial pressure will be slightly lower than the actual hydrogen partial pressure in the weld arc atmosphere. In order to compensate for this, another term, C_H^o, was added to equation (6.1.1), resulting in a modified version of Sieverts' law,

$$C_H = S_H (P_{H_2})^{\frac{1}{2}} + C_H^o \qquad (6.2.3)$$

Here, C_H^o refers to the hydrogen content of a weld made under nominally hydrogen free conditions. This term accounts for the amount of diffusible hydrogen absorbed by the weld pool from sources not considered in developing the spectroscopic calibration curve. Arata, et al. [32], included such a term in using Sieverts' law to predict the hydrogen content of underwater gas metal arc welds.

The diffusible hydrogen content of test welds fabricated under the cleanest possible conditions was measured to determine the value of C_H^o. Based on these tests, a value of 1.60 mL H_2/100 g deposited weld metal was assigned to this constant. This is similar to the value measured by other workers [32].

6.3 Comparison of Measured and Calculated Weld Hydrogen Contents: GMA Welds

The solubility of hydrogen in steel is strongly dependent on temperature; therefore, selection of weld pool temperature for calculations of weld hydrogen content is very important. Some workers have estimated the weld pool temperature to be 1600°C to 1700°C [5,7], but more recent work indicates that the weld pool is much hotter, with temperatures as high as 2300°C [34,35].

Mallett [7] obtained good agreement between theoretical and measured values of hydrogen by estimating the weld pool temperature to be between 1550°C and 1700°C. Therefore theoretical weld hydrogen contents were calculated for 1700°C as well as for weld pool temperatures of 2100°C and 2300°C on the basis of later work [35].

The calculated and measured values of the weld hydrogen contents are found in Table 6.1. Comparisons between the calculated and measured diffusible hydrogen content of the welded specimens are shown in Figure 6.1. At low hydrogen partial pressures, the measured weld hydrogen contents are very close to the calculated values obtained when a weld pool temperature of 1650°C to 1700°C is assumed. However, at higher arc atmosphere hydrogen concentrations, weld hydrogen contents calculated for higher weld pool temperatures agree more closely with the measured weld hydrogen contents.

When the shield gas hydrogen content is increased to 1.0 percent, a drop in the measured diffusible hydrogen content of the weld is observed. This is due to the generation of porosity in the weld as the shield gas hydrogen content increases. Hydrogen present in the form of porosity is non-diffusible, and either escapes from holes in the top of the weld or remains trapped in subsurface pores.

The apparent increase in hydrogen solubility as the shield gas hydrogen concentration increases is probably due to an increase in weld pool temperature as the hydrogen content of the arc atmosphere increases. Several factors contribute to this temperature increase.

The addition of hydrogen to the weld shielding gas tends to cause an unstable arc. An increase in arc current helps to stabilize the arc but also increases the arc temperature [64]. Hydrogen dissociates in the welding arc. However, near the anode surface, hydrogen is known to give up heat of association in the complex reactions occurring in the anode drop zone, increasing local temperature [65]. Furthermore, the presence of hydrogen in weld shielding gas produces some constriction of the welding arc. Hydrogen also has a thermal conductivity approximately ten times that of argon [66], so it is clear that a variety of causes exist for an increase in weld pool temperature as the hydrogen content of the weld shielding gas increases.

Table 6.1 Measured and Predicted Weld Diffusible Hydrogen Contents--GMA Welds

% Hydrogen in Shielding Gas	Average Measured Weld Diffusible Hydrogen Content (mL H_2/100 g deposited weld metal)	Predicted Weld Diffusible Content (mL H_2/100 g deposited weld metal) for Each Weld Pool Temperature		
		1700°C	2100°C	2300°C
0.0	1.65	1.65	1.65	1.65
0.05	2.35	2.39	2.70	2.86
0.10	2.7	2.68	3.13	3.34
0.15	2.85	2.90	3.45	3.72
0.20	4.30	3.08	3.72	4.03
0.25	4.6	3.25	3.95	4.30
0.30	5.69	3.40	4.17	4.55
0.5	5.46	3.89	4.88	5.38
0.75	5.38	4.38	5.61	6.21
1.00	3.73	4.80	6.21	6.90

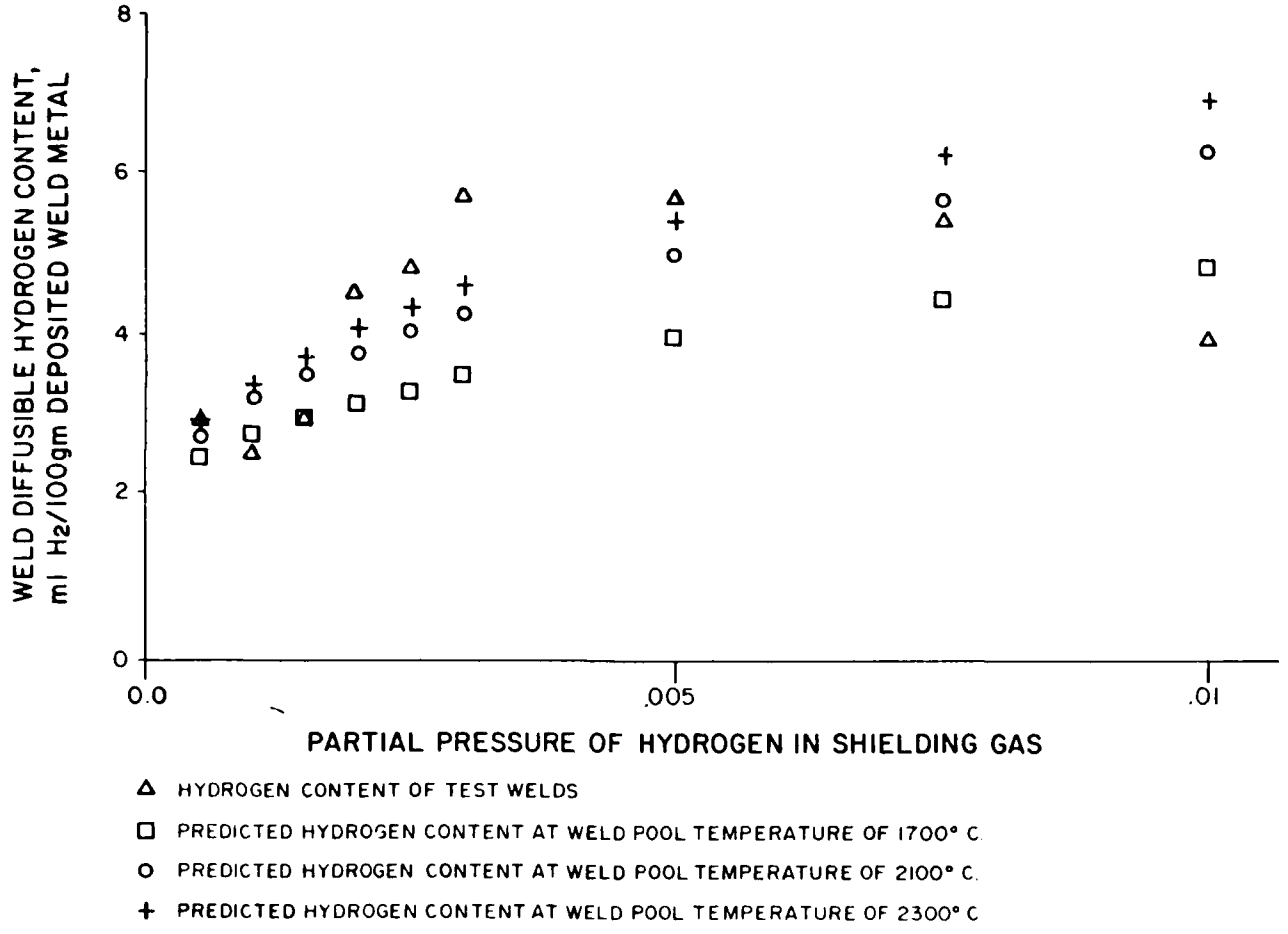

Figure 6.1 Comparison of experimentally measured weld hydrogen contents with weld hydrogen contents predicted by a modified version of Sieverts' Law.

Some observations made by Salter [35] support this hypothesis. He observed that an increase in hydrogen partial pressure in the weld arc atmosphere produced a change in the apparent optical intensity (brightness) of the "hot zone" immediately under the center of the welding arc. Although no appreciable increase in the size of this zone was observed, the increased brightness can be explained by an increase in the temperature of the weld pool in the zone immediately beneath the arc. In measurements of weld pool temperatures made in the same study, an increase in the partial pressure of hydrogen in the arc atmosphere was found to have a negligible effect on weld pool temperature. However, in a later study, an increase in anode temperature was observed as hydrogen was added to the argon shielding gas in GTA welding [65].

Convection occurs in the weld pool, allowing excess hydrogen absorbed in hotter parts of the weld pool to be carried to other parts of the weld pool by the stirring action. Lancaster [67] suggests that hydrogen absorption to the limit of solubility occurs at the arc root. Hydrogen is then distributed throughout the weld pool by metal circulation.

6.4 Absolute Intensity Measurements

Absolute intensity measurements of weld arc hydrogen partial pressure were made to determine whether more accurate prediction of weld diffusible hydrogen content could be made with this technique than with the relative intensity approach. The results of the absolute intensity measurements of hydrogen partial pressure in the GTAW arc atmosphere were not accurate enough to make such predictions. However, a number of other interesting results were obtained and are discussed in the following sections.

6.4.1 Temperature Measurements

The results reported in Chapter 5 showed that reasonably good agreement was found between the temperatures measured in this study and results reported in the literature. Furthermore, the expected increase in the average weld arc temperature as the hydrogen content of the weld arc atmosphere increased was observed. However, it must be recognized that the measured temperatures do not represent spatially resolved determinations of local weld arc temperatures.

A radial distribution of temperatures exists in a welding arc as shown in Figure 6.2(A) and (B). If local arc temperatures are to be determined, a small segment of the arc must be spatially resolved and the light emitted by it focussed on the entrance slit of a monochromator. However, welding arcs are approximately axisymmetric, so that the temperature varies along the line of sight through the arc as shown in Figure 6.2(C). The Abel inversion method is used to compensate for this temperature change, by converting intensity data in terms of W/cm^2-ster to a volume intensity in a local region which can be characterized by a single temperature in terms of W/cm^3-ster [68].

Griem [47] describes the use of this method, and it is used in most reported attempts to measure temperature distributions in welding arcs [49,52,64,69].

The Abel inversion was not used in these measurements because the optical system used was designed for performing relative intensity measurements of average weld arc composition and is not capable of spatially resolving small areas in the welding arc. Therefore, the intensity measurements were dominated by the light emitted from the brightest (i.e., hottest) part of the welding arc. Thus, the temperatures measured in this study are valid if they are considered to represent an upper bound on the average temperature of the welding arc [70].

The temperature measurements are also of interest because they support the conclusion in section 6.3 that increasing the hydrogen content of the weld arc atmosphere results in an increased weld pool temperature. It was also noted in section 6.3 that hydrogen absorption is controlled by the temperature in the hottest part of the weld pool where hydrogen solubility is highest. Thus, use of temperature measurements which represent an upper bound is reasonable in examining the effect of shield gas hydrogen content on weld arc and weld pool temperatures.

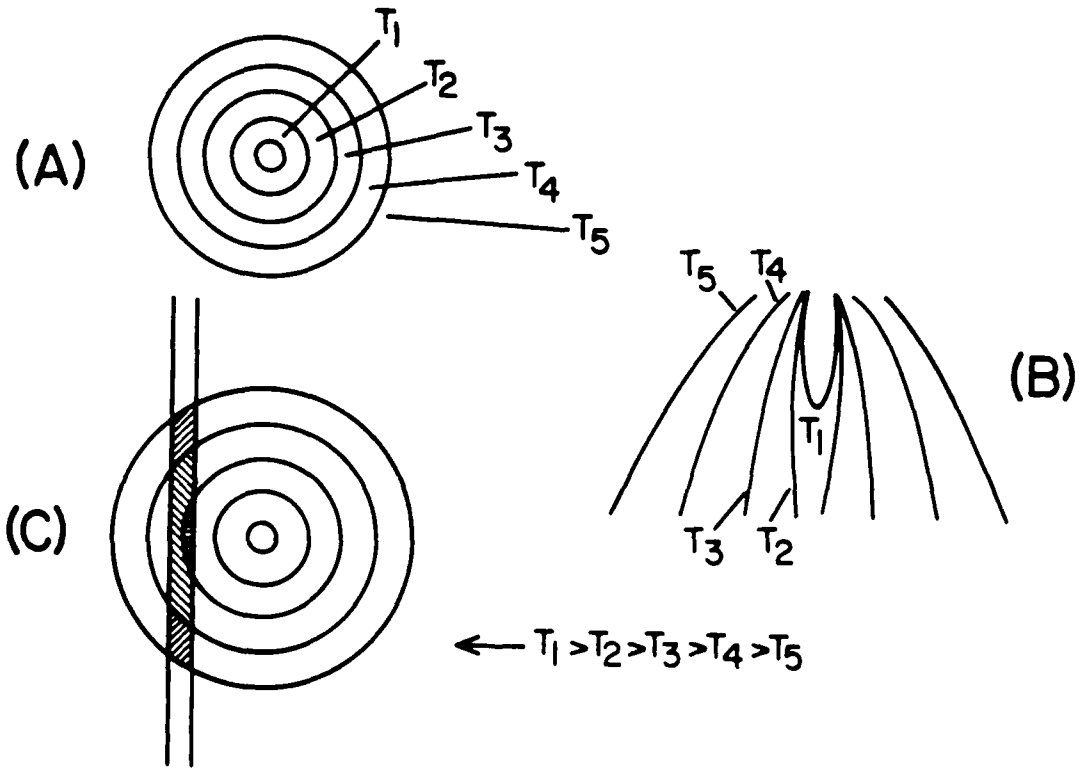

Figure 6.2 Temperature distribution in the welding arc and line of sight through zones of changing temperature.

6.4.2 Electron Density Measurements

Weld arc temperature measurements were performed in this study largely for the purpose of measuring the electron density of the weld arc plasma. As discussed in section 3.5.2, electron densities can be determined from the Stark width of a hydrogen line, and the temperature of the plasma. Electron density is a slowly varying function of temperature [47], so using maximum weld arc temperatures in determining electron density does not greatly affect the results. The electron densities measured in this study agree reasonably well with those reported in other work [50].

However, it is clear from Figure 5.9 that there are some inaccuracies in the electron density measurements. Electron density is observed to increase with the hydrogen content of the shielding gas. But, shield gas hydrogen content should not have a significant effect on electron density.

It is possible that the increase in the weld pool and weld arc temperature associated with the additional hydrogen increases the metal vapor pressure above the weld pool sufficiently to produce the observed increase in electron density. When the metal vapor pressure above the weld pool increases, a large number of easily ionized metal atoms are added to the arc atmosphere. The temperatures in the welding arc are capable of causing secondary ionization in some of these atomic species (particularly Fe, Cr and Mn). In this case the welding arc was struck on a tungsten work piece, however, so this effect should be far less significant than in experiments with lower melting point materials.

Electron density is calculated from measurements of the width of a hydrogen line at the point where the line intensity has dropped to one half of its maximum (i.e., the Stark width of the line). Griem [47] states that significant error will not be introduced by ignoring the continuum radiation level below the hydrogen peak. However, as seen in Figure 6.3, the effect of the continuum level on the Stark width of hydrogen lines as measured in this experiment is large. Furthermore, nonlinearity in the photodiode response could have affected the observed line intensity as the hydrogen content of the welding arc increased.

Changes which could be made to decrease these errors are discussed later in this section. However, an error of 16% in electron density measurements is considered to be small [47], so it is possible that greatly increased accuracy could not be achieved.

6.4.3 Hydrogen Ion Density Measurements

Hydrogen ion densities were measured from the absolute intensity of the Balmer series hydrogen lines as described in Chapter 3. Some of the problems which plagued the electron density measurements also affect measurements of hydrogen ion density. In general however, the spectroscopically measured hydrogen ion density increased with the hydrogen content of the shielding gas. Calibration difficulties are probably the major factor producing errors in these measurements.

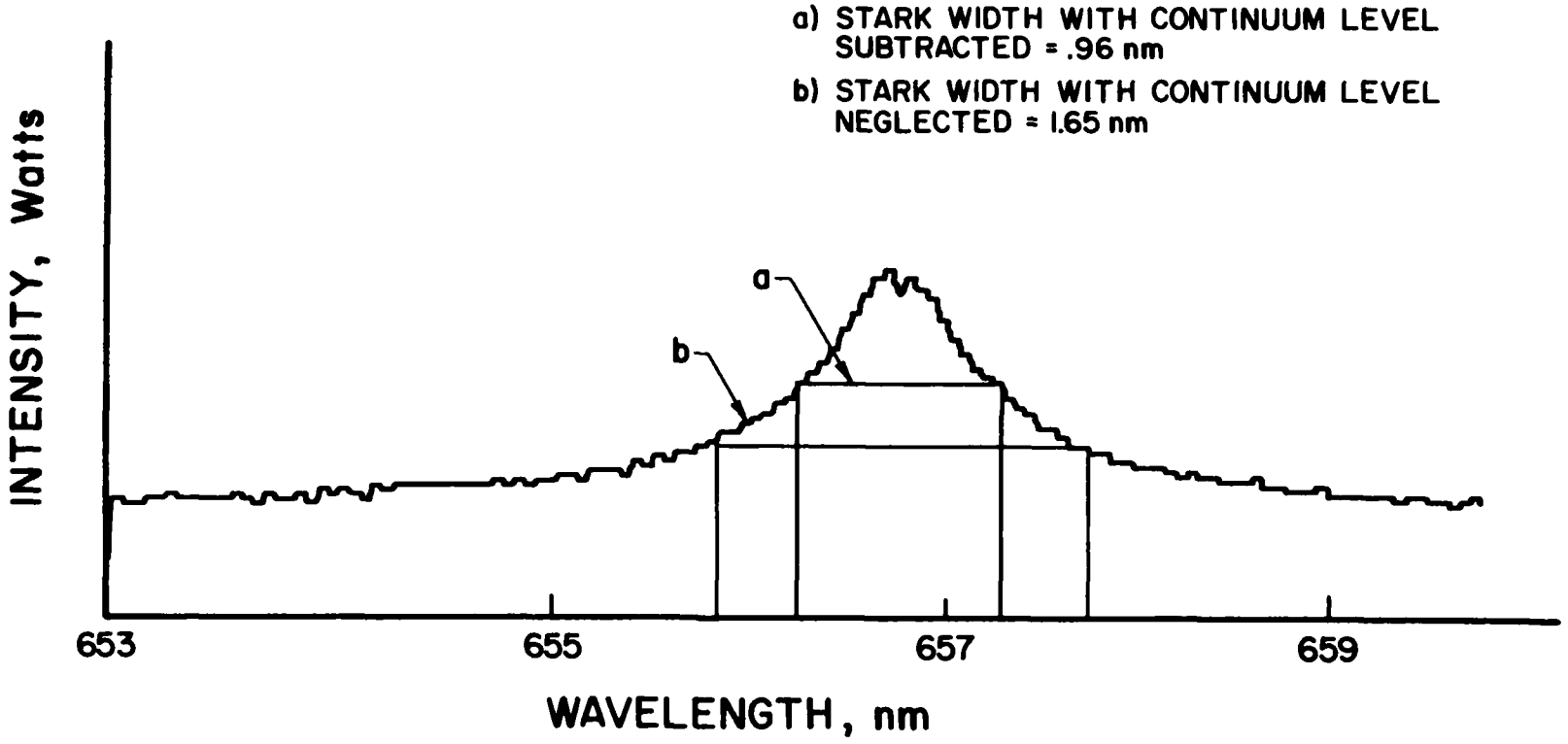

Figure 6.3 Effect of continuum radiation level on hydrogen line Stark width determination.

6.4.4 Measurements of Hydrogen Partial Pressure

The hydrogen partial pressure in the weld arc atmosphere was calculated by dividing the measured hydrogen ion density, which was determined as described in section 3.5.2, by the total electron density which was determined as described in section 3.5.2.2. As shown in Chapter 5, an increase in the spectroscopically measured hydrogen partial pressure was observed as the hydrogen content of the weld arc atmosphere increased. However, the results are clearly inaccurate, with a hydrogen free shield gas composition resulting in an average weld arc hydrogen partial pressure measurement in the welding arc of more than 1, which is clearly impossible.

Figure 6.4 shows the appearance of the hydrogen line at 656 nm when the weld arc atmosphere is nominally free of hydrogen. Determining the Stark width of this line is very difficult because it does not rise far above the background level, and the broadened shape of the line is hard to define. For this reason, the electron density measured at this hydrogen level was probably far below the actual electron density. This would explain the very high calculated hydrogen partial pressure. However, it is clear that either electron density was seriously underestimated in all measurements or that hydrogen ion density was overestimated, because the calculated hydrogen partial pressures are three orders of magnitude higher than expected. The error is consistent; the calculated hydrogen partial pressure increases with the amount of hydrogen added to the weld arc atmosphere.

6.4.5 Sources of Error in Absolute Intensity Measurements

Errors were larger in the absolute intensity measurements than in the relative intensity measurements for a number of reasons. Some of the errors were caused by the line of sight and optical system problems discussed earlier. In addition, weld arc plasmas are unstable and are not representative of the steady-state conditions needed for exact measurements of absolute line intensity. Another source of experimental error is smoke produced by the welding arc. This smoke reduces the amount of light focused by the lens on the fiber optic bundle and transmitted to the spectrograph. However, during calibration of the system with a standard lamp, no smoke is present. This introduces error in determining the intensity of the hydrogen emission lines of interest. Heating of the tungsten plate as the arc travels along it during data acquisition is another factor which cannot be compensated for during calibration with a standard lamp. As the anode grows very hot, the amount of blackbody radiation it emits at all wavelengths increases. This affects apparent line intensity during the time over which measurements are made. Self absorption of some of the radiation emitted by the welding arc also occurs in the weld arc plasma. This decreases apparent line intensity, contributing to errors in calibration of the system.

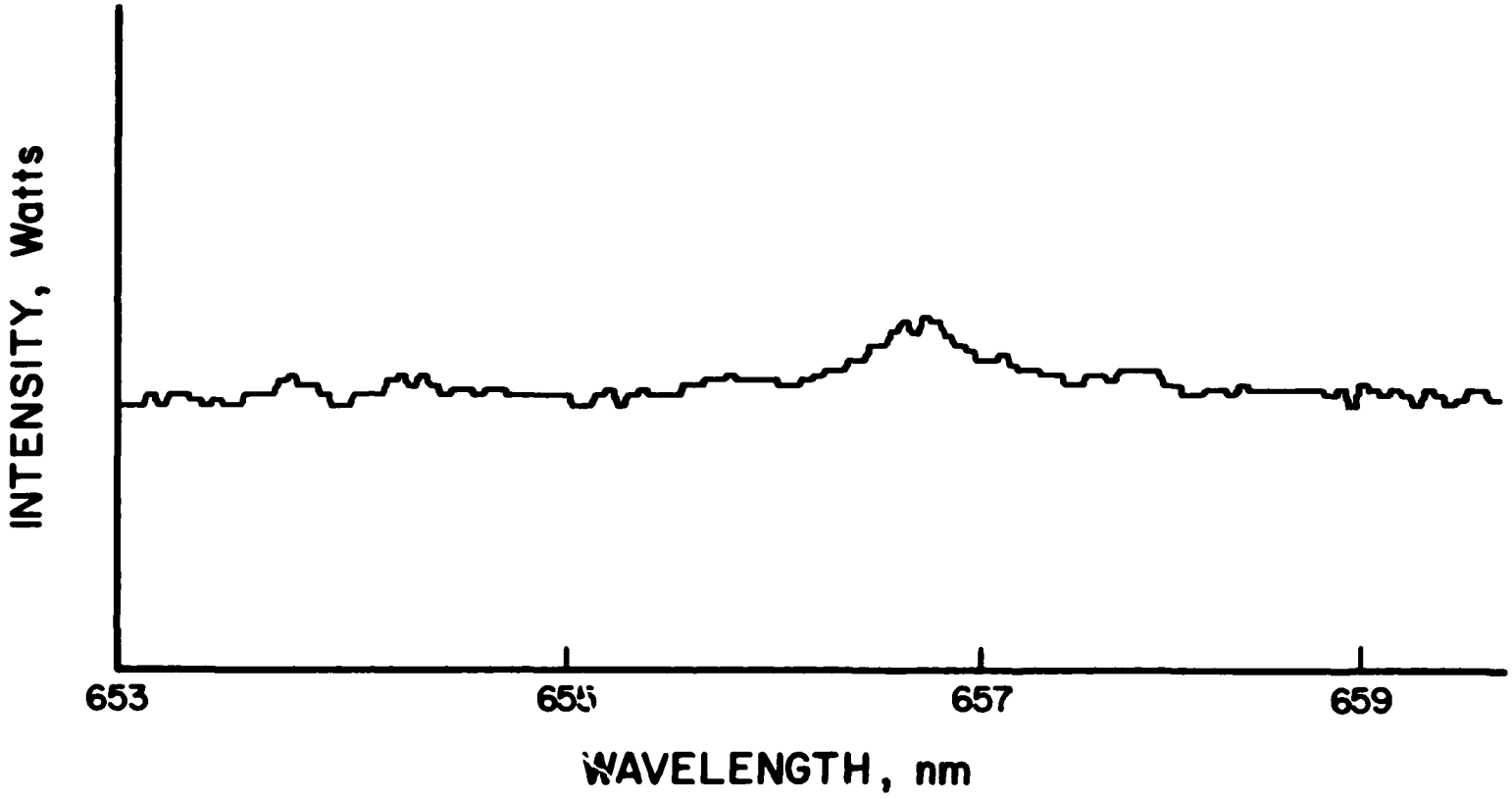

Figure 6.4 Hydrogen line appearance when shield gas hydrogen content is 0 percent.

An additional equipment-related problem exists. The response of the photodiode array drops off quickly at wavelengths below approximately 550 nm, and at 460 nm is only about 60 percent of that at 656 nm. In addition, the output of the calibrated lamp at the lower hydrogen wavelengths is about one-eighth of its radiance at 656 nm. As a result, the accuracy of the intensity calibration data obtained for the hydrogen lines at 486 and 434 nm is questionable. This problem does not plague the temperature measurements because it is the relationship between lines equally affected by the problem which is of interest. In determinations of hydrogen partial pressure in the arc atmosphere however, the number of atoms in various energy states is being measured. This quantity depends directly on the line intensity measurements, so calibration inaccuracies produce large errors.

The difficulties cited above in determining the partial pressure of hydrogen present in the weld arc atmosphere through use of absolute intensity measurements could be overcome through the use of more sophisticated hardware and software. Improvements in hardware would have to include an optical system capable of spatially resolving small areas in the welding arc. A more sensitive photodiode array with a flatter response at low wavelengths would also improve the accuracy of the data. A two-dimensional photodiode array would also help. Software changes should include use of the Abel inversion to eliminate errors associated with variations in arc temperature and composition along the line of sight.

If these changes were made, the spectroscopic system could be used to determine local changes in arc composition as well as to make temperature measurements. A number of questions exist in the literature which such a system could answer.

The interactions occurring immediately above the weld pool in the anode drop zone are known to be vey complex and are not well understood. For example, it has been proposed that metal ion vapor above the weld pool can have a significant effect on the composition of the welding arc immediately above the weld pool [34,65,67,71]. A spatially resolved mapping of weld arc composition would be of great use in understanding this effect and other questions about the anode drop zone and the gas-metal interactions occurring at the pool-arc interface.

6.5 Discussion of Implant Test Results

For the simplest purposes of quality control, the data presented in Chapter 5 could be used to establish a weld arc hydrogen level which should not be exceeded under production conditions. For example, the lower critical stress (LCS) in the implant test of an armor steel specimen welded under hydrogen free conditions is 55 ksi (377 MPa). When the hydrogen content of the shielding gas is increased to 0.25 percent, the lower critical stress drops appreciably to 43 ksi (295 MPa). If an analysis of structurally significant welds was performed and the minimum acceptable implant strength determined, such data could be used to establish the maximum weld arc hydrogen content allowable at various welding stations in a manufacturing facility.

Such a rudimentary application of this research could be fielded readily in a manufacturing situation. The relative emission line intensity results reported in Chapter 5 show that a hydrogen partial pressure of much less than 0.0025 in the welding arc can be detected spectroscopically. Thus, the technique is sufficiently sensitive to measure arc atmosphere hydrogen levels capable of causing deterioration in the mechanical properties of welds in the material studied. A fieldable system capable of measuring weld arc hydrogen levels in real time by mimicking the spectrograph through use of narrow pass band filters has been tested. Implant test data could be used to establish a cut off weld arc hydrogen level at which such a system would, for example, alert an operator or record the time and location of the suspect weld for later nondestructive inspection.

6.5.1 Use of Weld Diffusible Hydrogen Content Data to Predict Implant Test Results

Other ways of analyzing implant data exist [72,73] which would allow some integration of the design, quality control, and manufacturing functions by establishing fitness-for-purpose criteria for welding consumables quality. Christensen [72], for example, proposed a procedure in which implant test data can be used to determine the electrode coating type and diameter to prevent hydrogen induced cracking at a given ambient welding temperature and plate thickness. The method can also be used to estimate implant rupture strength if plate composition and electrode type and size are known.

Christensen's method relies on estimates of the volume percent of martensite present in the joint microstructure and on indirect estimates of weld diffusible hydrogen content (through correlation with electrode type and size). As a result, it is not particularly useful when weld diffusible hydrogen content can be determined through spectroscopic measurement in real time as discussed earlier in this chapter. However, Ito, Ikeda and Nakanishi [73] used a similar technique in a later investigation to obtain estimates of the implant rupture strength of a weld from its plate thickness, preheat temperature, and diffusible hydrogen content.

As shown in Figure 6.5, Ito, et al., related the diffusible hydrogen content, preheat temperature, and plate thickness of a given weld to a change in implant rupture strength from that obtained under a set of standard conditions. In this procedure, the time required for a weld to cool from peak temperature to 100°C is either known or is estimated from plate thickness and preheat temperature as shown in part a of Figure 6.5. This cooling time is related graphically to a change in implant rupture strength as illustrated in Figure 6.5(B). The weld's lower critical stress in the implant test under standard conditions is then estimated from P_{cm} (a cracking parameter dependent on the composition of the material being welded and the diffusible hydrogen content of the weld) as shown in Figure 6.5(C). The change in implant rupture strength estimated from part b of the figure is then added to or subtracted from the standard value to predict the final implant strength of the joint.

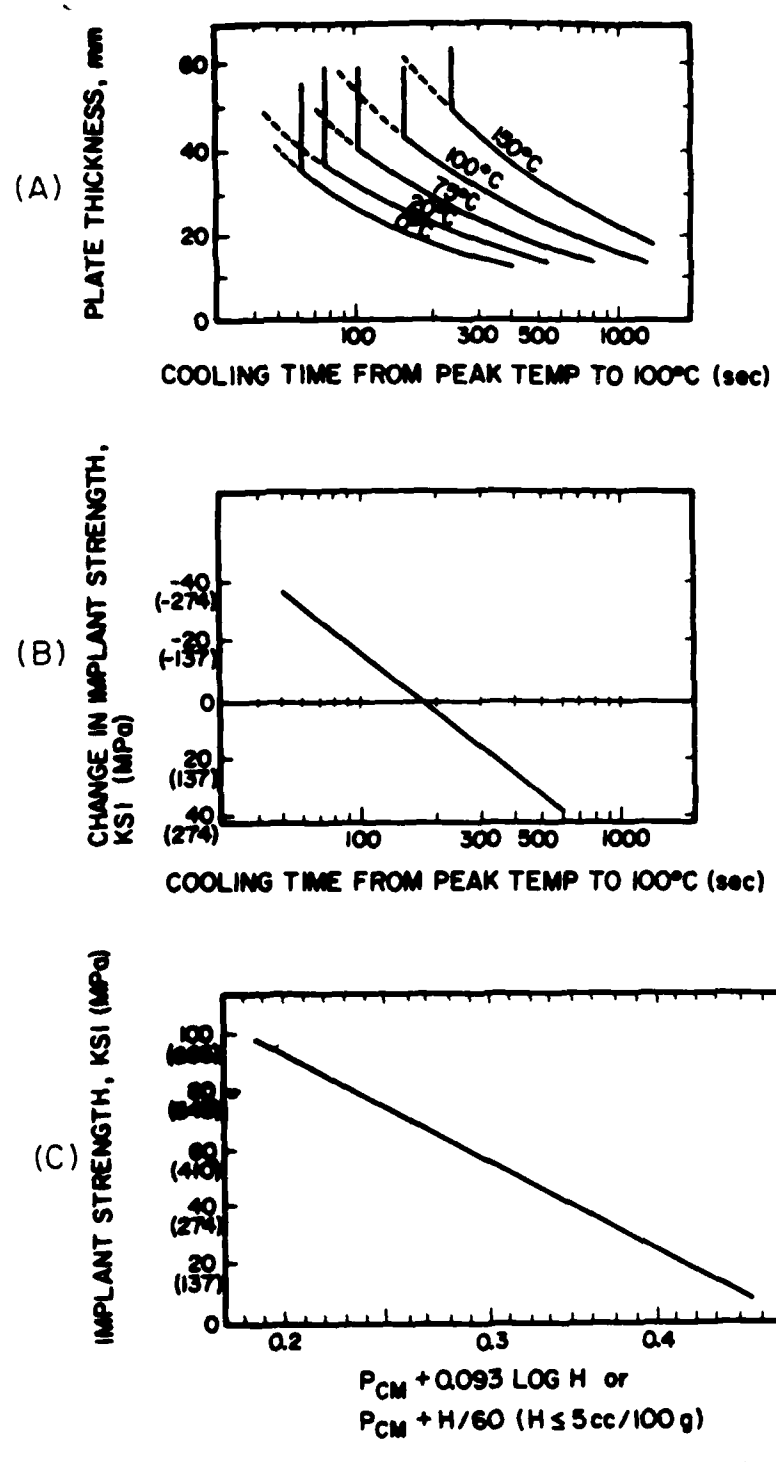

Figure 6.5 Ito's method for predicting lower critical stress from base metal composition and weld hydrogen content.

Like the better known carbon equivalent, P_{cm} is a parameter dependent on the composition of the base metal. It is an index of the relative cracking susceptibility of the weld and is dependent on the hydrogen content of the weld as well as the alloy composition. Generally, the higher the P_{cm}, the more susceptible the joint is to cracking.

$$P_{cm} = C + \frac{Si}{30} + \frac{Mn}{20} + \frac{Cu}{20} + \frac{Ni}{60} + \frac{Cr}{20} + \frac{Mo}{15} + \frac{V}{10} + 5B$$

is the formula used to determine this parameter. For the armor steel used in this study, P_{cm} is 0.387. This is rather high, and this material is indeed highly susceptible to hydrogen induced cracking.

Ito's method was applied to the material used in this study to determine whether the implant strengths of the welds could be predicted accurately. Using part (A) of Figure 6.5, the time required for a weld in a 25 mm plate with a preheat temperature of 150°F to cool to 100°C is predicted to be 300 seconds. However, when this cooling time was measured for implant tests performed under the conditions used in this study, the time required for the weld to cool to 100°C was found to be approximately 500 seconds, and this was the value used in estimating changes in implant strength. According to Ito, et al., the effect of preheating to 150°F on the implant rupture strength (i.e., the effect of increasing the cooling time of the weld to 100°C to 500 seconds on the lower critical stress) will be an increase of approximately 32 ksi over that predicted by Figure 6.5(C) for the appropriate P_{cm}.

Table 6.2 gives the results predicted using Ito's method and the measured lower critical stresses. As shown in Figure 6.6, this method provides good correlation with the experimental results. This suggests that spectroscopic measurement of weld arc hydrogen content could be used to estimate the mechanical properties of a welded joint directly in real time.

Table 6.2 Measured and Calculated Values of Lower Critical Stress

% Hydrogen in Shielding Gas	Measured		Calculated	
	(Ksi)	(MPa)	(Ksi)	(MPa)
0.0	55	377	56	384
0.05	58	397	52	356
0.10	53	365	50	342
0.20	51	356	48	329
0.25	43	295	45	308
0.5	29	199	42	287

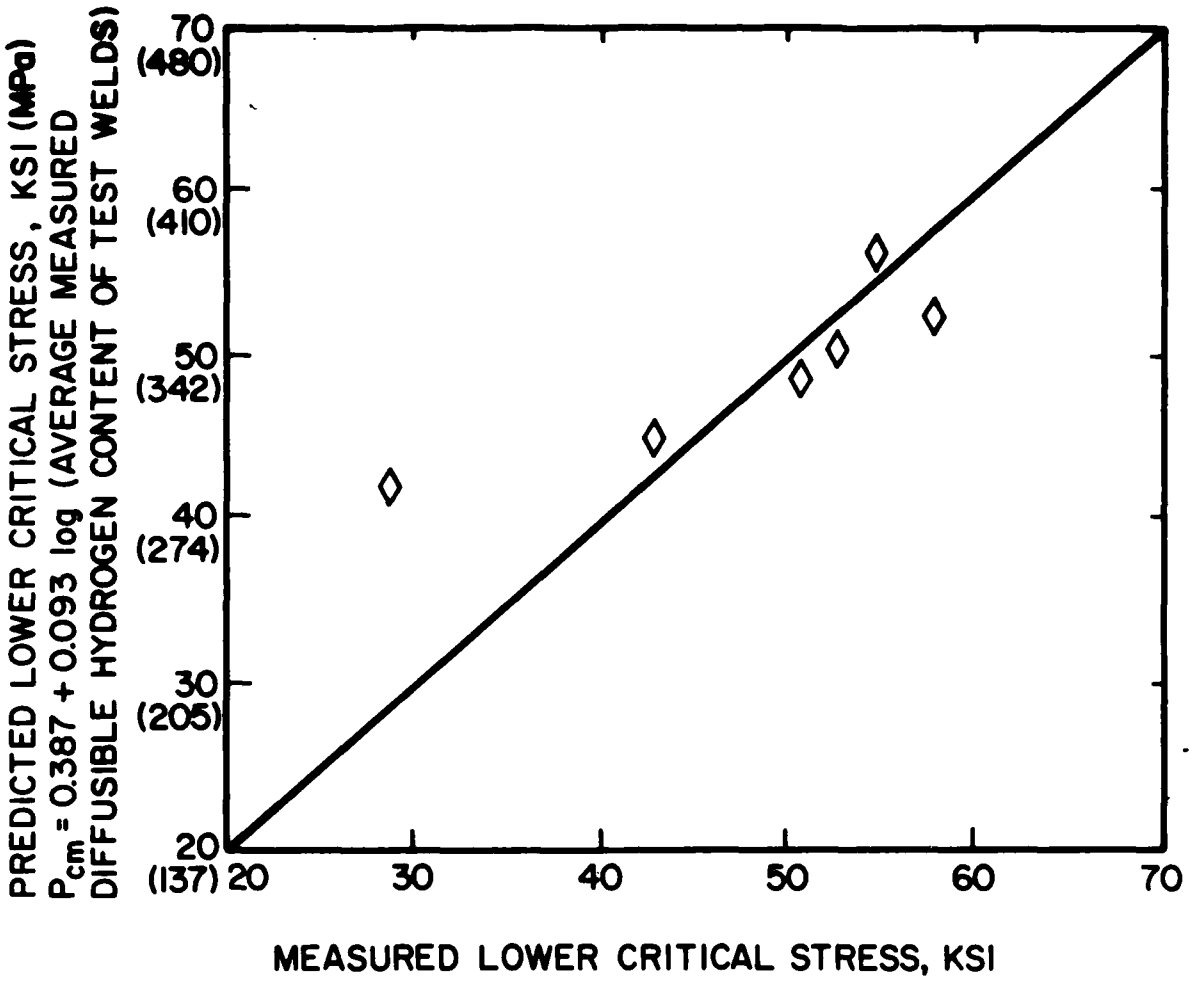

Figure 6.6 Comparison of measured and predicted lower critical stress using Ito's method.

Ito's method uses the diffusible hydrogen content of the weld to determine the lower critical stress, along with other constant parameters such as plate thickness and composition. However, the objective of this work is to relate the mechanical properties of a weld to spectroscopic data which can be obtained in real time. It was shown earlier that the diffusible hydrogen content of a weld can be related to the partial pressure of hydrogen in the welding arc as measured spectroscopically. Ito's method provides a procedure for correlating weld diffusible hydrogen content with implant strength. Therefore, it should be possible to use spectroscopic data with Ito's method to determine lower critical stress.

This can be done by replacing $P_{cm} + 0.093_H \log H$ as the equation for implant rupture strength with $P_{cm} + \log [S_H(I_{H_{REL}} - 0.7)/287.5]^{\frac{1}{2}}$. This is similar to the procedure used to predict the diffusible hydrogen content of welds from spectroscopic data. Figure 6.7 compares the predicted

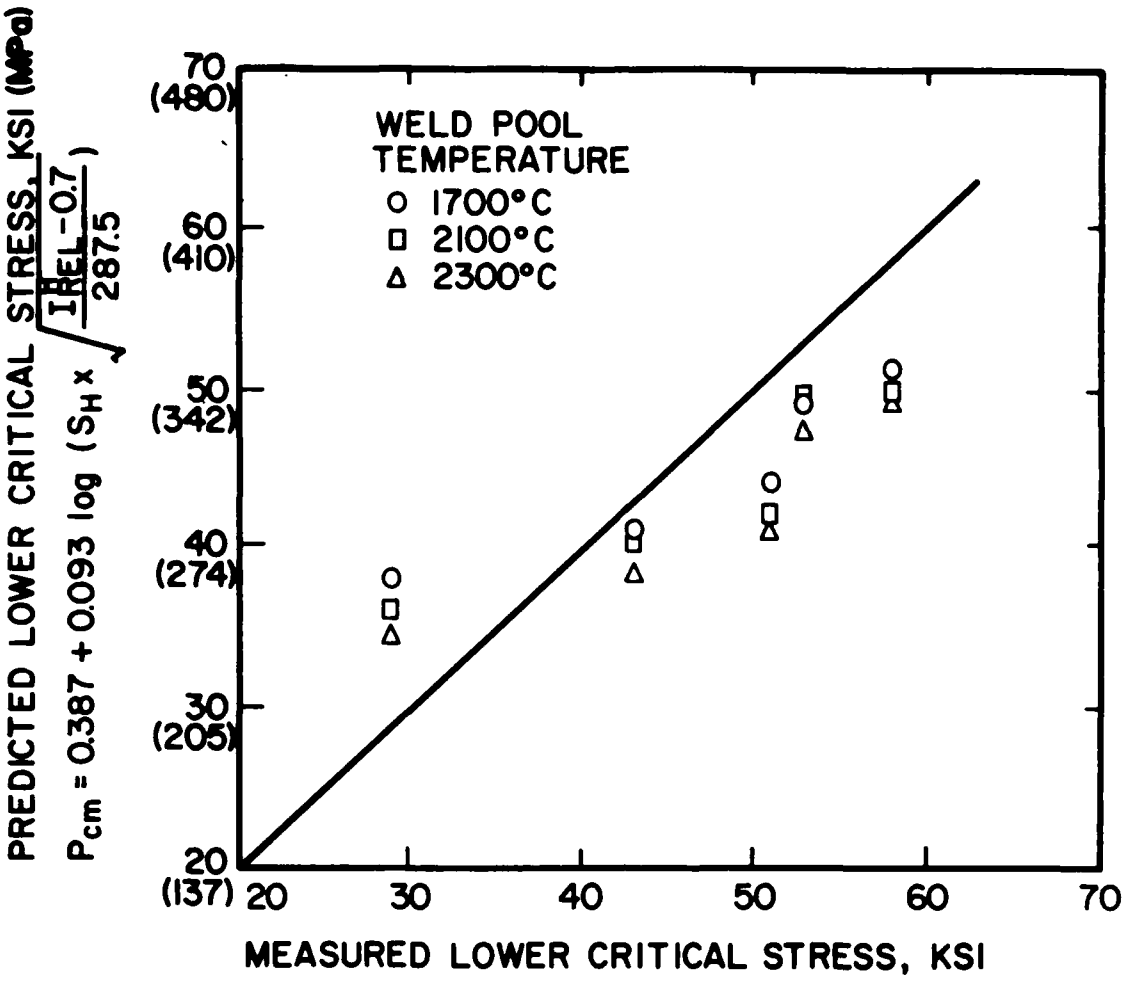

Figure 6.7 Comparison between predicted lower critical stress when spectroscopically determined hydrogen contents are used in Ito's method and measured lower critical stress.

lower critical stress if spectroscopically derived data is substituted for measured weld diffusible hydrogen contents with the experimentally determined lower critical stress.

Agreement is good between the LCS values predicted when measured or spectroscopy-determined weld diffusible hydrogen contents are used and agreement is good between measured and predicted LCS values whether measured weld hydrogen contents or spectroscopic data are used in evaluating P_{cm}. Some deviation exists because the measured and spectroscopically determined weld hydrogen contents are not identical. However, since the error in the determination of the lower critical stress using the implant test is generally considered to be about 15 percent [72,73], it is clear that most of the data fall well within the bounds of likely experimental error. For low weld hydrogen contents, the spectroscopic method is conservative: the predicted lower critical stress is slightly lower than that measured experimentally. When 0.5 percent hydrogen is added to the weld arc atmosphere, the predicted lower critical stress is considerably higher than the measured lower critical stress. However, this arc atmosphere hydrogen level is well

above any acceptable limit (it results in a decrease of over 50 percent in lower critical stress) and would require immediate attention in any welding operation involving medium or high strength steel.

6.5.2 Use of Implant Test Data to Establish Design, Quality Control, and Manufacturing Requirements

A technique has been presented which allows the diffusible hydrogen content of welds and their mechanical properties to be estimated quite accurately in real time. This capability, together with the data base developed in this study, provides a basis for integration of many design, quality control, and manufacturing functions. Using the relative intensity spectroscopic technique described here, a simple testing program could establish the average weld arc hydrogen partial pressure associated with various welding processes or brands of consumables.

Designers could use this information to select materials sufficiently resistant to hydrogen induced cracking to perform well under the selected welding conditions. Similarly, the data could be used to select a welding process suitable to the material being used or to ensure that joint restraint did not exceed that allowable for a given combination of welding process and material. For example, the degree of restraint in a particular joint could be analyzed during the design process.

This restraint could be associated with a maximum arc atmosphere hydrogen partial pressure which would not result in hydrogen induced cracking. The data could then be used to establish nonarbitrary filler wire quality requirements as part of the design process.

Following design, the information could also be used by value engir ring and quality control departments. During development of purchasing specifications and procurement of consumables, the allowable weld arc hydrogen content established during the design cycle might be found to be unrealistically low for reasons of cost or unavailability of consumables of the required quality. The joint design could then be modified prior to starting fabrication of components and discovering that joint redesign was necessary because of cold cracking of finished assemblies.

The real time capabilities of the spectroscopic technique could also be used as part of the input to a sophisticated adaptive feedback control system in manufacturing. If a weld arc hydrogen partial pressure slightly higher than average was detected, a method similar to that proposed by Ito et al. could be used to adjust preheat or interpass temperature. This type of data could be used with some form of artificial intelligence to allow continuous adjustment of welding parameters by a welding robot based on arc hydrogen content. Very high weld arc hydrogen contents would, of course, require notification of a human operator.

7. SUMMARY

The objectives of this study were to predict the diffusible hydrogen content of a weld as it is being fabricated, and to relate it to the hydrogen induced cracking susceptibility of the joint.

It has been shown that spectroscopic techniques based on measurement of the relative intensity of hydrogen emission lines during arc welding can be used to determine the partial pressure of hydrogen present in the weld arc atmosphere. These data can be used to predict the diffusible hydrogen content of weld specimens.

In addition, the results of this study show that spectroscopic measurements of the amount of hydrogen in the weld arc atmosphere correlate well with the mechanical properties of the resulting weld as evaluated using the implant test. This suggests that these data and the measurement technique developed could be used to improve integration of design, quality control and manufacturing in welded fabrication.

REFERENCES

1. Swinden, and Reeve L., Trans. Inst. Welding, Jan. 1938, pp. 7-24.

2. Seeve, L., Weld. J., Nov. 1945, pp. 618s-623s.

3. Hopkins, G. L., Weld. J., Nov. 1944, pp. 606s-608s.

4. Herres, S. A., Weld. J., Jun. 1944, pp. 43s-49s.

5. Christensen, N., Gjermundsen, K., and Rose, R., Brit. Weld. J., June 1958, pp. 272-281.

6. Cottrell, C. L. M., Brit. Weld. J., Apr. 1954, pp. 157-176.

7. Mallett, M. W., Weld. J., Julu 1946, pp. 396s-399s.

8. Makara, A. N. and Mosendz, N. A., Auto. Weld., Sept. 1964, pp. 1-10.

9. Aristov, V. S., Badasen, P. P., and Penkov, O.M., Weld. Prod., Feb. 1970, pp. 7-9.

10. Aristov, V. S., Badasen, P. P., Kudinov, E. D., and Ryabinkin, V. P., Weld. Prod., Oct. 1966, pp. 10-11.

11. Dorschu, K. E., Weld. Res. Council Bull. No. 231, Oct. 1977.

12. IIS/IIW Doc. 452-74, "Weld Metal Hydrogen Levels and the Definition of Hydrogen Controlled Electrodes."

13. Bradstreet, B. J., Weld. J., Jan. 1964, pp. 43s-48s.

14. Interrante, C. G., Dalder, E. N. C., and Yeo, R.B.G., Weld. J., Sept. 1969, pp. 384s-388s.

15. Chew, B., Weld. J., May 1976, pp. 127s-134s.

16. Smith, D. C., Rinehart, W. G., and Johannes, K. P., Weld. J., July 1956, pp. 313s-322s.

17. Chew, B., Met. Con., July 1982, pp. 373-377.

18. Millar, J. C., Austr. Weld. Res., June 1972, pp. 19-28.

19. Coe, F. R., Weld. J., Aug. 1968, pp. 355s-363s.

20. Coe, F. R., Met. Con., and Brit. Weld. J., Feb. 1969, pp. 108-109.

21. Stout, R. D., AISI Report 51-423, 1982.

22. Coe, F. R., and Moreton, J., Brit. Weld. J., June 1967, pp. 313-320.

23. Coe, F. R., Welding Steels Without Hydrogen Cracking, The Welding Institute, Abingdon Hall, Cambridge, 1973.

24. Graville, B. A., Cold Cracking Control in Welds, Dominion Bridge Co. Ltd., Montreal, Canada, 1975.

25. Kyte, W. S., and Chew B., Weld. J., Feb. 1979, pp. 54s-58s.

26. Christensen, N., Weld. J., Apr. 1961, pp. 145s-154s.

27. Chew, B., Weld. J., Sept. 1973, pp. 386s-391s.

28. Evans, G. M. and Weyland, F., Deut. Ver. Schweisstechnik Ber., No. 50, 1978, pp. 21-33.

29. Hirai, Y., Minakawa, S., Tsuboi, J., "Prediction of Hydrogen Content in Deposited Metals with Basic Type Covered Electrodes," IIW Doc. II-929-80.

30. Sieverts, A., Zeit. Metallkunde, Vol. 21, 1929,p. 37.

31. Mallett, M. W., and Rieppel, P. J., Weld. J., Nov. 1946, pp. 748s-759s.

32. Arata, Y., Hamasaki, M., and Sakakibara, J., Trans. JWRI, Mar. 1981.

33. Ball. D. J., Gestal, W.J. and Nippes, E. F., Weld. J., Mar. 1981, pp. 50s-54s.

34. Howden, D. G., and Milner, D. R., Brit. Weld. J., June 1963, pp. 304-316.

35. Salter, G. R., Brit. Weld. J., June 1963, pp. 316-325.

36. Fabling, F. T., and Chew, B., Weld. Res. Int'l., Apr. 1973, pp. 81-87.

37. Kozlov, R. A., Weld. Prod., Nov. 1953, pp. 47-59.

38. Boniszewski, T., and Morris, A.G. C., Weld. and Metal. Fab., Apr. 1981, pp. 131-142.

39. Kotecki, D. J., and La Fave, R. A., Weld. J., Mar. 1985, pp. 31-37.

40. Sohrman, B., Budgivfars, S., Dahlskog, H., Elvander, J., and Nilsson, G., Proc. 2nd Int'l Conf. Joining of Metals (JOM-2), Helsingors, DK, 1984.

41. Quintana, M., Weld. J., May 1984, pp. 141s-149s.

42. Quintana, M., and Dannecker, J., Proc., Symposium on Hydrogen Embrittlement: Test Methods, May 1985.

43. Pokhodnya, I. K., and Pal'tsevich, A. P., Auto. Weld., Jan. 1980, pp. 37-39.

44. Granjon, H., Met. Con. and Brit. Weld. J., Nov. 1969, pp. 509-515.

45. Christensen, N. and Simonsen, T., Scand. J. Met., Feb. 1981, pp. 120-126.

46. Howarth, O., Theory of Spectroscopy, Halsted Press, John Wiley and Sons, New York, 1973.

47. Griem, H. R., Plasma Spectroscopy, McGraw-Hill, New York, 1964.

48. Matsunawa, A., Katayama, S., Tokumura, T., and Ariyasu, T., Proc. 3rd Int'l. Colloquium on Welding and Melting by Electrons and Laser Beam, pp. 53-60.

49. Kobayashi, M. and Tsuga, T., Proc., Int'l. Conf. on Arc Physics and Weld Pool Behavior, The Welding Institute, 1979.

50. Glickstein, S. S., Weld. J., Aug. 1976, pp. 222s-229s.

51. Ludwig, H. C., Weld. J., July 1959, pp. 296s-300s.

52. Key, J. F., Chan, J. W. and McIlwain, M. E.,

53. Mills G. S., Weld. J., Mar. 1977, pp. 93s-96s.

54. Vinogradov, V. A., et al., Weld. Prod., Dec. 1974, pp. 5-6.

55. Blackmon, D. R., and Kearney, F. W., Weld. J., Aug. 1983, pp. 37-39.

56. Shea, J. E., and Gardner, C. S., J. Appl. Phys., Sept. 1983, pp. 4928-4938.

57. Davis, R. C., and Gardner, C. S., RRL Publication No. 517, July 1982, University of Illinois.

58. Thornton, J. A., "An Investigation of the Energy Exchange Processes in Nonequilibrium Plasmas," Litton Publication 11-68-190.

59. International Institute of Welding, Commission IX, Welding in the World, 1/2, 1985, pp. 12-20.

60. Reader, J., Corliss, C. H., Wiese, W. L., and Martin, G. A., Wavelengths and Transition Probabilities for Atoms and Atomic Ions, NSRDS-NBS 68, Dec. 1980.

61. Coe, F. R., Met. Con., Jan. 1986, pp.20-25.

62. Cary, H. B., Modern Welding Technology, Prentice-Hall, New Jersey, 1979, p. 358.

63. Fast, J. D., Interactions of Metals and Gases, Vol. 1 Thermodynamics and Phase Relations, Academic Press, New York and London, 1965.

64. Haddad, G. N., Farmer, A. J. D., Weld. J., Dec. 1985, pp.339s-342s.

65. Howden, D. G., Weld. J., Mar. 1986, pp. 125s-132s.

66. CRC Handbook of Chemistry and Physics, ed. R. C. Wheat, CRC Press, Boca Raton, Florida, 1984.

67. Lancaster, J. F., The Metallurgy of Welding, Brazing and Soldering, American Elsevier, New York, 1970.

68. Deutsch, M., and Beniaminy, I., J. Appl. Physics, Jan. 1983, pp. 137-143.

69. Etemadi, K., and Pfender, E., Rev. Scientific Instruments, Feb. 1982, pp. 255-257.

70. Eddy, T. L., IEEE Trans. in Plasma Science, June 1976, pp. 103-111.

71. Block-Bolten, A., and Eagar, T. W., Met. Trans. B, Sept. 1984, pp. 461-469.

72. Christensen, Nils, International Institute of Welding Document IX-824-73.

73. Ito, Y., Ikeda, M. and Nakanishi, M., International Institute of Welding Document IX-969-76.

DISTRIBUTION

Chief of Engineers
ATTN: DAEN-IMS-L (2)

Defense Technical Info. Center
ATTN: DDA (2)

CRREL, ATTN: Library

WES, ATTN: Library